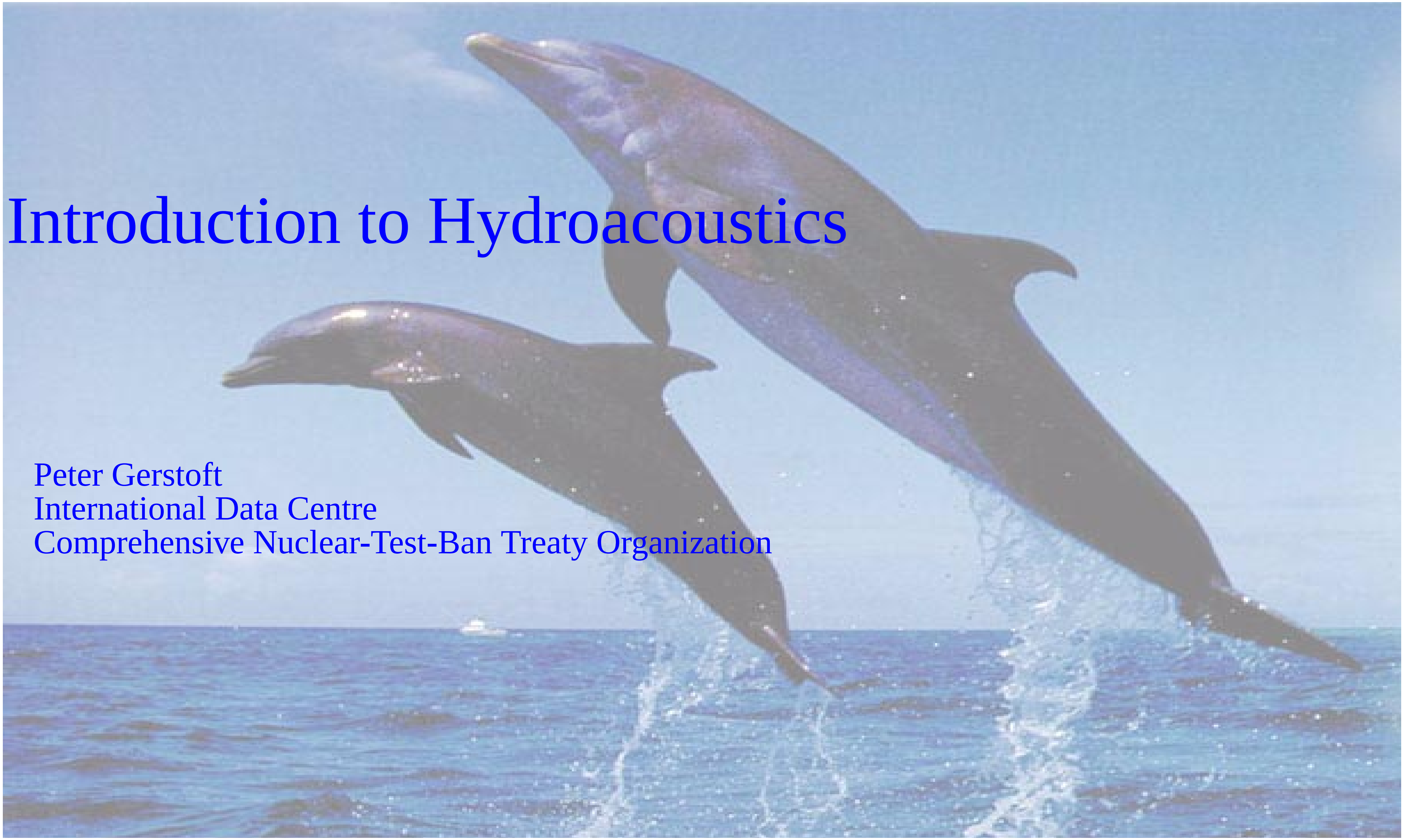

Introduction to Hydroacoustics

Peter Gerstoft
International Data Centre
Comprehensive Nuclear-Test-Ban Treaty Organization

Introduction to hydroacoustics (3 days) contents:

The Physics

- The environment
- Features of acoustic propagation
- Computational ocean acoustics
- T and H-phases
- Examples of acoustic arrivals
- Atoll explosion
- T-phases
- Bubble pulse
- California explosions

Hydroacoustic processing

- Detection and Feature eXtraction (DFX)
- Analysis of one arrival
- Station Processing (StaPro)
- Global Analysis (GA)- location
- Event Screening

Hydroacoustic processing is not as mature as seismic processing.
CTBT related hydroacoustics is a mixture of naval ocean acoustics and seismology.
A functional hydroacoustic network will only be available in next few years.

Underwater nuclear explosion
at Bikini Atoll on 24 July 1946

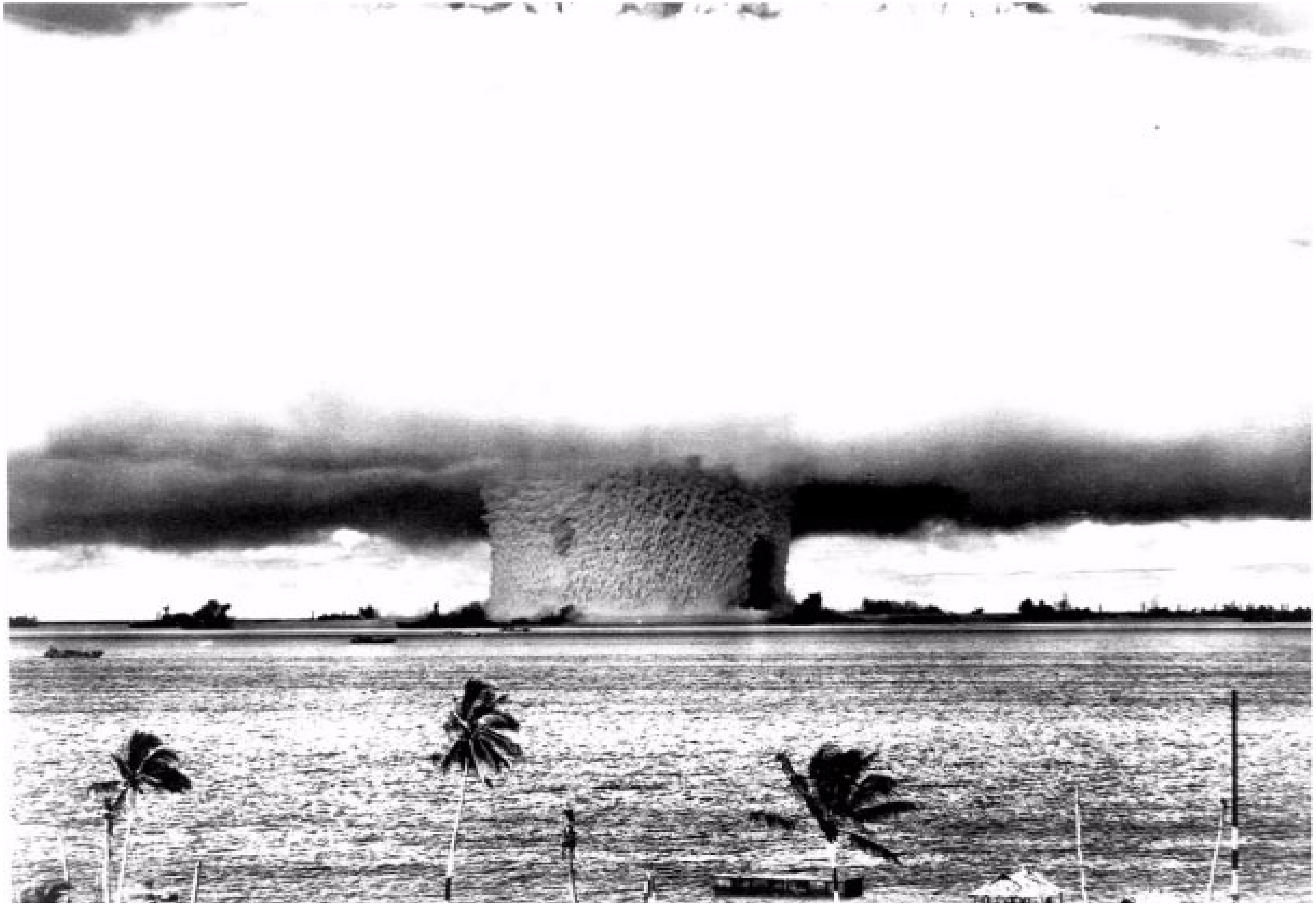

Crozet Island - France

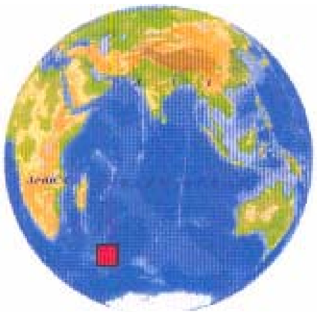

Hydrophone Station

- Site survey complete
- Installation underway
- Expect operation April 2000

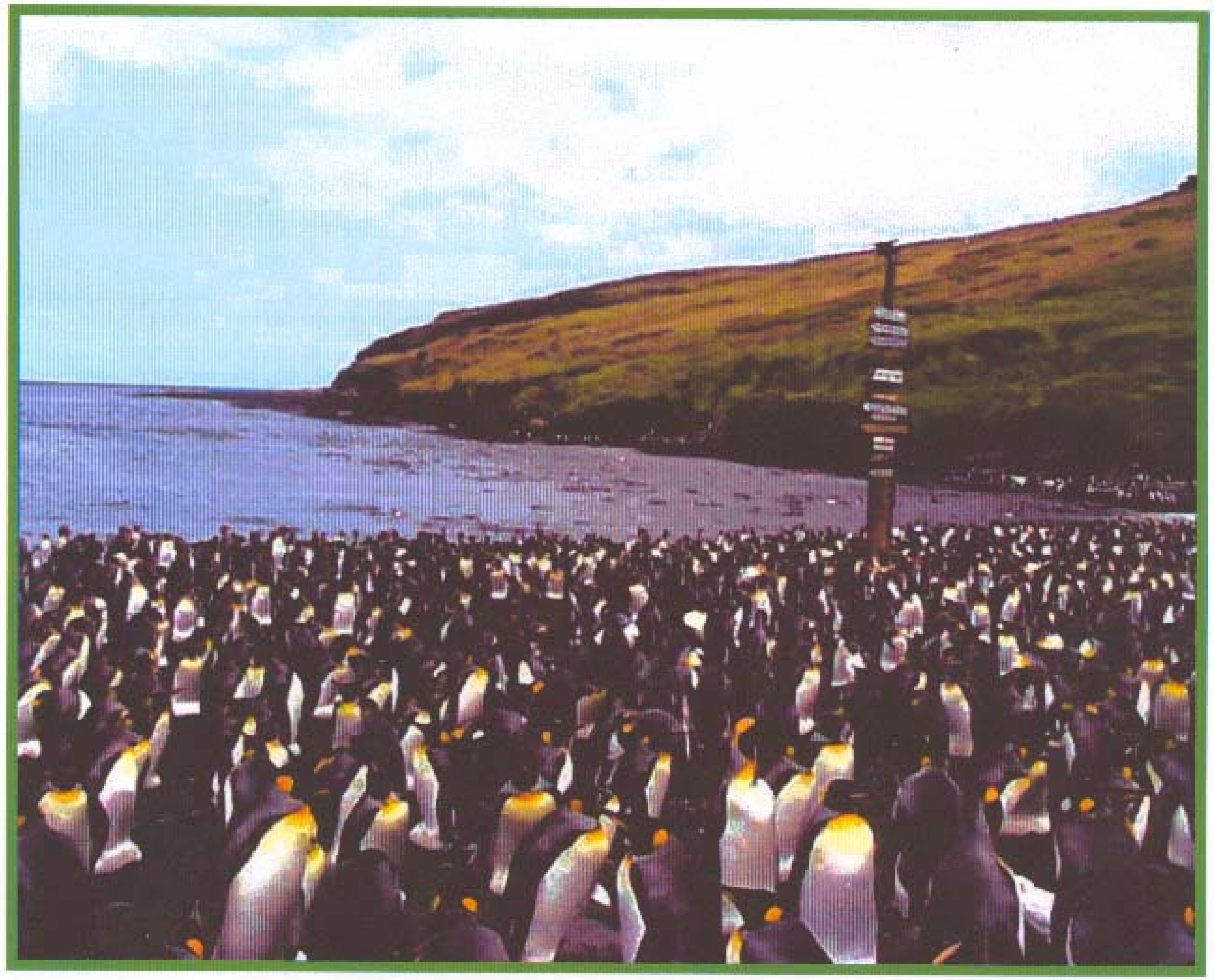

Ocean sound speed profile

Sound speed increases with pressure, temperature and salinity.
The pressure increases linearly with depth.
The temperature is constant in the deep ocean and also in the mixed layer.
The salinity variation can often be neglected.

The SOFAR Channel: No interaction with ocean boundaries.

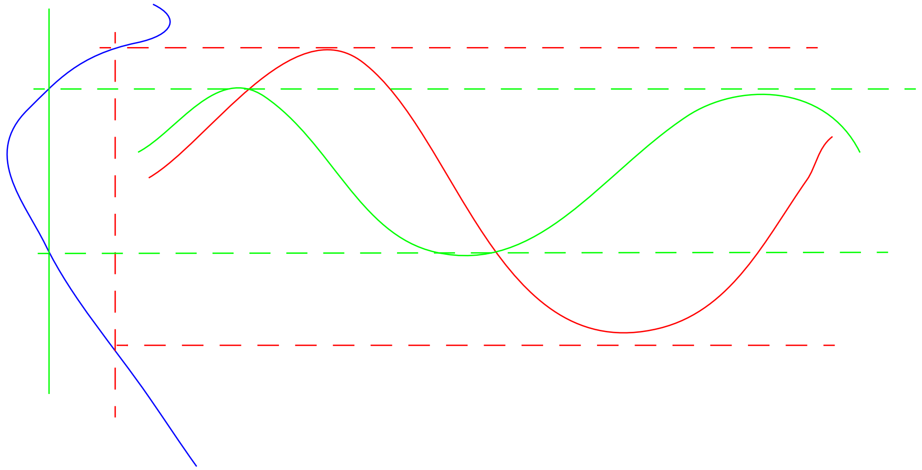

Mixed layer has constant temperature. A surface duct.

Ocean is not frozen in time or space!
The sound speed shows seasonal variability.

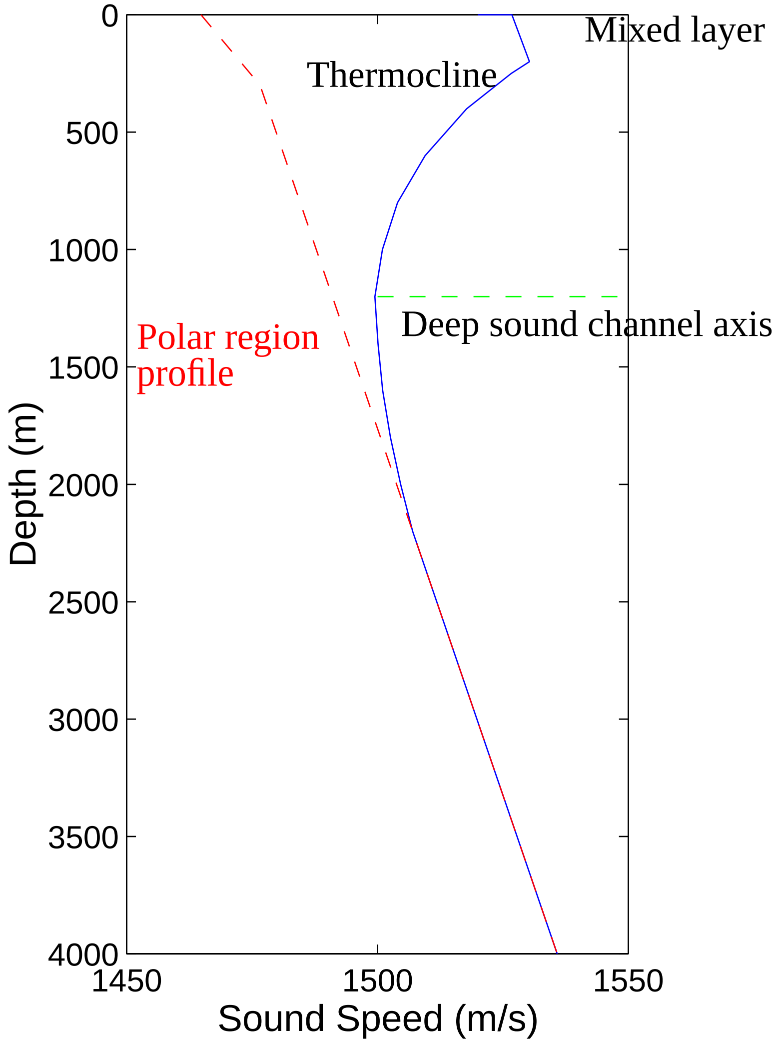

Ocean environment is not stationary in time or space

Examples of variation in ocean environment;

Global scale: e.g. Global warming (years)

Subbasin scale (1,000), e.g. Gulf steam (weeks months)

Mesoscale eddies fronts, meanders (days-weeks)

Submesoscale: 10km; internal waves, tides (hours-days)

These features will affect the ocean sound speed
and thus the travel time and the shape of received waveform.
It is much more difficult than in seismics to reproduce the
received waveform

Temperature profiles in the Norwegian sea in a two week period.

1deg C =4.5 m/s

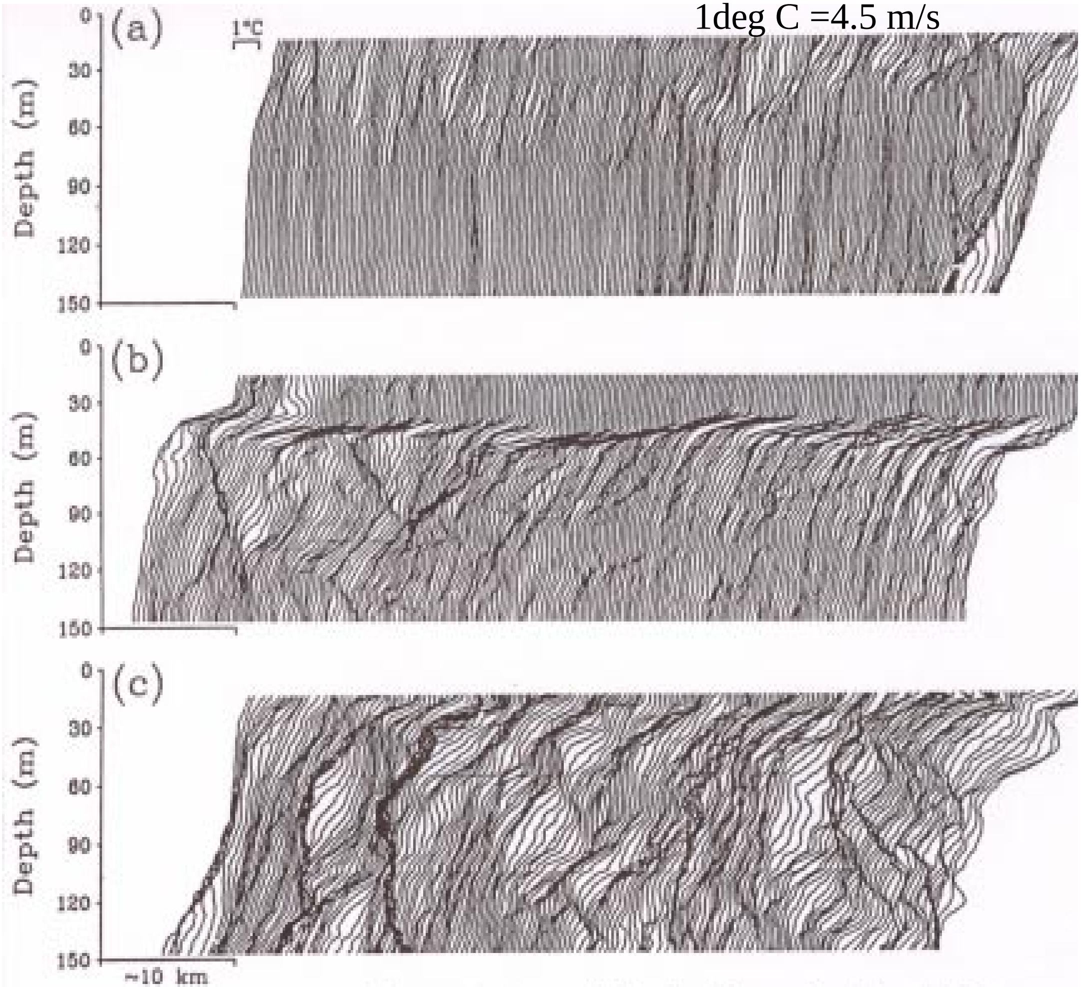

Fig. 1. Temperature profile sections recorded in the Norwegian Sea. (a) Laterally stable ocean. (b) Stable surface layer with some lateral variability below the thermocline. (c) Strong lateral variability in upper 150 m.

Bathymetry

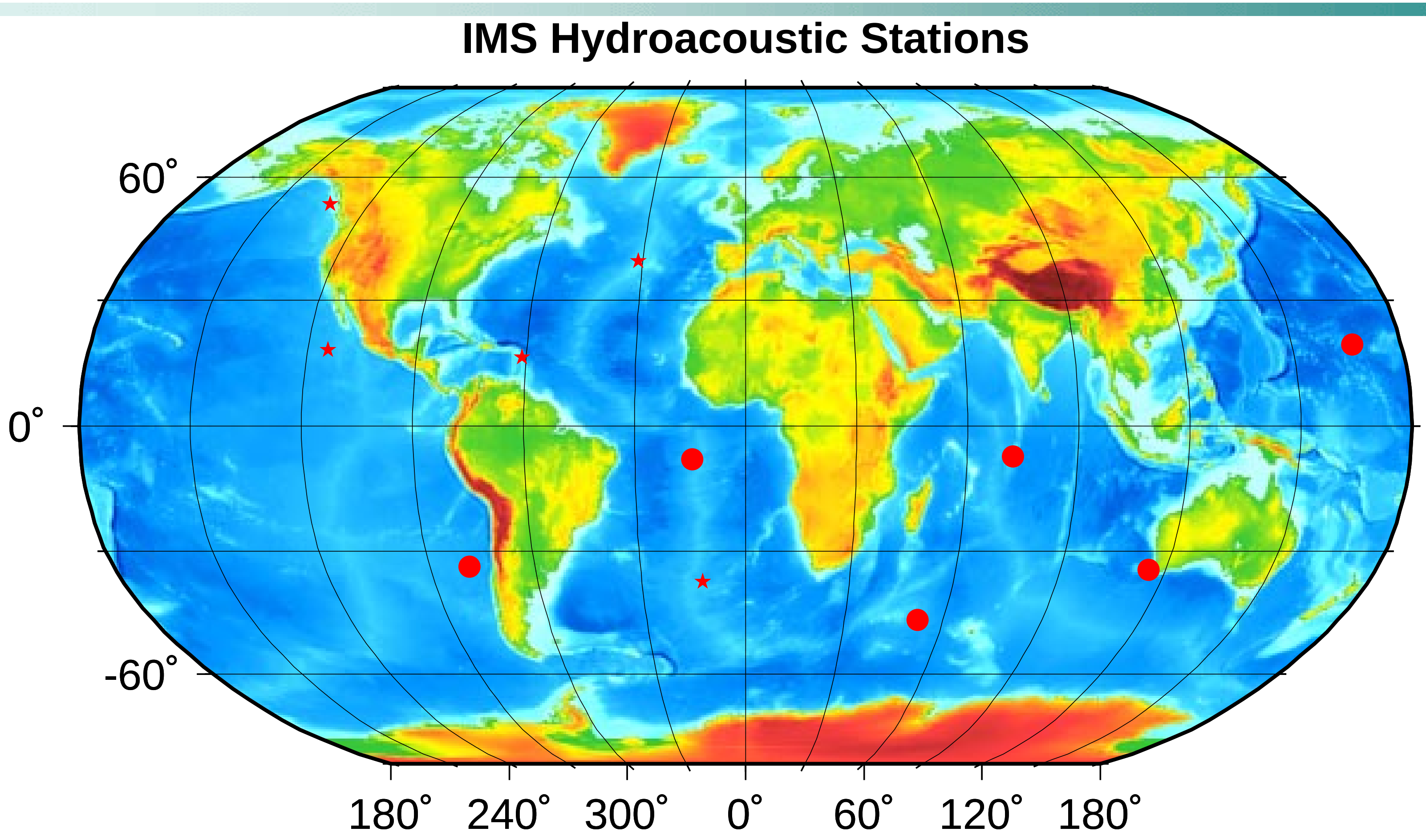

The lower boundary of the ocean is ocean bottom.
Usually, long range acoustic energy propagates without bottom interaction for ocean depths > 4000 m.

Reflection coefficient

Bottom: Penetrable boundary

Most acoustic paths will during the propagation interact with the bottom

For low grazing angles there is perfect reflection.
Bottom scattering is can also be important.

Typically, ocean acoustic energy will propagate at grazing angles less than 15 deg.

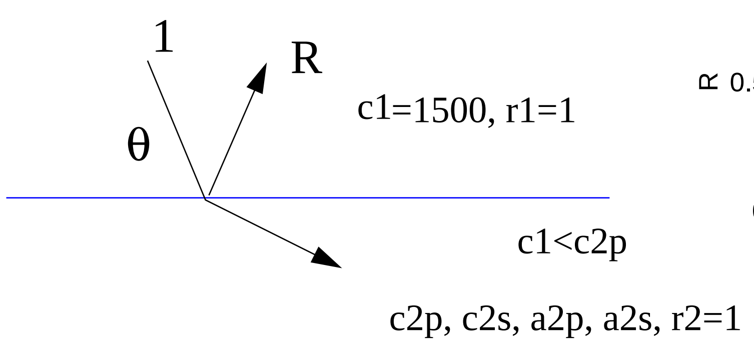

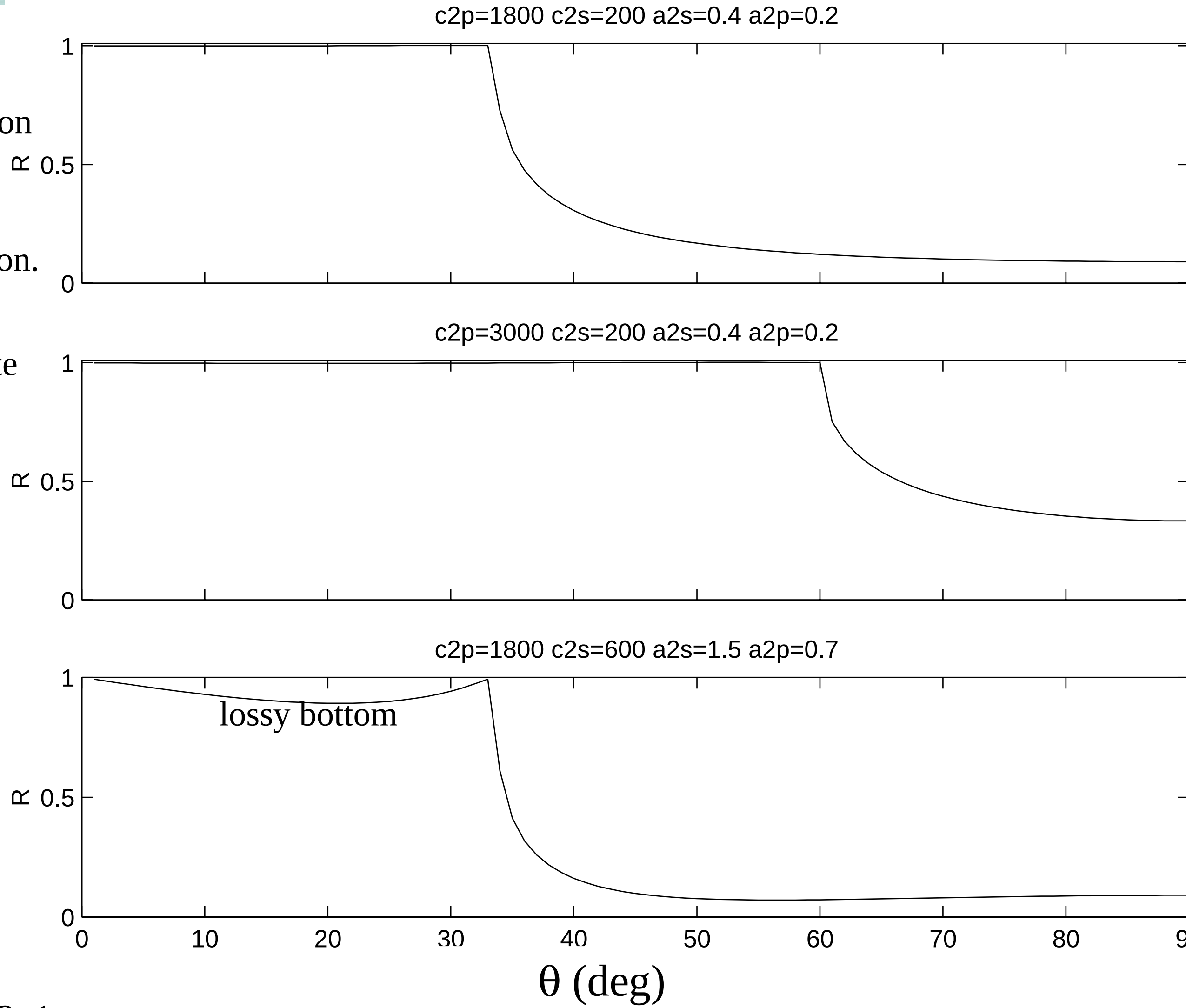

Propagation path

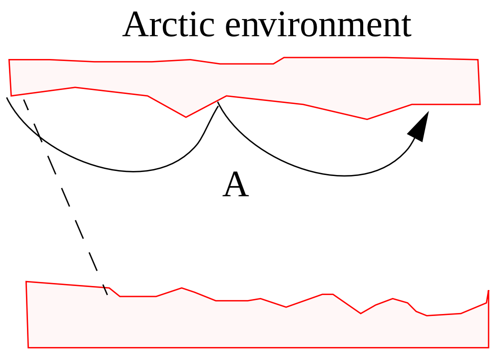

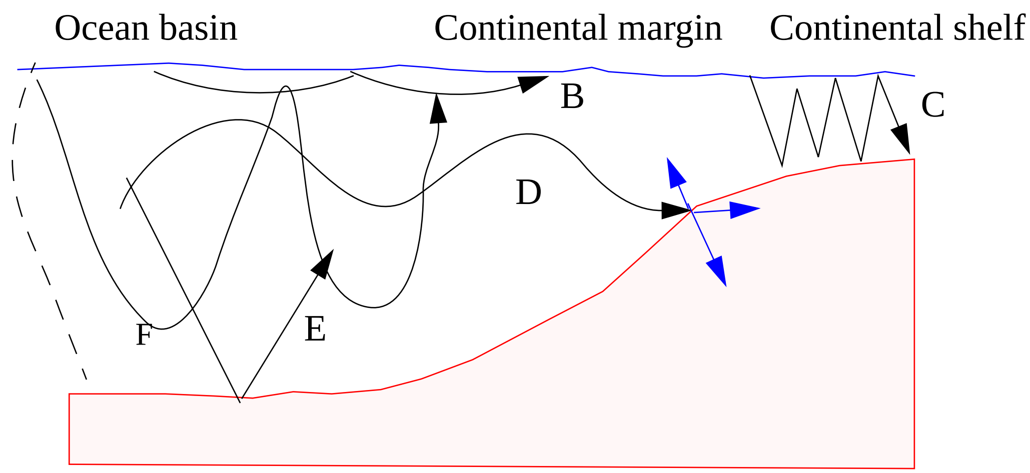

A: Arctic propagation
B: Surface duct
C: Shallow water
D: SOFAR channel
E: Bottom bounce
F: Convergence zone

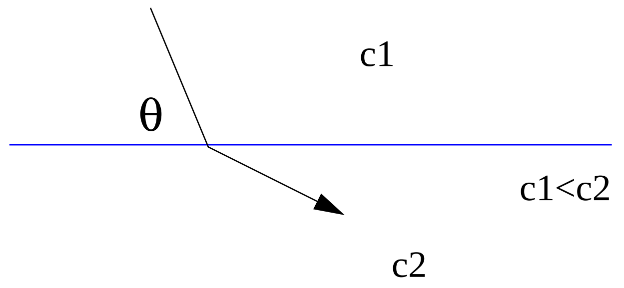

Use of Snells law gives the basic path: $\cos(\theta)/c = \text{const}$
c is local sound speed and θ is angle with interface.

Arctic and SOFAR propagation

Arctic Environment:

Surface channel
Absorption at sea surface

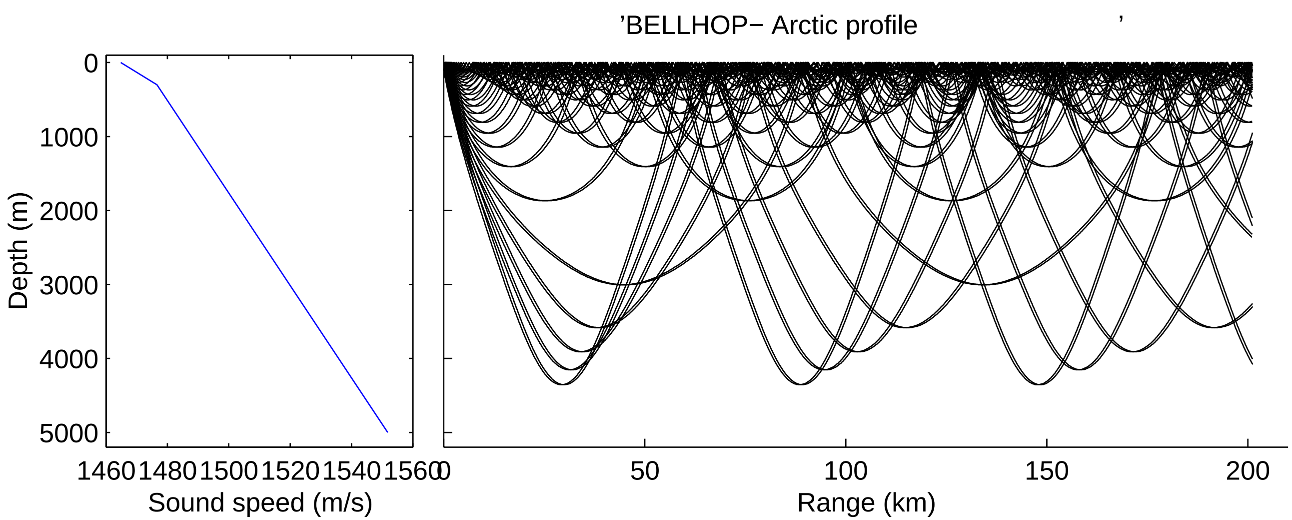

SOFAR environment

No interaction with ocean boundaries
Little attenuation.

The rays that interact with boundaries will be attenuated.

The steeper rays arrives before shallow rays, as they spend more time in faster media.

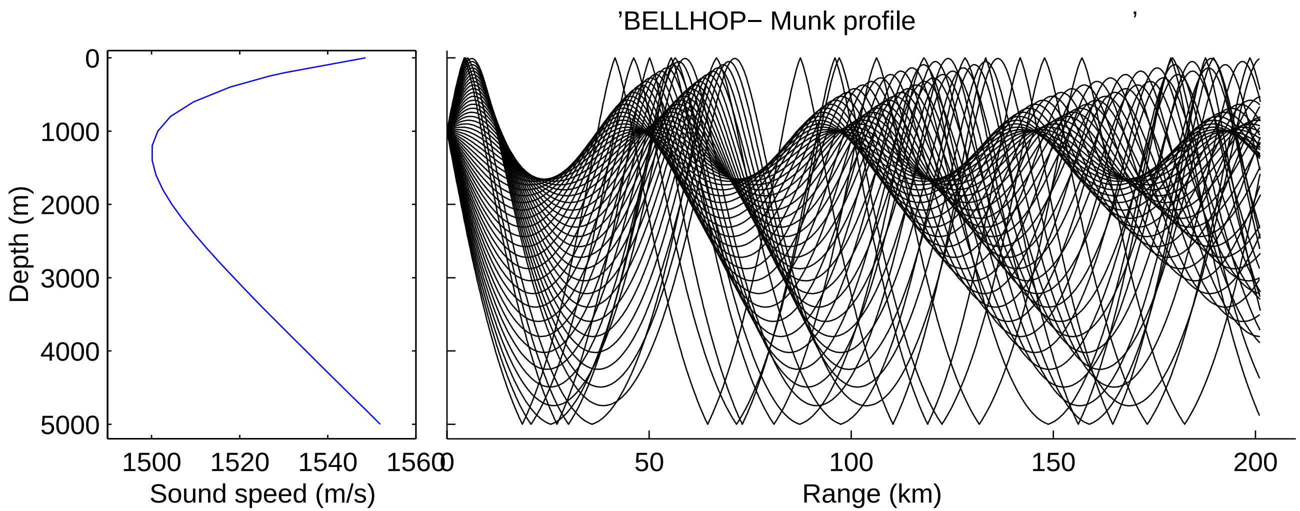

Normal modes

The preferred way to solve long range ocean acoustic propagation problem is via normal modes. The solution to the wave equation is solved via separation of variables. The pressure *p* at frequency *f*, range *r* and depth *z* is:

$$P(f, r, z) = S\sum_{j}^{N} v_j(z_s) v_j(z) \frac{\exp(ik_j r)}{\sqrt{k_j}}$$

where $v_j(z)$ are the normal modes and z_s is the source depth.

k_j is the horizontal wavenumber for mode j,
lower modes has lower phase speed,
they arrive later at a given range.

N is the number of propagating modes, it depends on environment and increases with frequency.

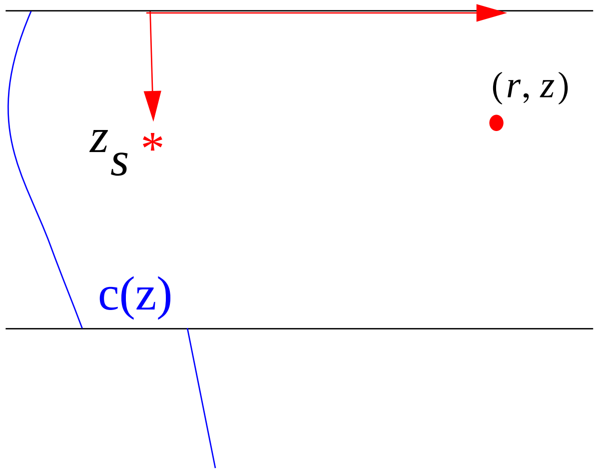

The analogy to ocean acoustic modes is modes on a vibrating string

The interference between modes varies in range due to the complex exponential in the above formula.
For 2 modes the formula simplifies

$$P(f, r, z) = C_1 v_1(z) \exp(ik_1 r) + C_2 v_2(z) \exp(ik_2 r)$$

Where C's are constants. Thus at some ranges the field can be zero.

Range dependent acoustic propagation can also be solved with this method.

Normal modes (2): Example of modes from SOFAR environment

Note how nice the envelope follow the sound speed

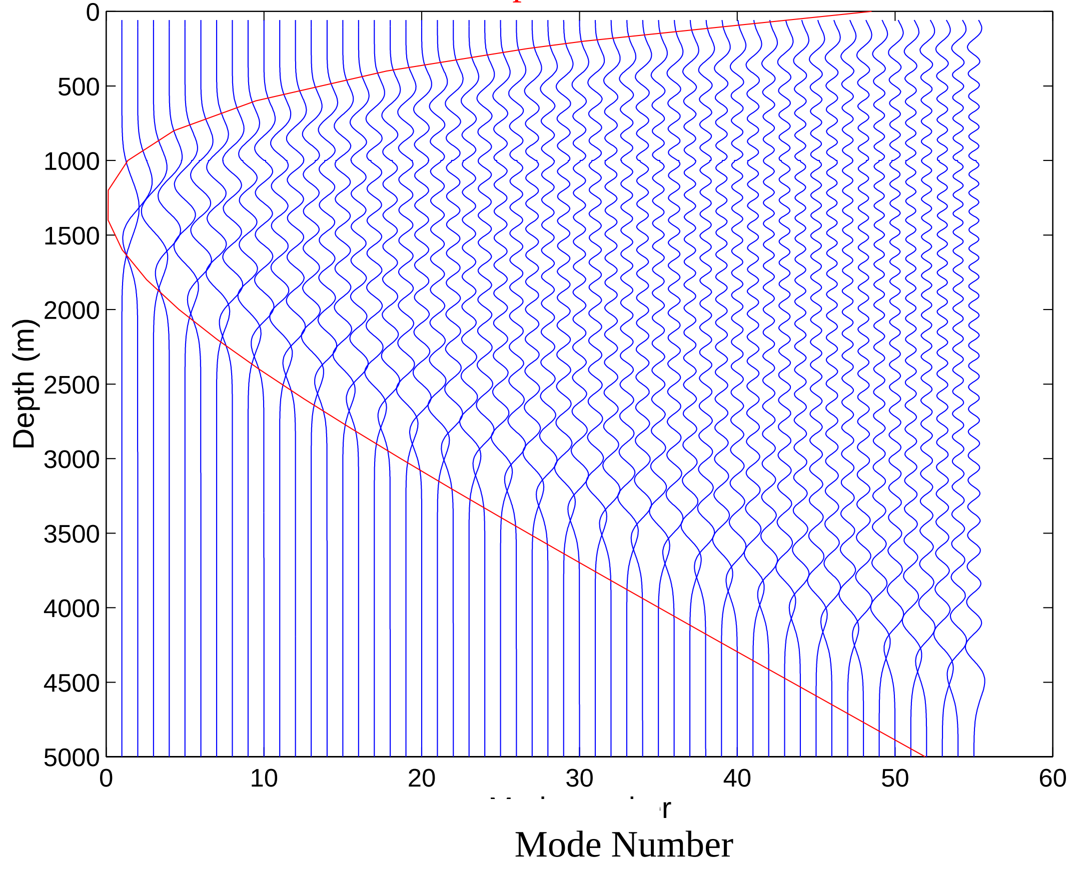

Time series

From the pressure in the frequency domain the time series is obtained by Fourier synthesis

$$p(r, z, t) = \int_{-\infty}^{\infty} p(r, z, \omega) S(\omega) \exp(-i\omega t) d\omega$$

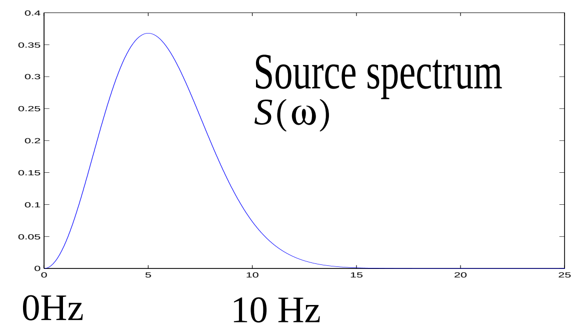

Reduced travel time:

Instead of plotting p(r,z,t) the pressure p(r,z,t-r/v), v is the reduction velocity.
since the ocean sound speed varies little the arrival will be nearly stationary in reduced time.

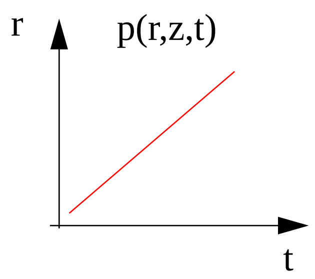

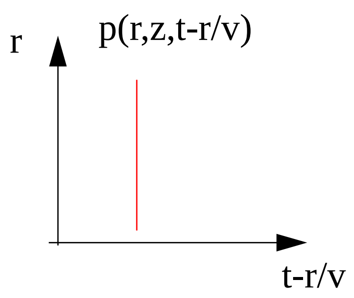

Time series versus depth for SOFAR environment (1)
Two ranges

Based on normal mode theory and Fourier synthesis (wavelet had a center frequency of 10Hz and source depth 1000m).

At range 50 km:

-the bottom reflected energy arrives first.

-The main energy is in upper part of SOFAR channel, it can be understood by looking at ray diagram.

At range 1000 km:

- The main arrival is late.
- “symmetry” around sound axis.

-Main energy close to sound axis.

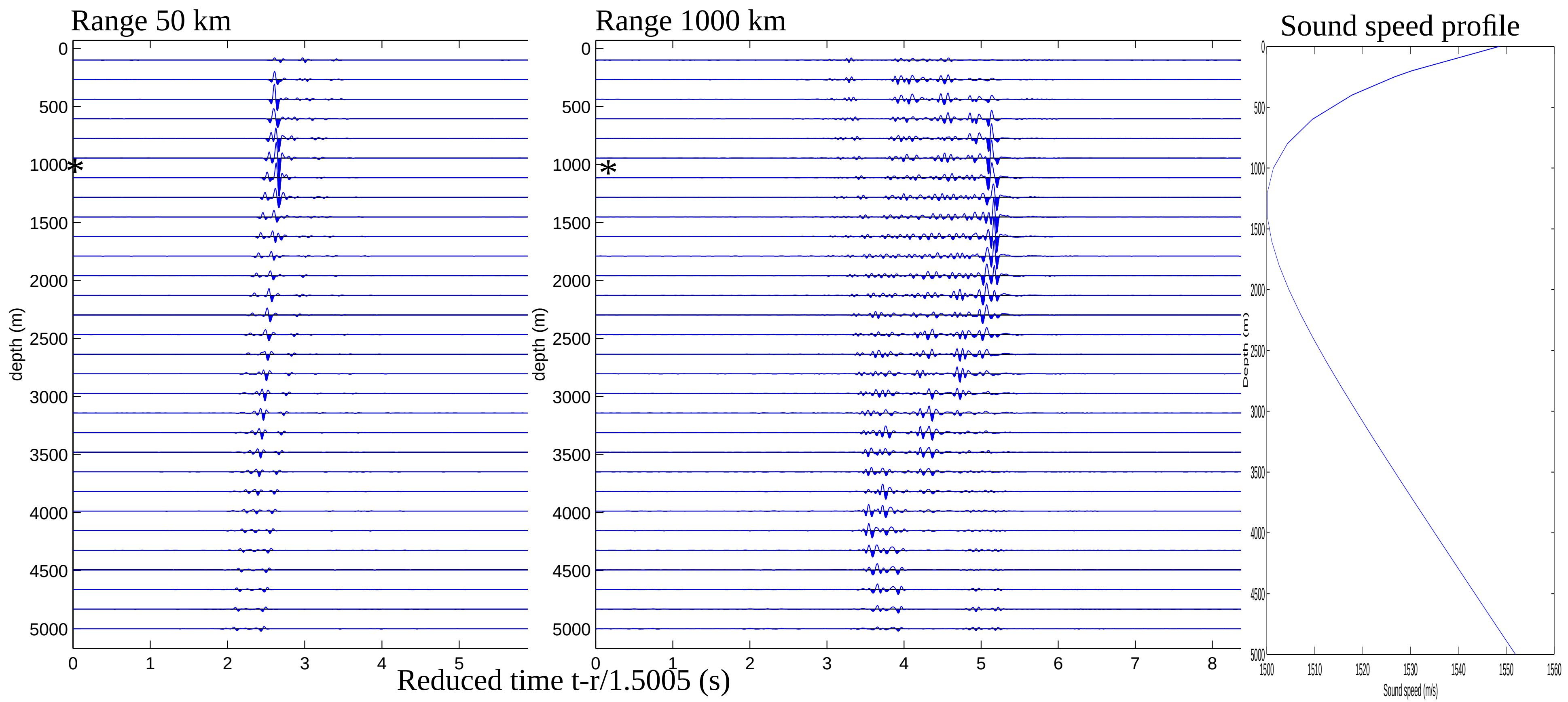

Time series versus depth for SOFAR environment (2)
Two center frequencies, SD=1000 m

Based on normal mode theory and Fourier synthesis (For a range of 1000km and source depth 1000m).

Notice the strong late arrival. It is propagating close to the sound speed axis.

The arrival time and structure are frequency dependent

The higher order modes propagates at steeper angles, has higher phase velocity, arrives earlier and is vertically spread out.

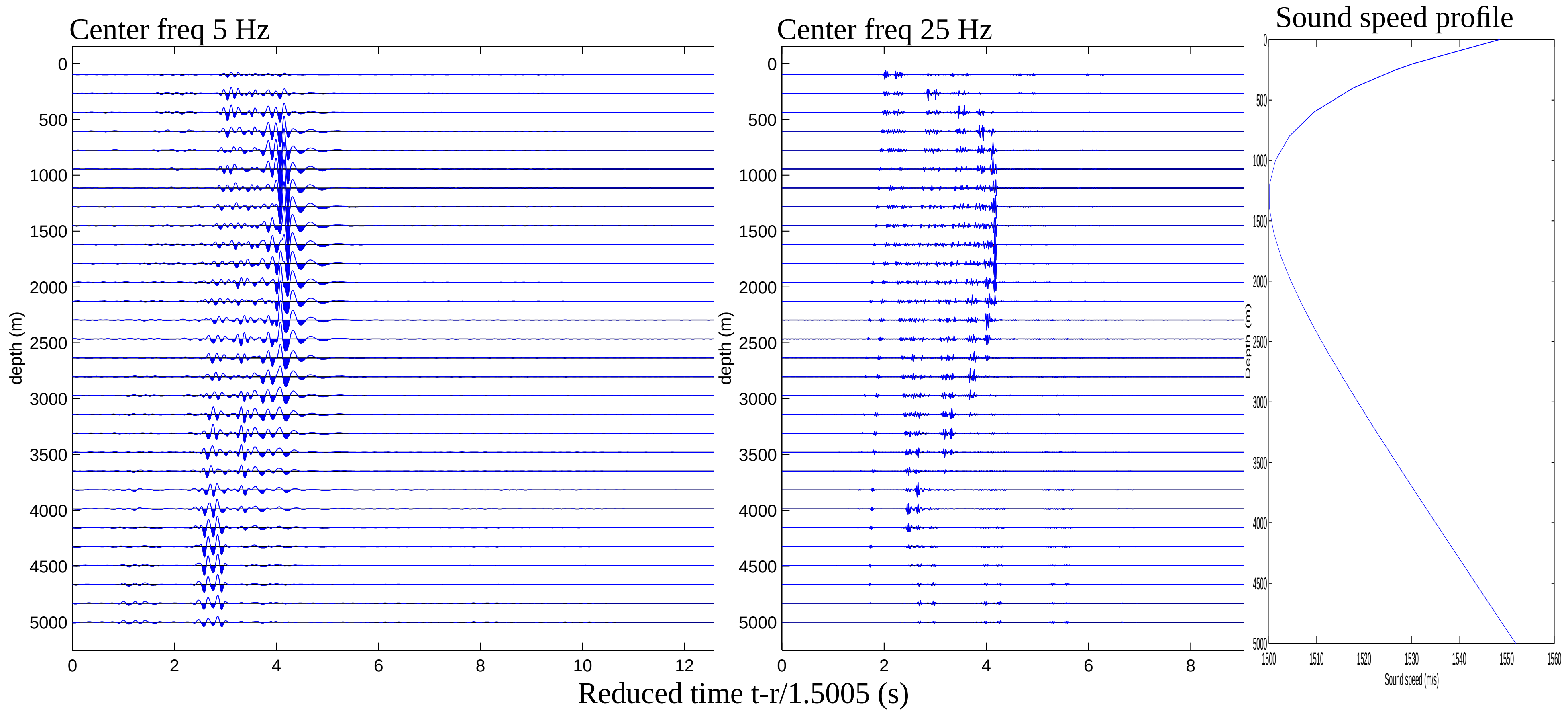

Time series versus depth for SOFAR environment (3)
Two center frequencies, SD=200 m

Based on normal mode theory and Fourier synthesis (For a range of 1000 km and source depth 200 m).

The wave propagates with a higher velocity, the reduction velocity has been increased.
The energy of the arrival is now more spread out in depth.

The arrival time and structure are frequency dependent

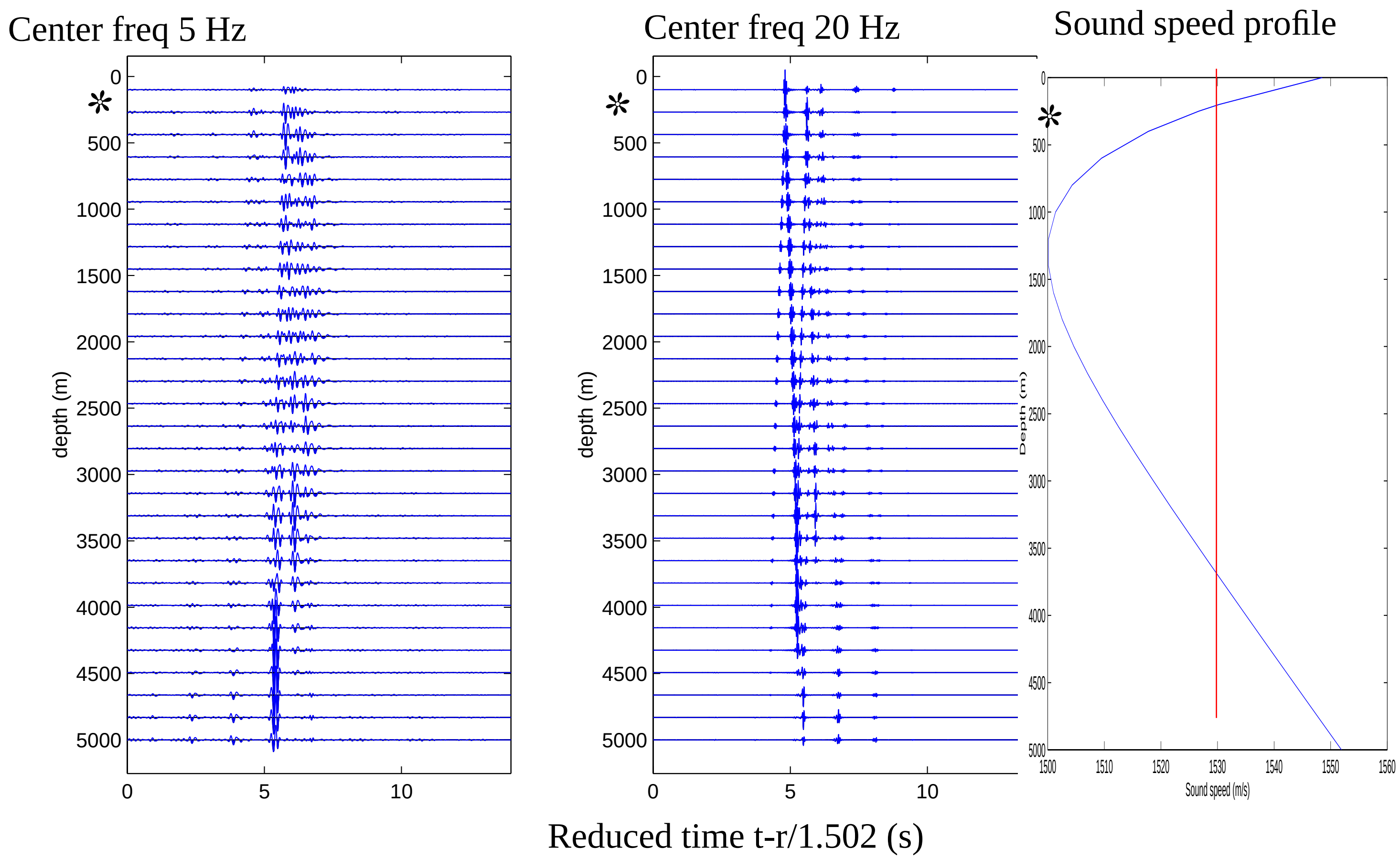

Decibel (dB)

Intensity is the product of pressure and velocity. For an acoustic media

$I = P\,V = P\,(P/\rho c)$

Signal Level based on "energy"

$SL = 10 \log(I/Io)$ [dB re 1μPa]

Signal Level based on "amplitude"

$SL = 20 \log(P/Po)$ [dB re 1μPa]

where $I = P\,(P/\rho c)$
Io and Po are reference intensity and pressure; equal to Po= 1μPa [and $Io = Po\,(Po/\rho c)$].

[For velocity Vo=1nm/s and
$SL = 20 \log(V/Vo)$ [dB re 1nm/s]
This is relevant for T-phase stations, which record velocity.]

Example: SL1=20dB and SL2=60 dB (often the reference unit is neglected).
The difference is 40dB. Using the above formulas 20log(P2/P1)=40.
Thus P2=100*P1

If SL2=80 dB we find P2=1000*P1

Transmission loss:

An acoustic signal travelling through the ocean become distorted due to multipath and various loss mechanisms.

Referenced to the intensity at 1 m from the source

TL= -10 log[I(r,z)/Io]=-20 log[P(r,z)/Po]

Spherical spreading: TL=20log(r)   [dB re 1 m]

Cylindrical spreading: TL=10log(r)   [dB re 1 m]

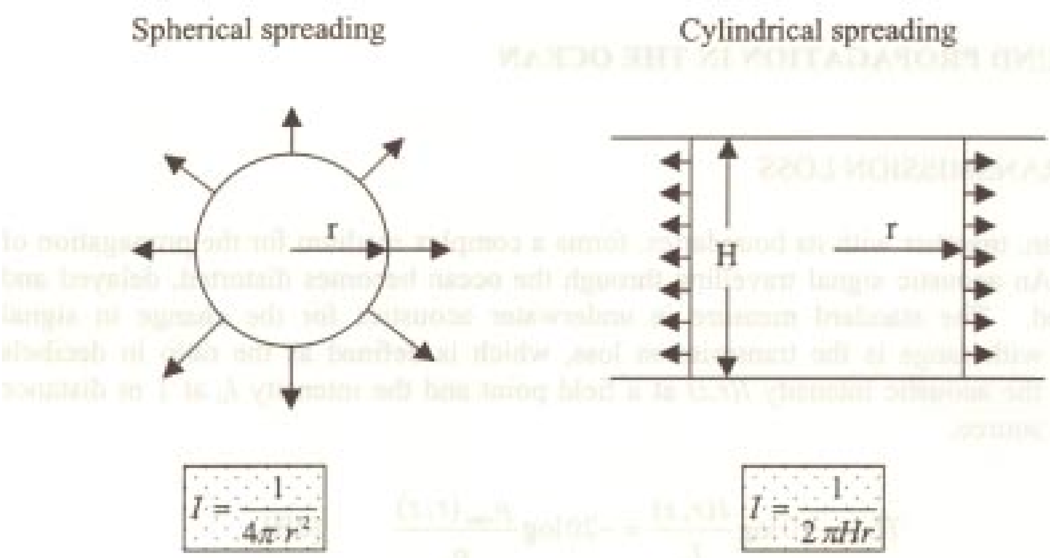

In the ocean waveguide we have cylindrical spreading for r>>D

TL(100 km)   = (1 km spherical) +(remainder cylindrical)= 20log(1000)+10log(100) = 60 dB + 20 dB= 80 dB

TL(10,000 km) = (1 km spherical) +(remainder cylindrical)=20log(1000)+10log(10000) 60 dB + 40 dB= 100 dB

Most seismic waves are spherical attenuated, as they are not propagating in a waveguide.

What is the seismic TL @ 10,000 km?

Seismic TL=(10,000,000 spherical)= 20log(10,000,000)=140 dB

Thus the difference between seismic and hydroacoustic propagation at this range is 40dB---A factor 100.

Attenuation

When sound propagates in the ocean part of the acoustic energy is continuously absorbed, i.e., energy is transformed into heat.
Scattering also causes decay of sound intensity with range.
Attenuation covers both effects.

Based on attenuation it is seen that sound propagation in the ocean is optimal at about 5-50 Hz.

Seismic attenuation is much larger and a typical propagation frequency is about 1 Hz (depending on range)

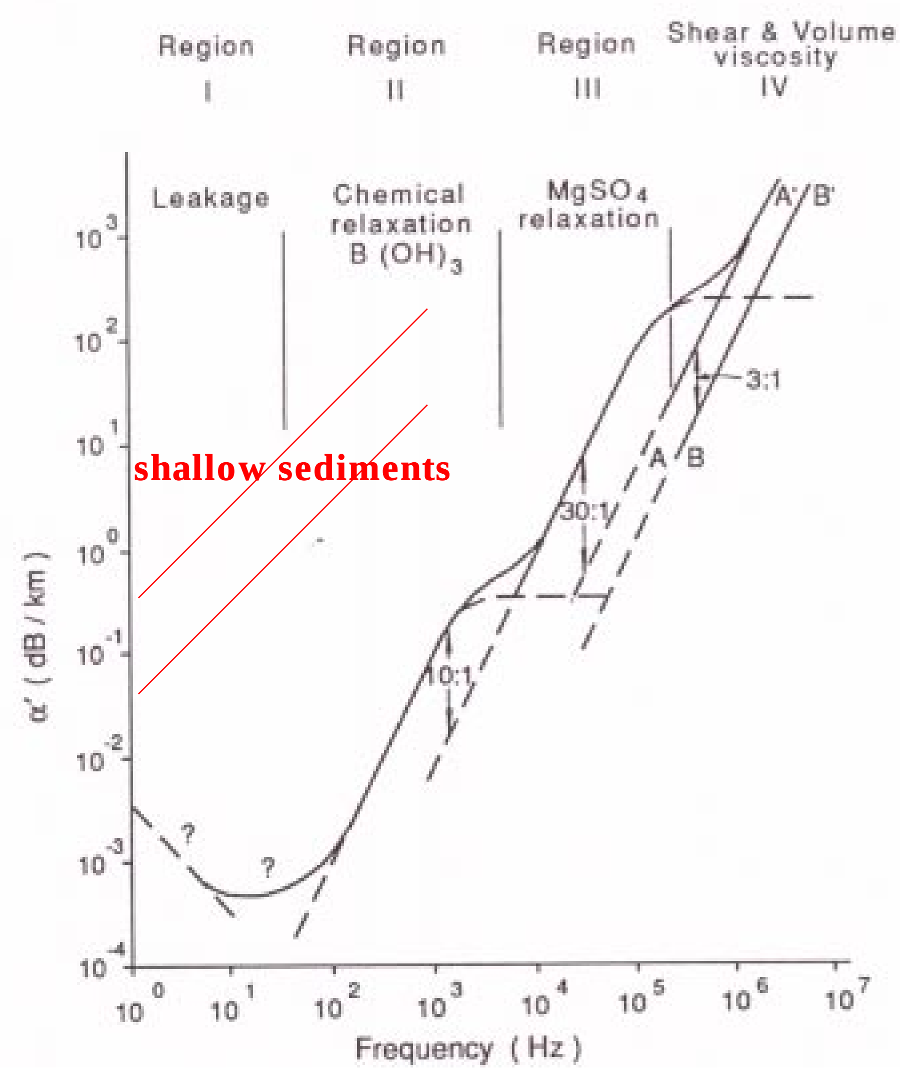

Propagation past a seamount in the Northeast Pacific

Varying bathymetry has strong influence on range-dependent propagation

Only shallow beams propagate past this seamount.

Rays at steeper angles will suffer loss due to interaction with the seamount.

The seamount has caused a propagation loss of about 20-30 dB.

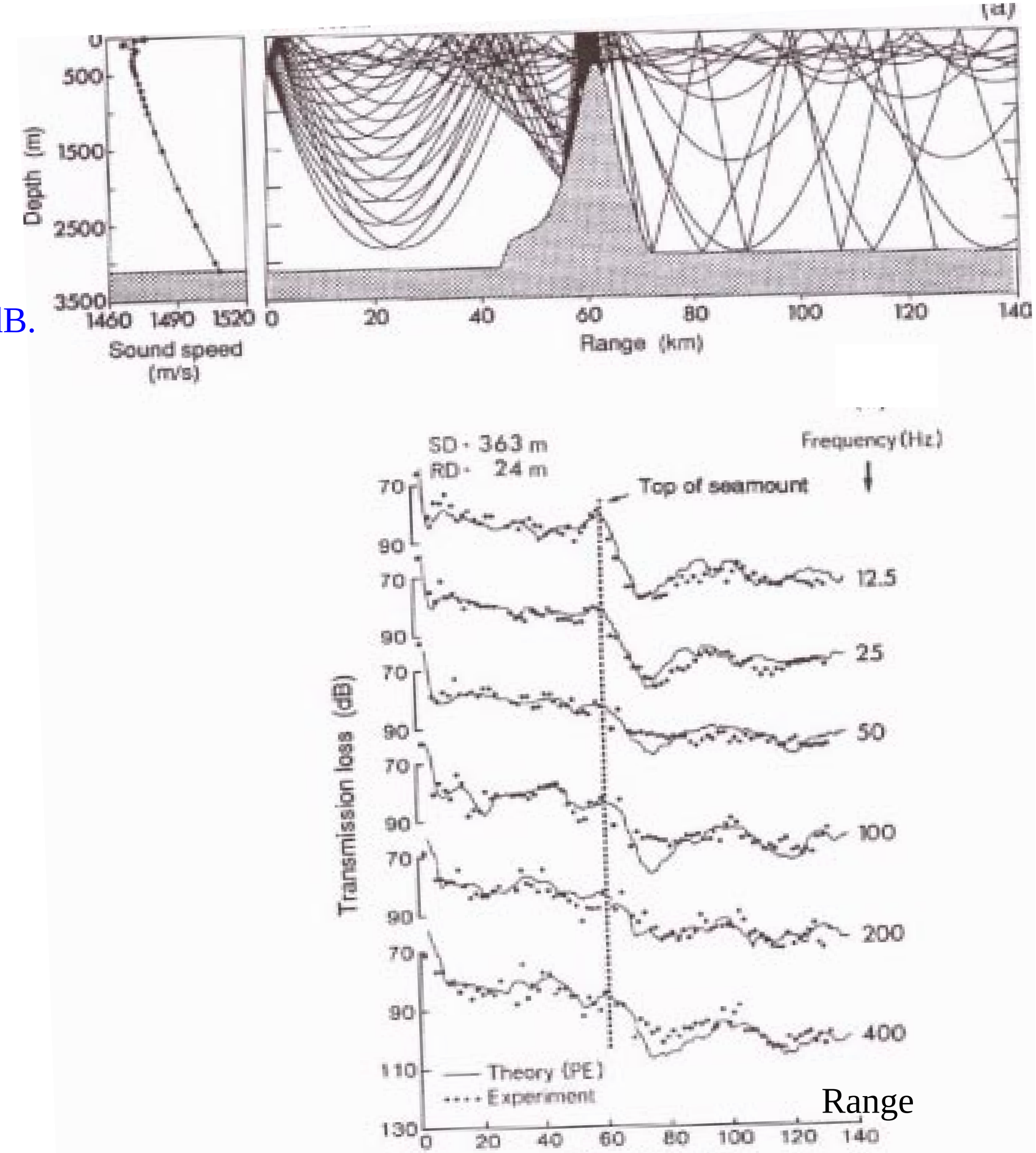

Transmission Loss from WK30

Based on a Parabolic Equation, PE-model.
A set sound speed profile and bathymetry is extracted from databases.

The Transmission loss is not yet used in the automatic processing
(The transmission loss could be used to determine the pressure at a given range).

Sound speed profiles:

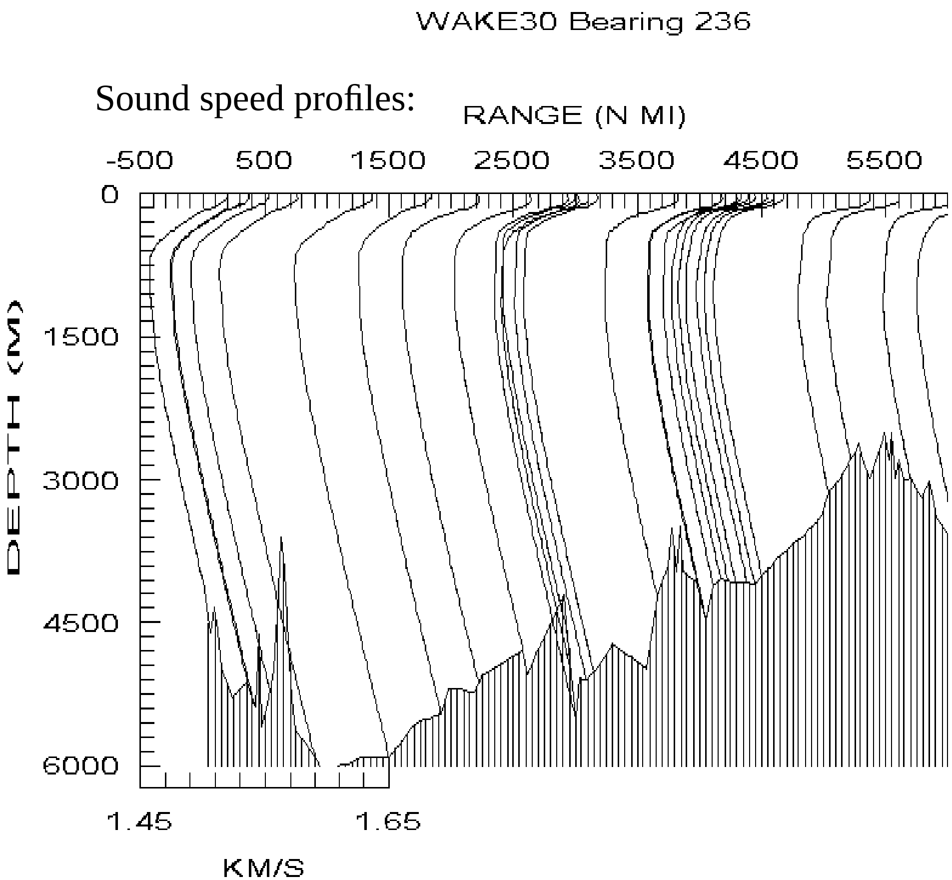

Transmission loss versus range and depth.

(Red is small and blue large TL)

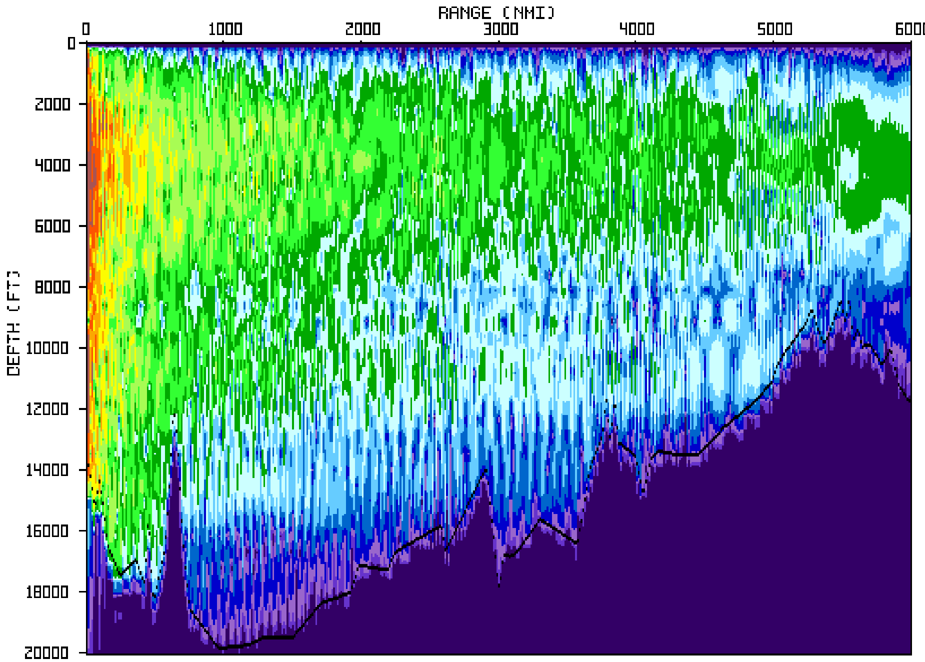

Perth-Bermuda, 1960 (Heaney et al, JASA 1991)

300lb charges were used.
Modeled by adiabatic mode theory in vertical and ray theory in the horizontal.
Horizontal refraction: rays bend towards slower (colder) water, but refraction at Heard Island bend north.

Modelling shows 30 s difference between geodesic and great circle path

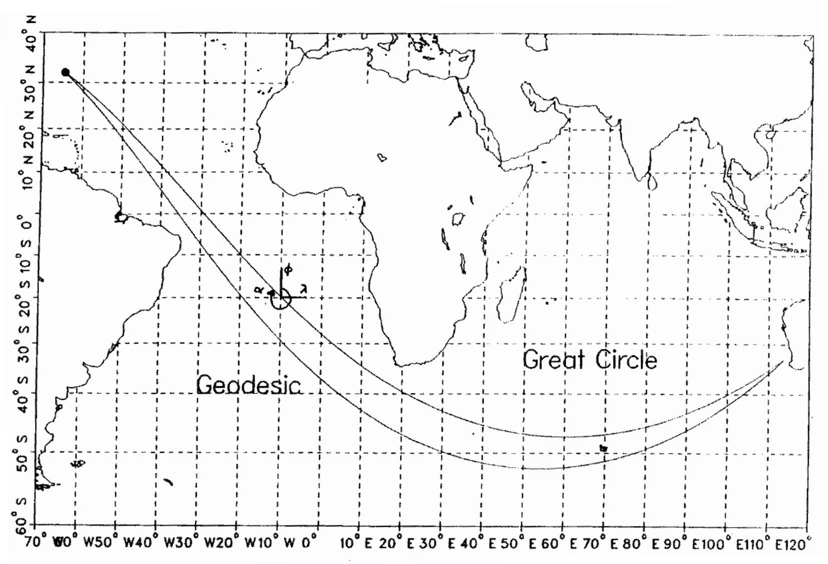

Horizontal refraction:
the acoustics paths is repelled by
- high sound speed (warm water)
- shallow depths
- high latitudes

Perth-Bermuda, 1960 (Heaney et al, JASA 1991)

Modes have different phase velocity and thus have different horizontal refracted.

Based on raytracing in the horizontal plane, the arrivals were found for mode 1, other paths was blocked.

The southern path travel trough colder and slower water and therefore this mode later than ones from the northern paths.

Mode 1 propagation path

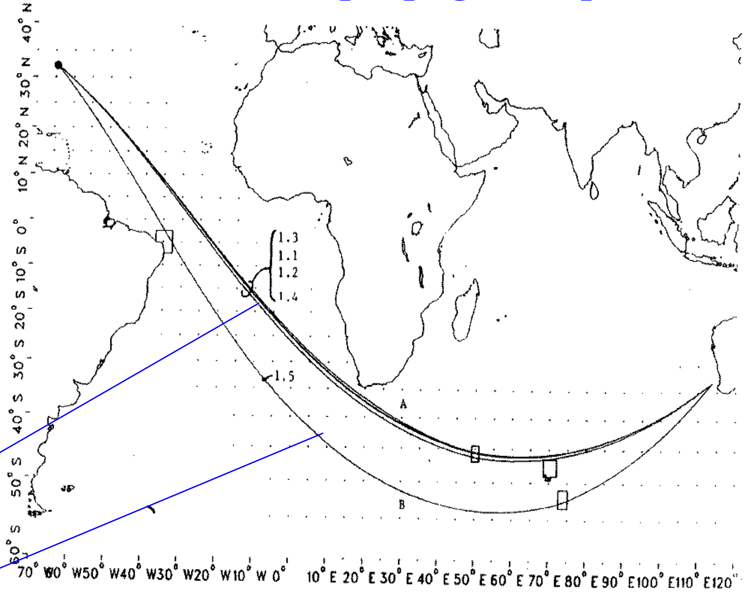

This is a new shot

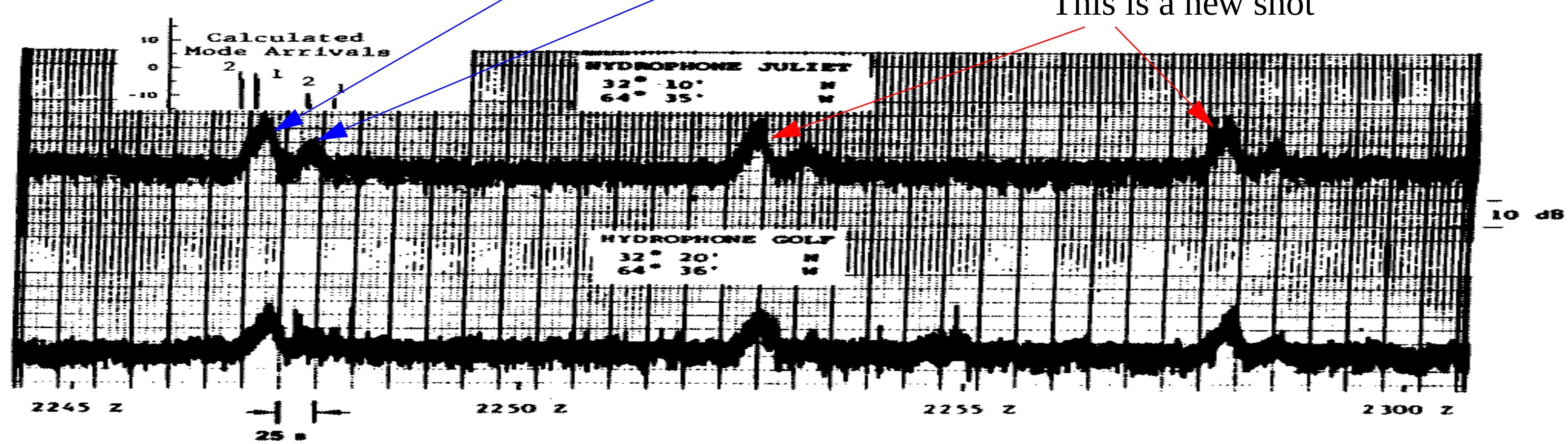

Heard Island feasibility test (1991)

The oceans can be used to monitor global warming.
By recording the change in traveltime the integrated effect of change in temperature can be estimated.
The Heard Island feasibility test was designed to test that a signal can be received across several oceans.
The passage between Australia and New Zealand was partly blocked, as Samoa did not receive the signal,
and Withney (and Monterey) received it south of New Zealand.

The figure shows the paths without taking horizontal refraction into account.
When considering propagation across oceans it must be taken into account. It is complicated!

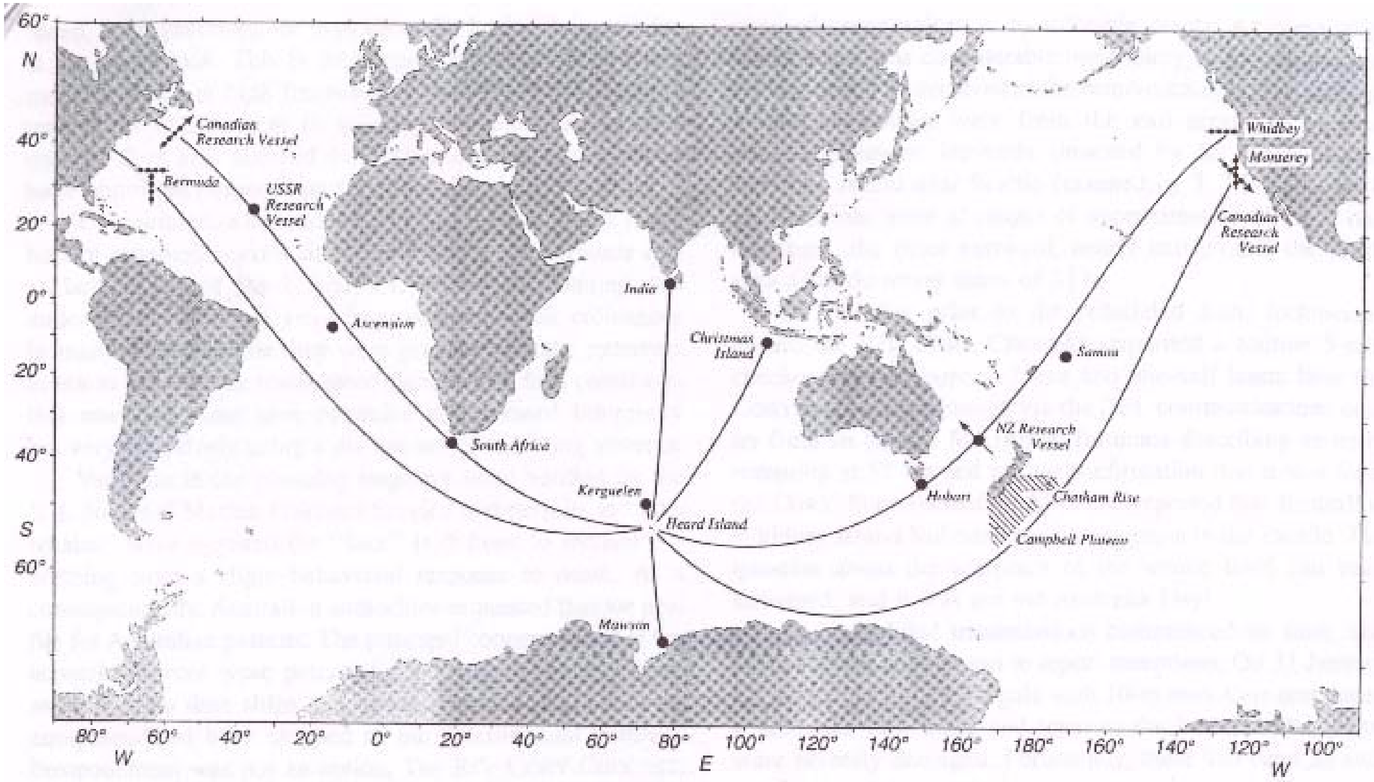

Bubble pulse (1)

Shock wave and buble pulses from an explosion

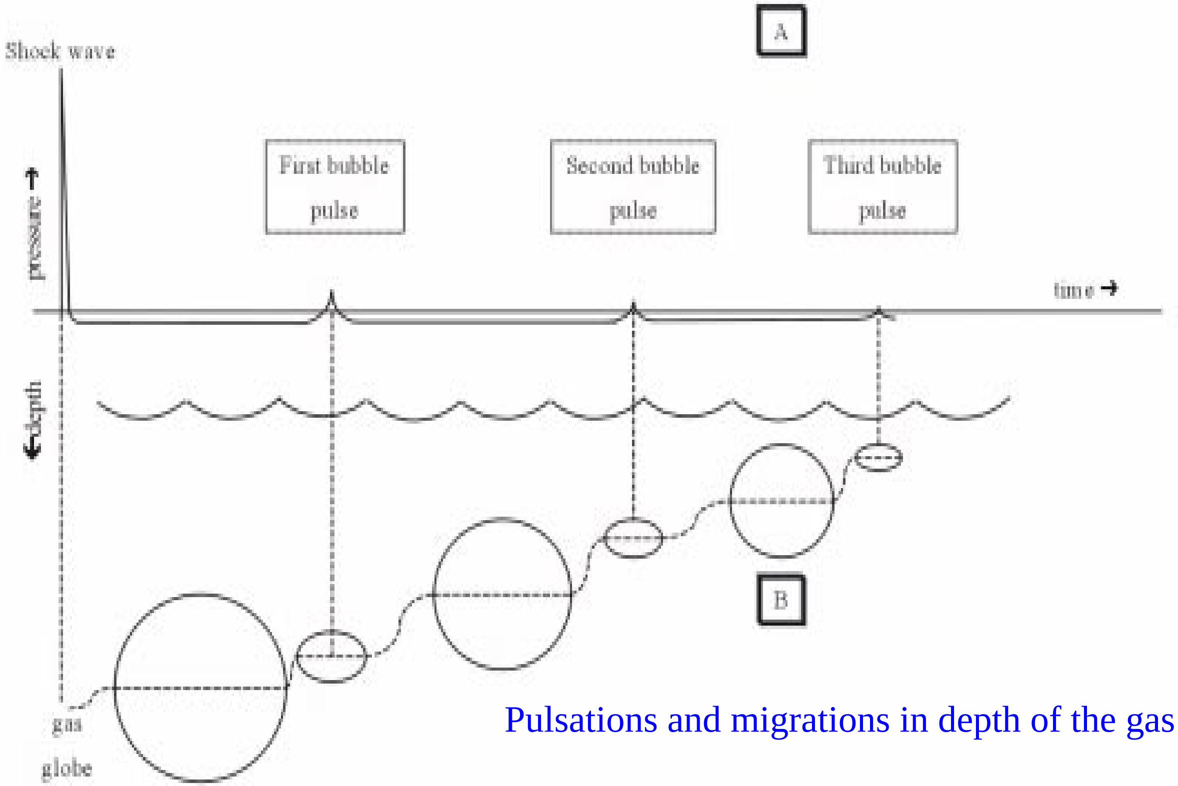

Pulsations and migrations in depth of the gas bubble.

T-phase and H-phase

H-phase stems from an in-water source, T-phase is of terrestial origin

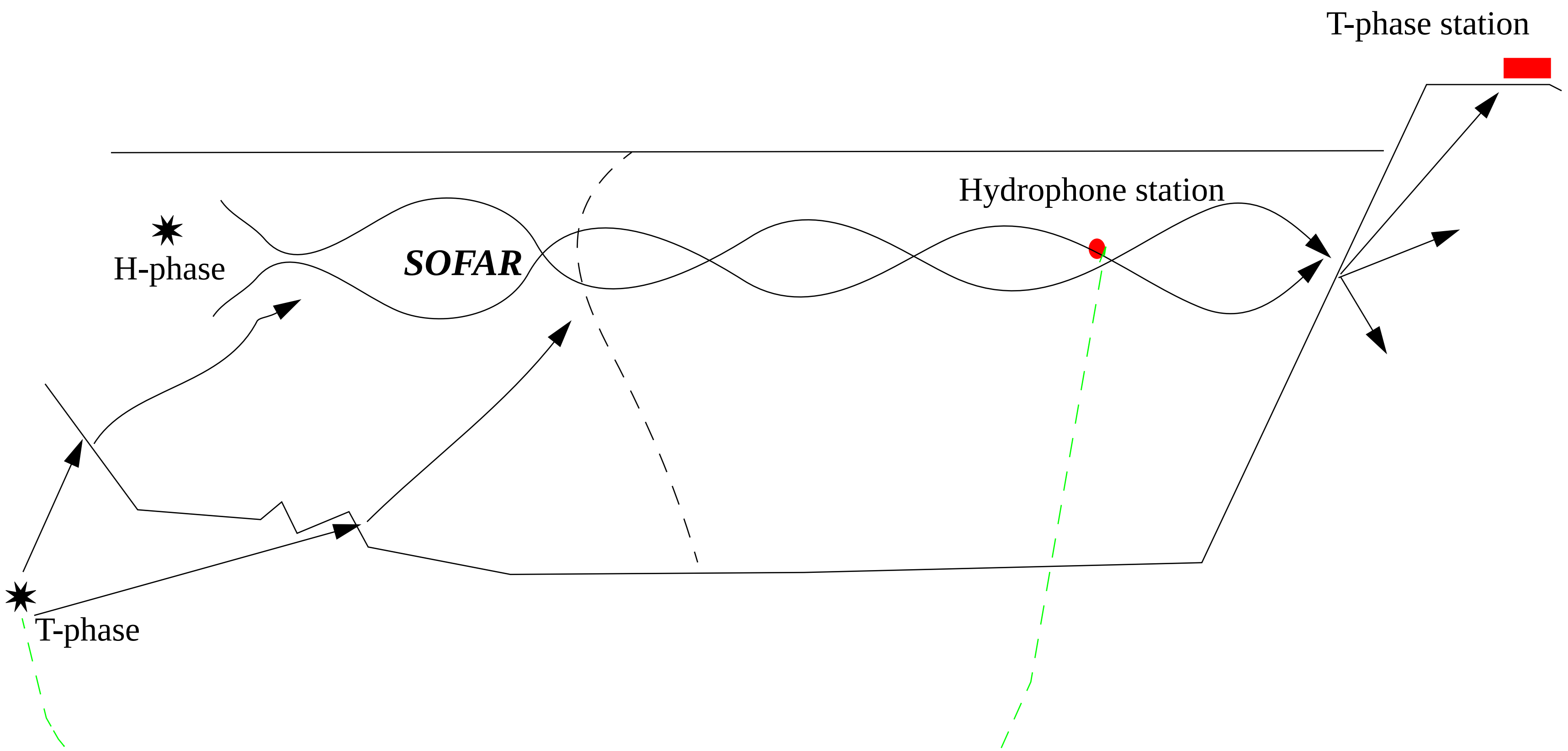

Hydrophone stations consist of one hydrophone (records pressure) placed in the SOFAR channel.
Future design calls for 3 hydrophones placed 1.5 km apart.

T-phase stations record vertical velocity. Future design will record 3-component velocities.
The transmission loss from the SOFAR channel to the T-phase station is probably 20-40dB.
T-phase stations are much cheaper and are still on research level.

Received signal:

The received signal can be expressed as a product of four factors

$$R(t)=T(t) * O(t) * C(t) * S(t)$$

where

- S(t) is source function. Earthquake has longer duration than an explosion.
- C(t) is the coupling from seismic source to ocean channel. High frequencies attenuated.
- O(t) is the ocean propagation, multipath effects, little attenuation
- T(t) is the propagation from ocean to T-phase station. High frequencies attenuated.

C(t) and T(t) is not yet well understood.

Features of H and T phases

H-phase

- Generated by impulsive in-water events (explosion, volcano)
- Travel long distance though SOFAR channel
- Can be recorded on T-phase stations (but H-phases at VIB is picked by analysts)
- Impulsive short duration (multi-pathing can increase duration)
- Energy at both low and high frequencies (2-100 Hz)
- May have bubble pulse (a bubble pulse is due to an explosion)

T-phases:

- Generated by solid earth sources (explosion, earthquake)
- Converted from elastic waves to hydroacoustic waves at seabottom
- Travel long distance though SOFAR channel
- Little energy above 30 Hz
- Long duration, often longer than a minute.
- Peak frequency below 10 Hz

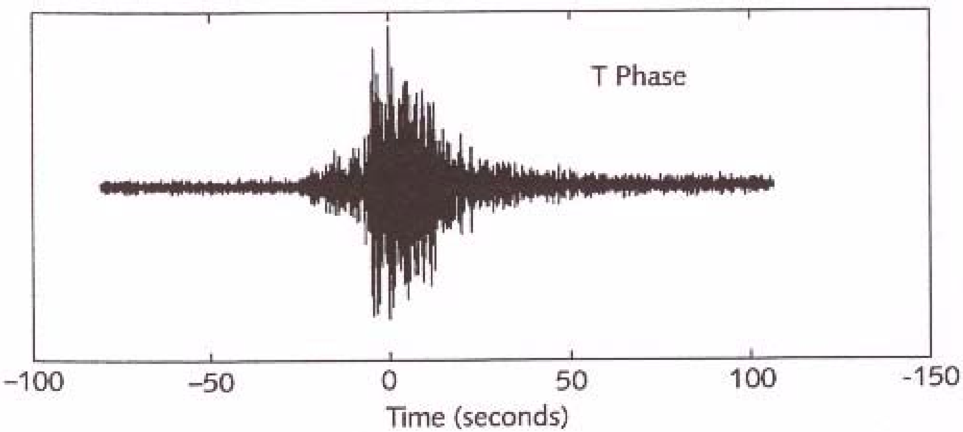

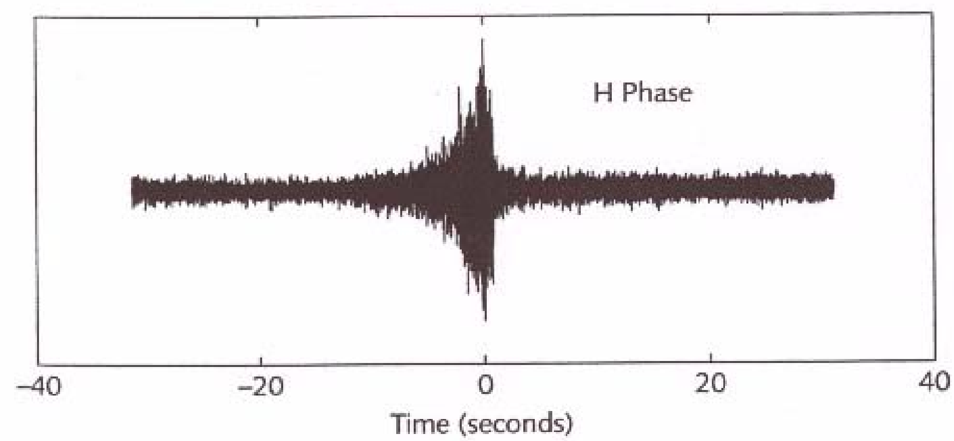

The 5-10 s build-up of the phase is typical of long range waveguide propagation

Wave equation

$$\frac{1}{c^2(x,y,z,t)}\frac{d^2}{dt^2}p(x,y,z,t)+\nabla p(x,y,z,t) = S(x,y,z,t)$$

where p(x,y,z,t) is the pressure and c(x,y,z) is the sound speed and S is the source function (density is constant, no shear).
Introducing the Fourier transform

$$p(t) = \int_{-\infty}^{\infty} p(\omega)\exp(-i\omega t)dt$$

We obtain the Helmholtz equation

$$\left[\frac{\omega^2}{c^2}+\nabla\right]p(\omega,r,z) = \frac{\delta(r)\delta(z-z_o)}{2\pi r}S(\omega)$$

where we assume radial symmetry and a point source at range r=0. $k = \frac{\omega}{c} = \omega s$ is the wavenumber and the slowness $s = \frac{1}{c}$.

In hydroacoustics it advantageous to solve the problem in frequency domain and then apply a Fourier transform to obtain the time domain solution. The many bounces and the weakly range dependence makes the Fourier approach advantageous.
One exception to this is the investigation of acoustic coupling from the ocean to a T-phase station. Here a direct time domain method would be advantageous, as e.g. the Finite Difference method (FD).

Classification of Propagation models

Wave equation

High frequency approximation
Ray Theory

Range independent
Wavenumber integration
Normal modes

Weakly range dependence
Adiabatic modes

Range dependence
Coupled modes
Coupled wavenumber integration
Parabolic equation

Strong range dependence
Finite difference
Finite elements
Boundary elements
Hybrid methods

More CPU-time

Usually in ocean acoustics models in the three middle boxes are used

Fangataufa, 23:30 1 Oct. 1995

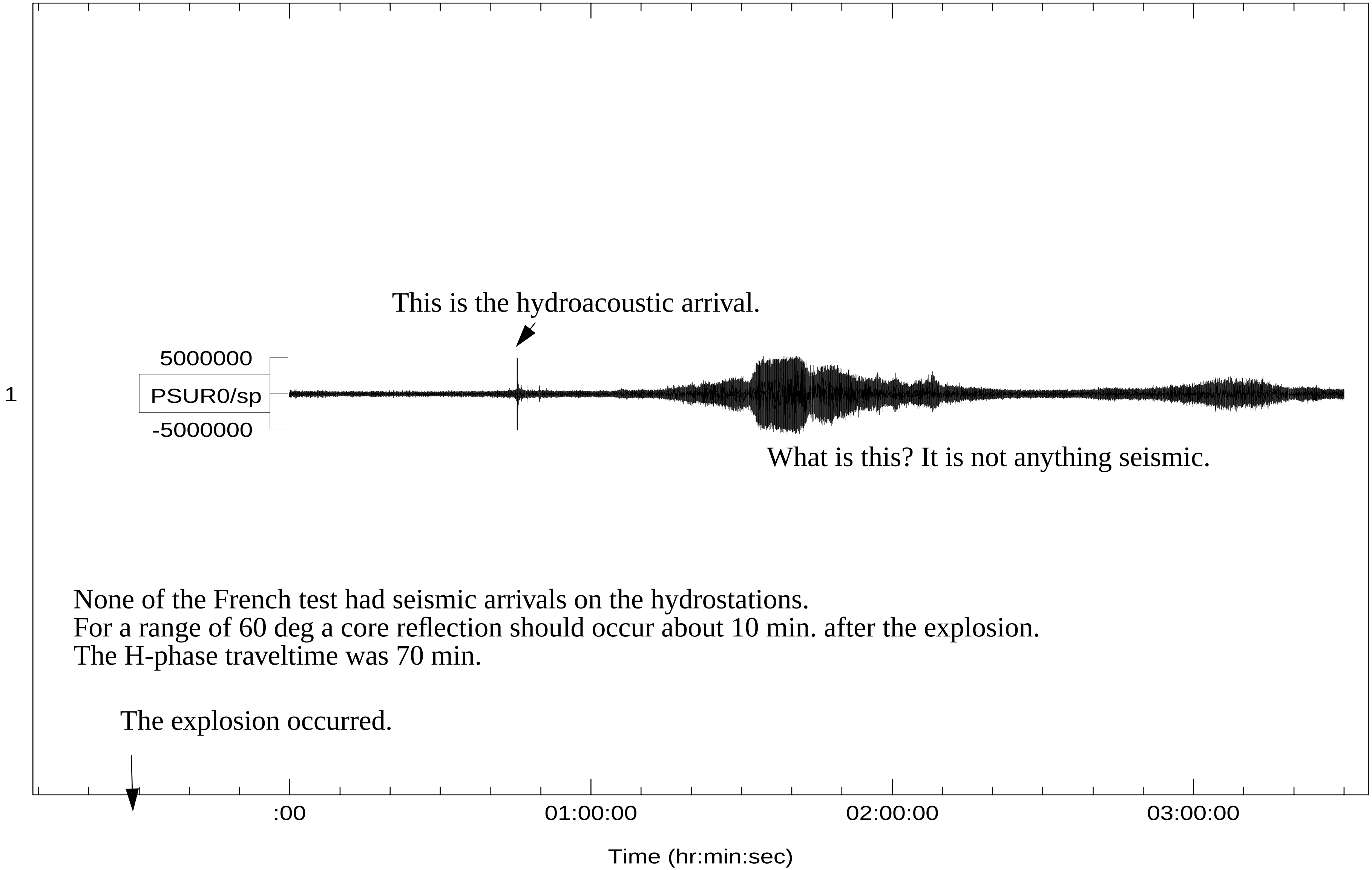

None of the French test had seismic arrivals on the hydrostations.
For a range of 60 deg a core reflection should occur about 10 min. after the explosion.
The H-phase traveltime was 70 min.

Fangataufa, 23:30 1 Oct. 1995- Spectrograms

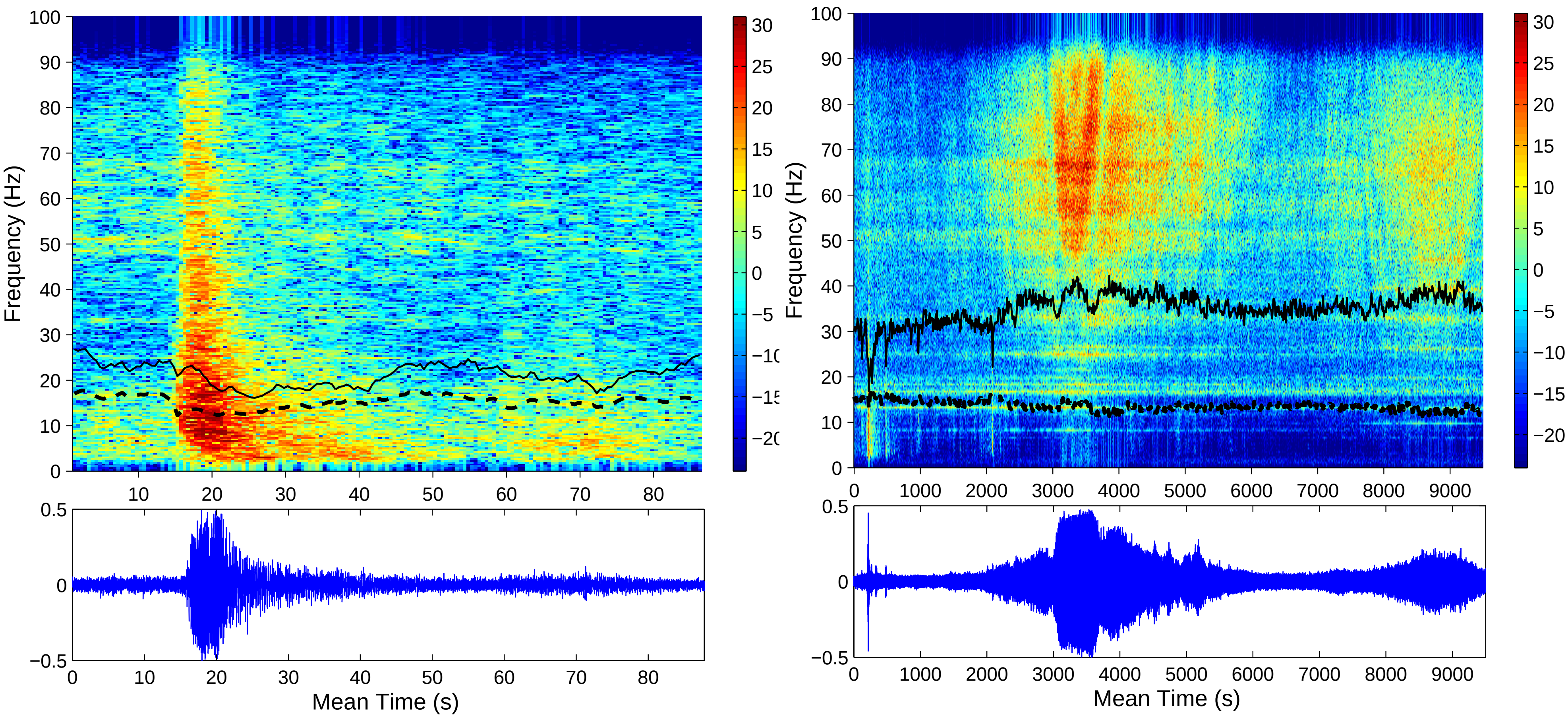

The spectrogram for the explosion shows high frequency contents for the whole frequency range.
The noise arrival is not clipped-- that can be seen by zooming in on the timeseries.
The long duration and the high frequency content makes it clear that it is not a real ocean or seismic arrival.

The solid line shows the average frequency and the dashed line the standard deviation.

PSUR time series of event on September 5, 1995 at Mururoa

Time series recorded at Point Sur, filtered into overlapping one-octave pass bands from 1-2 Hz to 24-48 Hz.

For this explosion energy at the higher frequencies arrives earlier than the low frequencies.

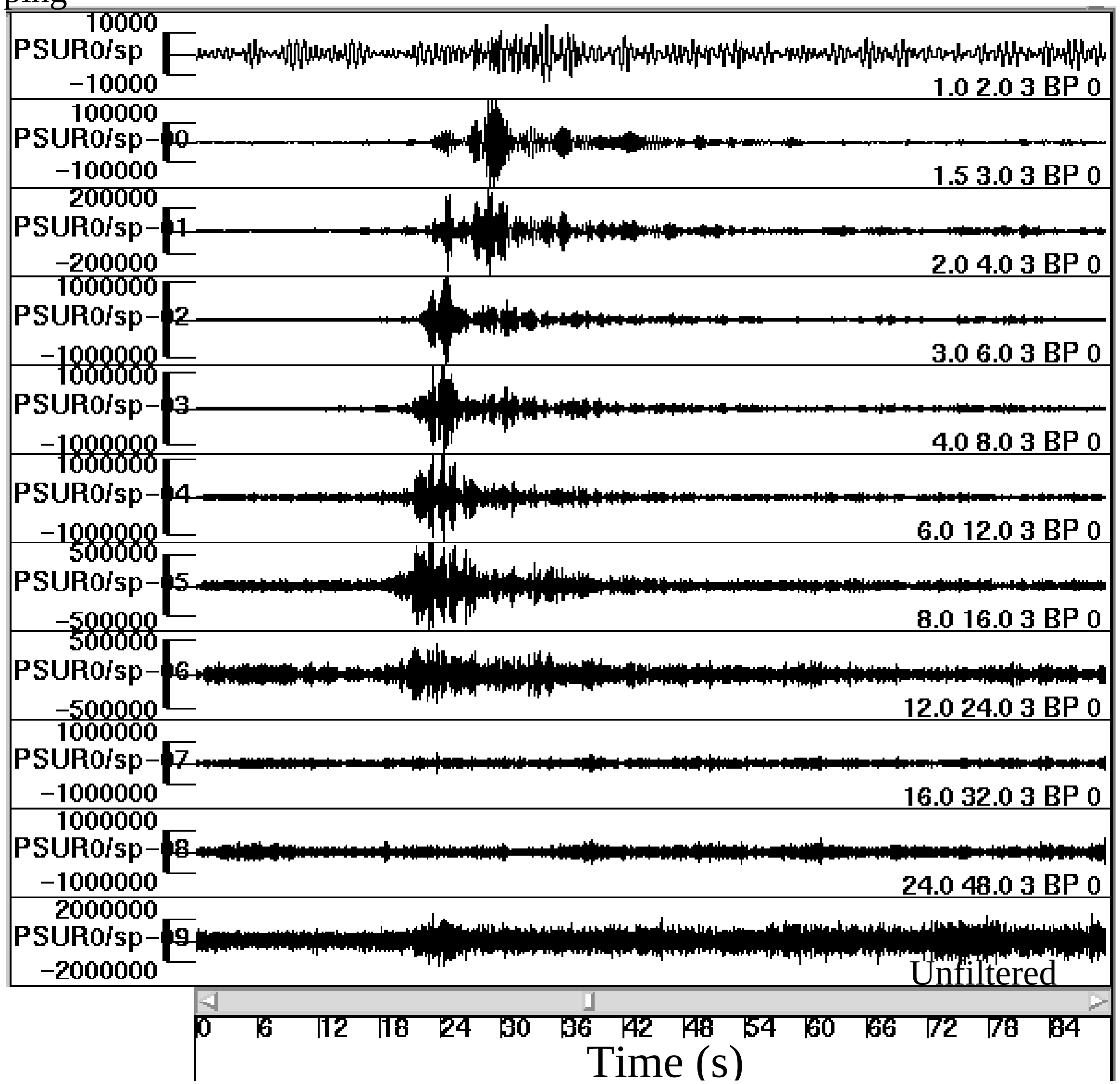

Event on October 1, 1995 at Fangataufa

Time series recorded at Point Sur, filtered into overlapping one-octave pass bands from 1-2 Hz to 24-48 Hz.

For this explosion energy at the higher freq. arrives slightly earlier than the low frequencies.

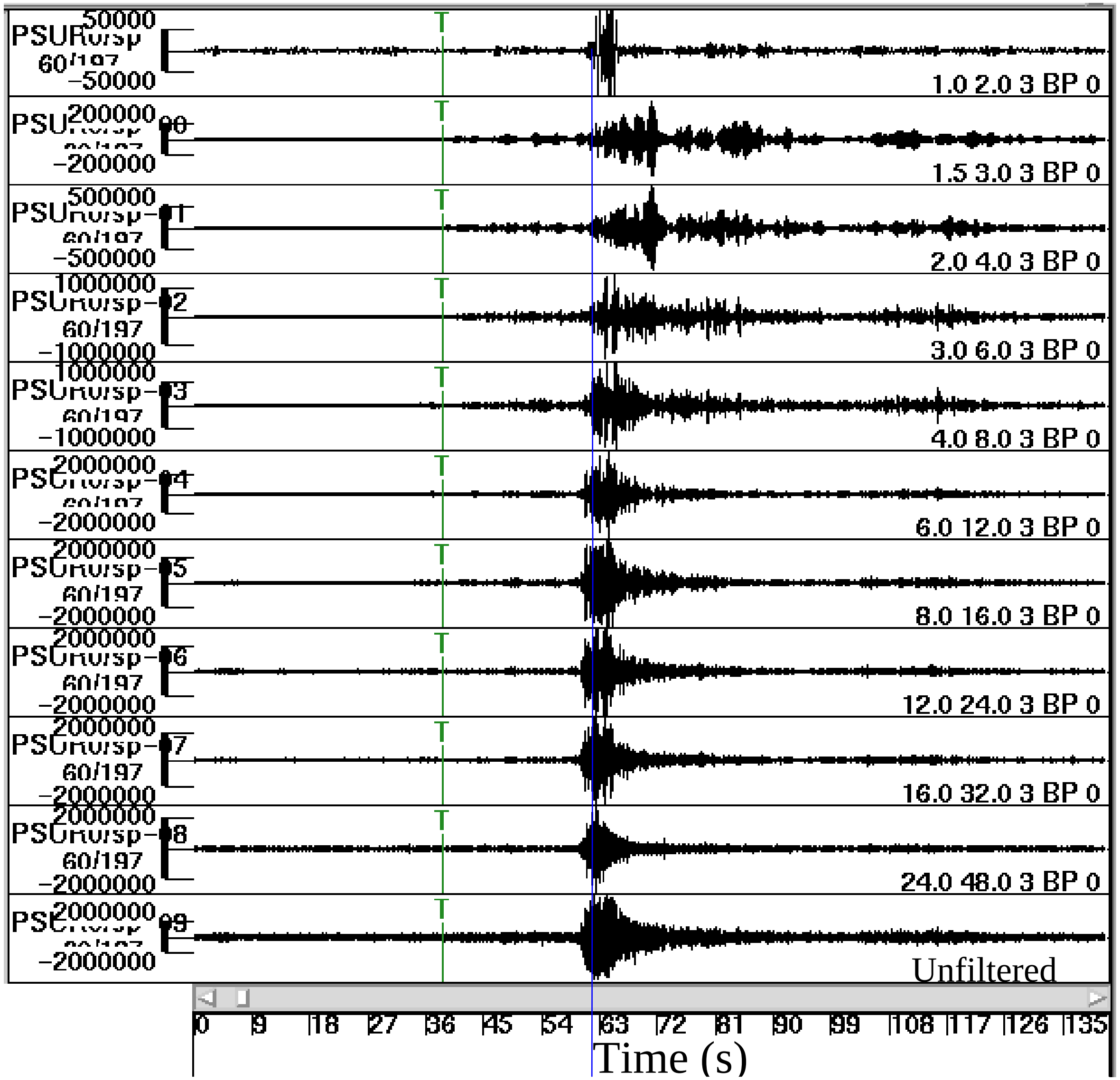

Event on October 27, 1995 at Mururoa

Time series recorded at Point Sur, filtered into overlapping one-octave pass bands from 1-2 Hz to 24-48 Hz.

For this explosion energy at the mid-freq. arrives slightly earlier than the lower or higher frequencies.

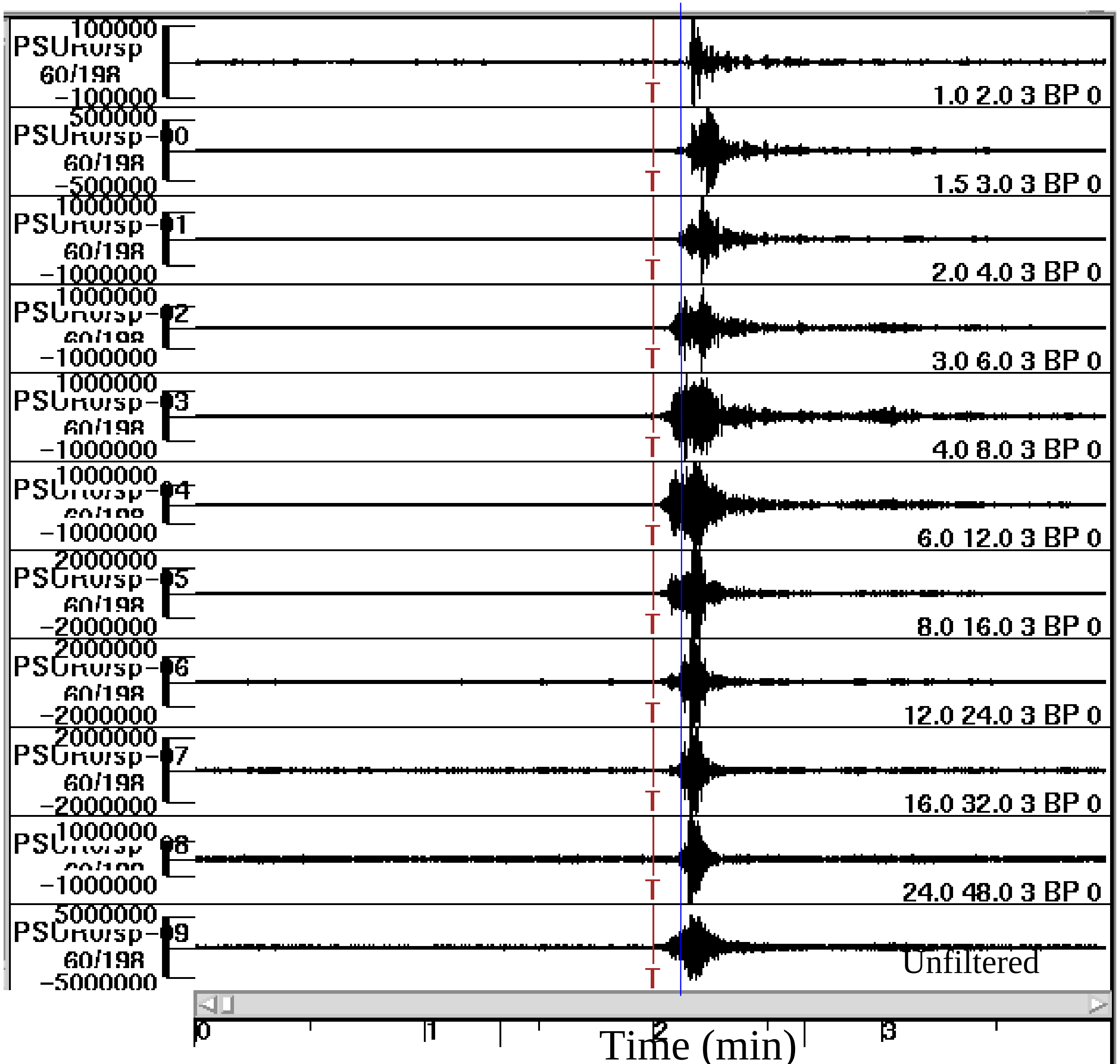

Spectra of French Atoll explosions at PSUR

Hydroacoustic explosions should have high frequency energy, the French Atoll explosions do not always have it, as they are partly underground.

The Fangataufa explosion has lot of energy in the whole spectrum, whereas the Mururoa only has little energy above 30Hz

Compare the spectra energy with the energy in the timeseries on previous slides

Event on September 5, 1995 at Mururoa

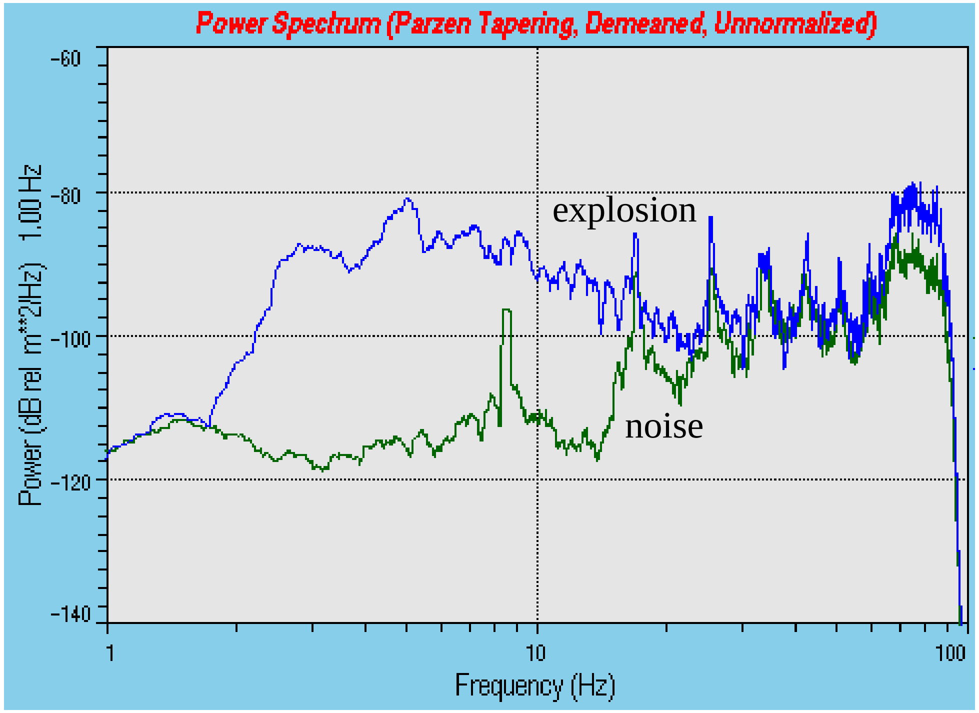

Event on October 1, 1995 at Fangataufa

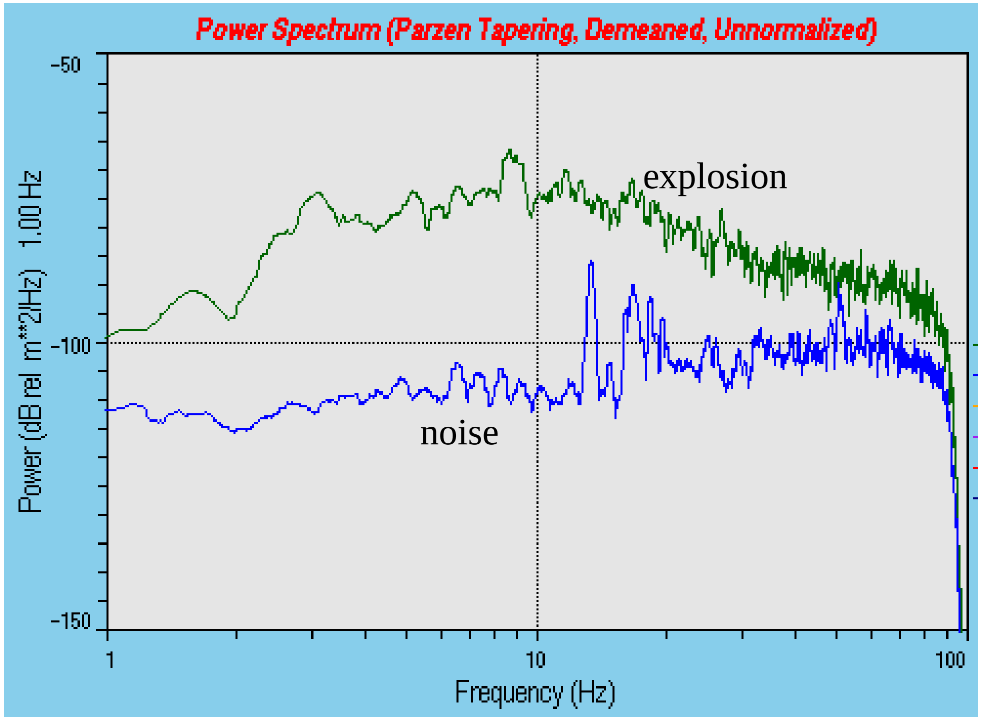

French atoll explosions: WK30 and PSUR

Bandpass filter 3-6 Hz

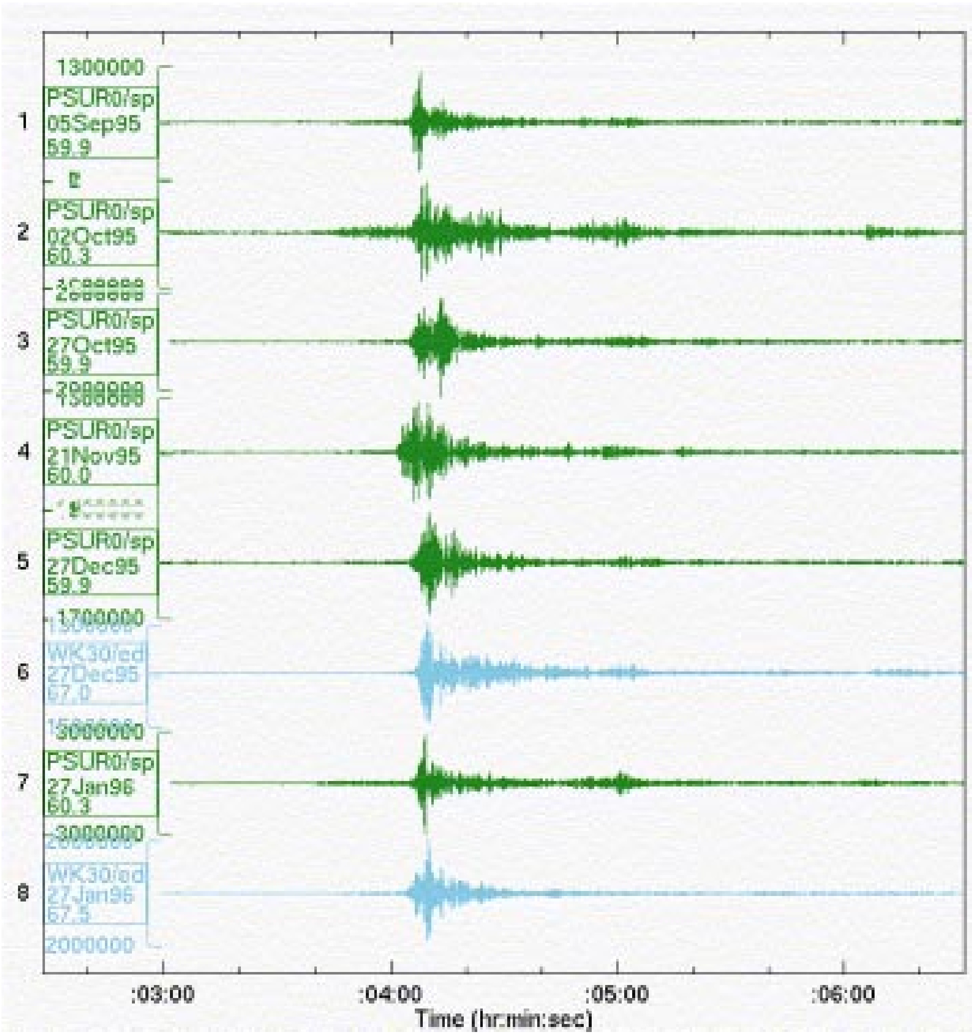

Bandpass filter 32-64 Hz

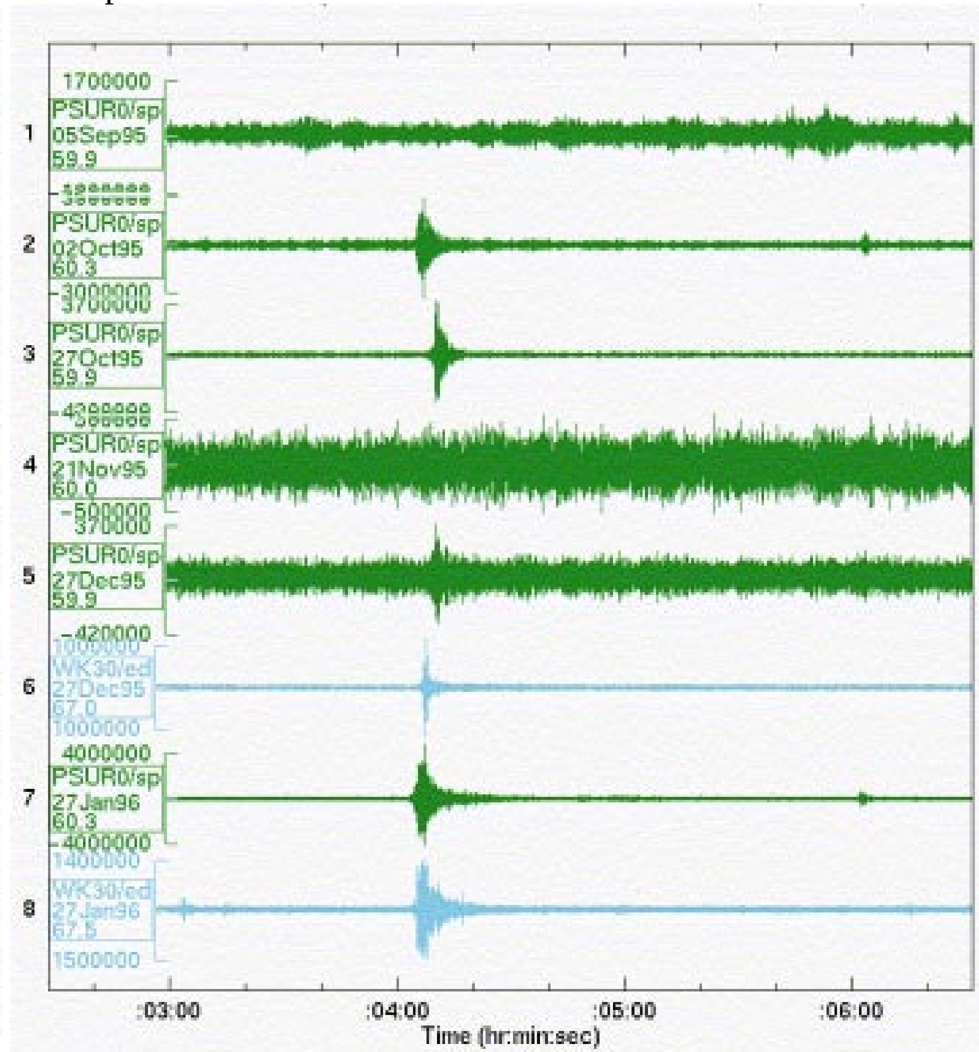

An important criteria for detecting H-phases is the ratio of energy in the two bands.
Not all the French Atoll explosions have high frequency energy.

French atoll explosions: spectra at WK30

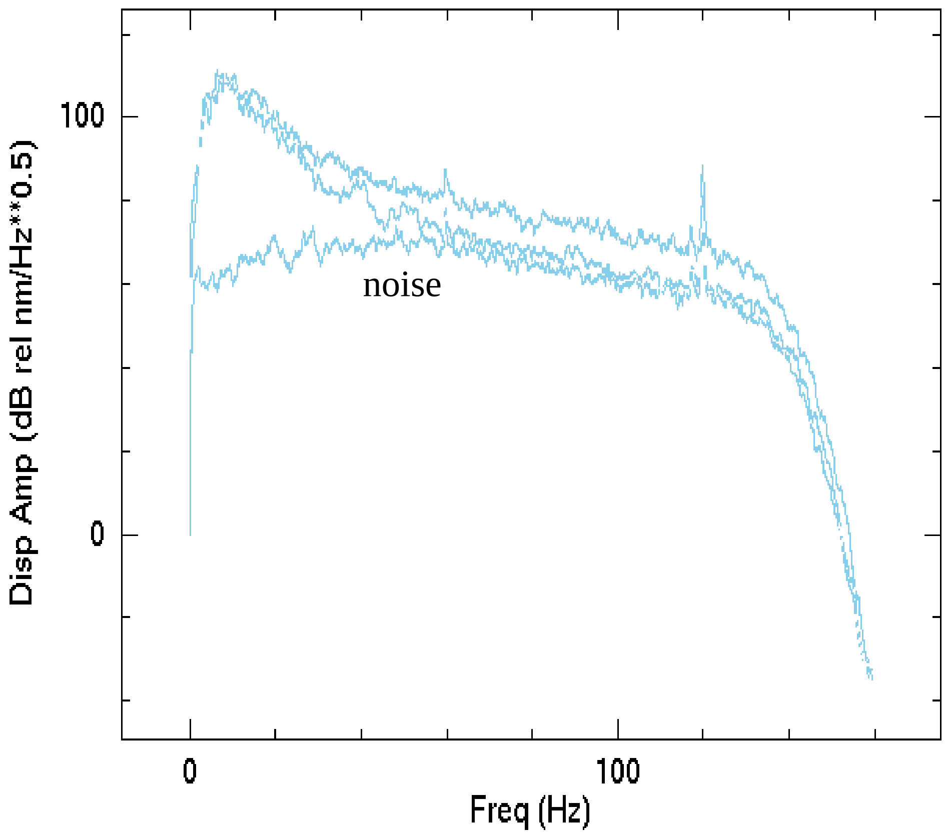

H-phases have usually energy in the spectrum up to 80 Hz. Again not all the Atoll explosions detected this,
The propagation though the solid earth attenuates the higher frequencies more than the lower.

Chase21 explosion: ASC

Chase21 was a naval ship that was exploded off Bermuda June 1970.

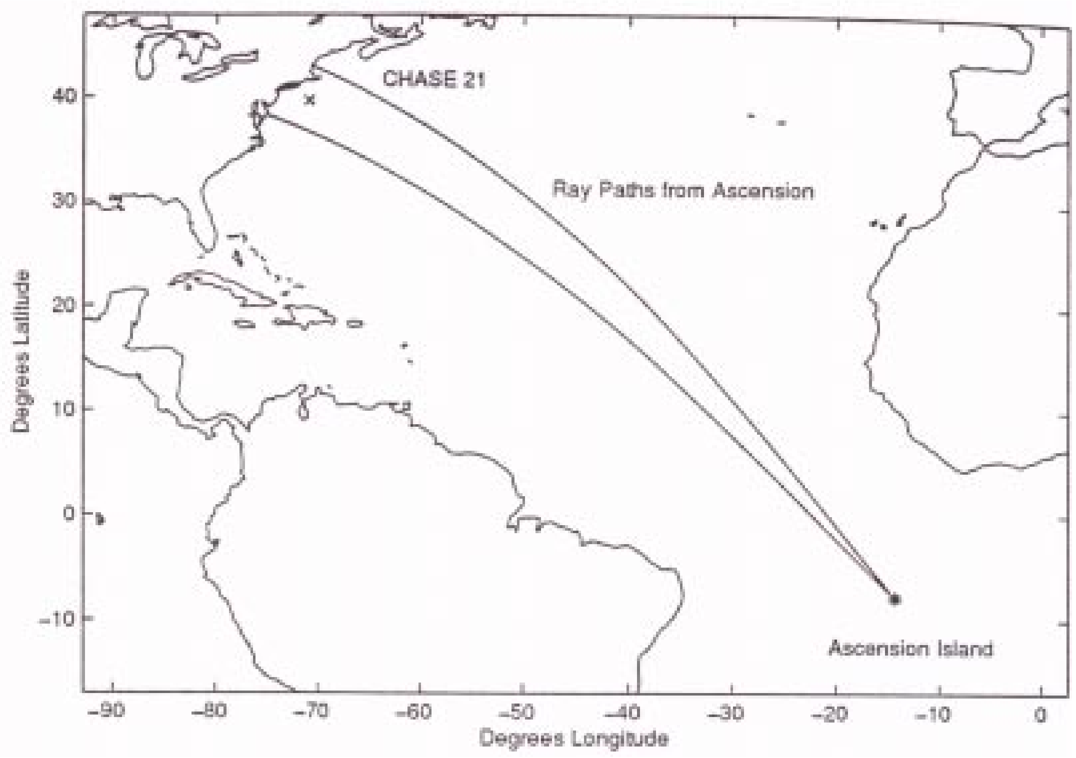

Geometry of Ascension Island hydrostations

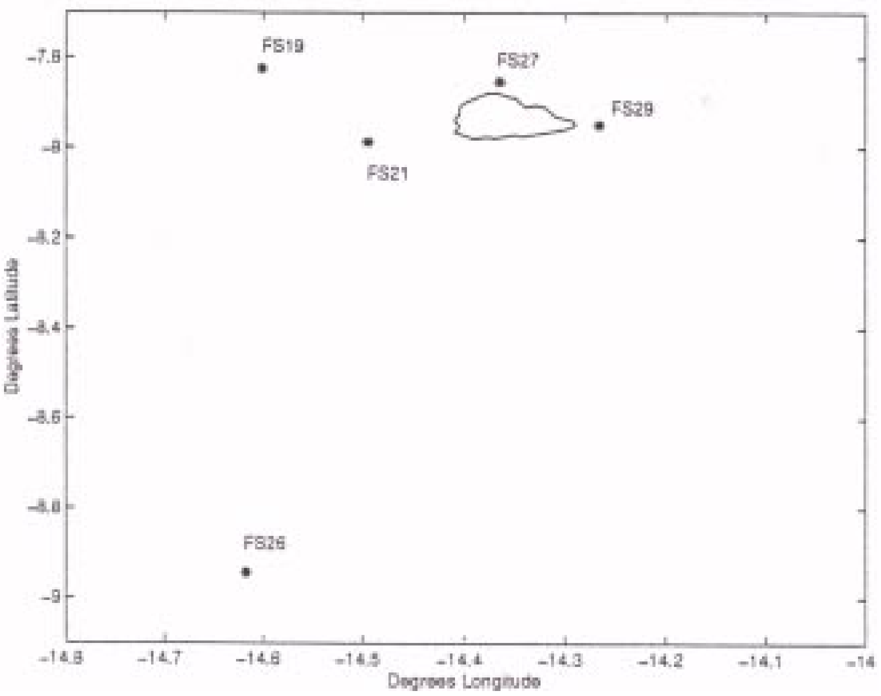

Chase21 explosion: ASC

The second arrival is about 9 min after the first arrival.
Variation in received level and incoherent beamforming indicate a different path scattered off South America.
(9 min is about 800 km),
However often the reflection coefficient from a sloping bottom is quite low.

ASC band filter 3-6 Hz

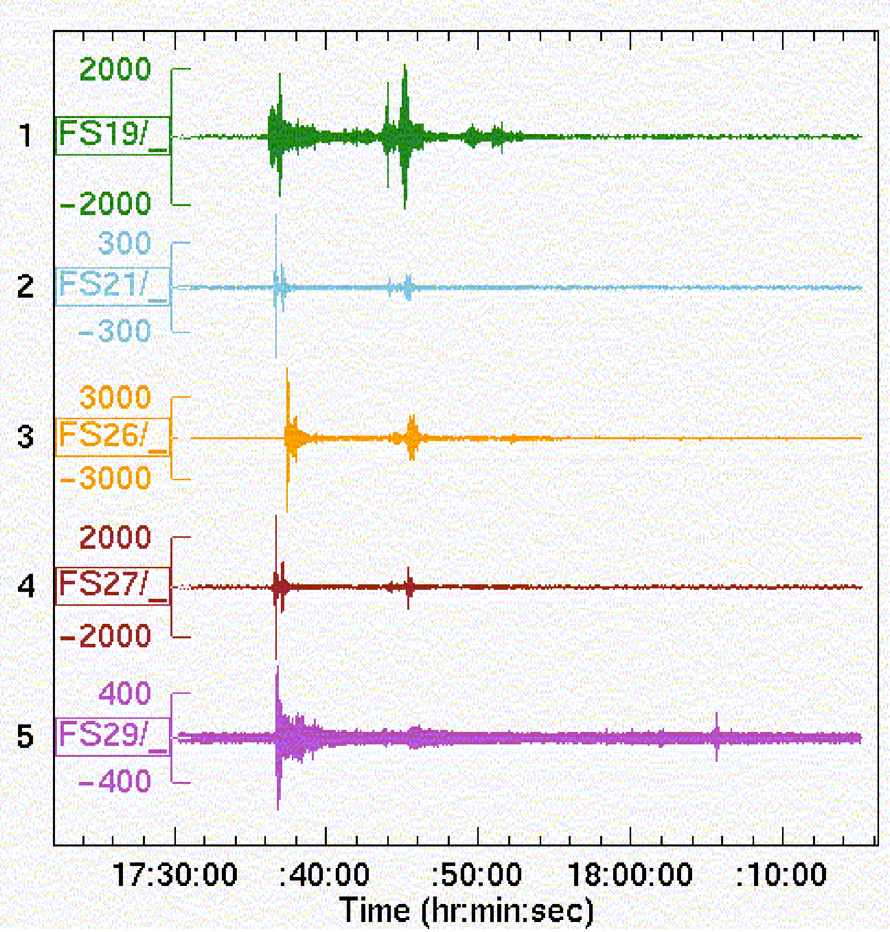

ASC band filter 32-64 Hz

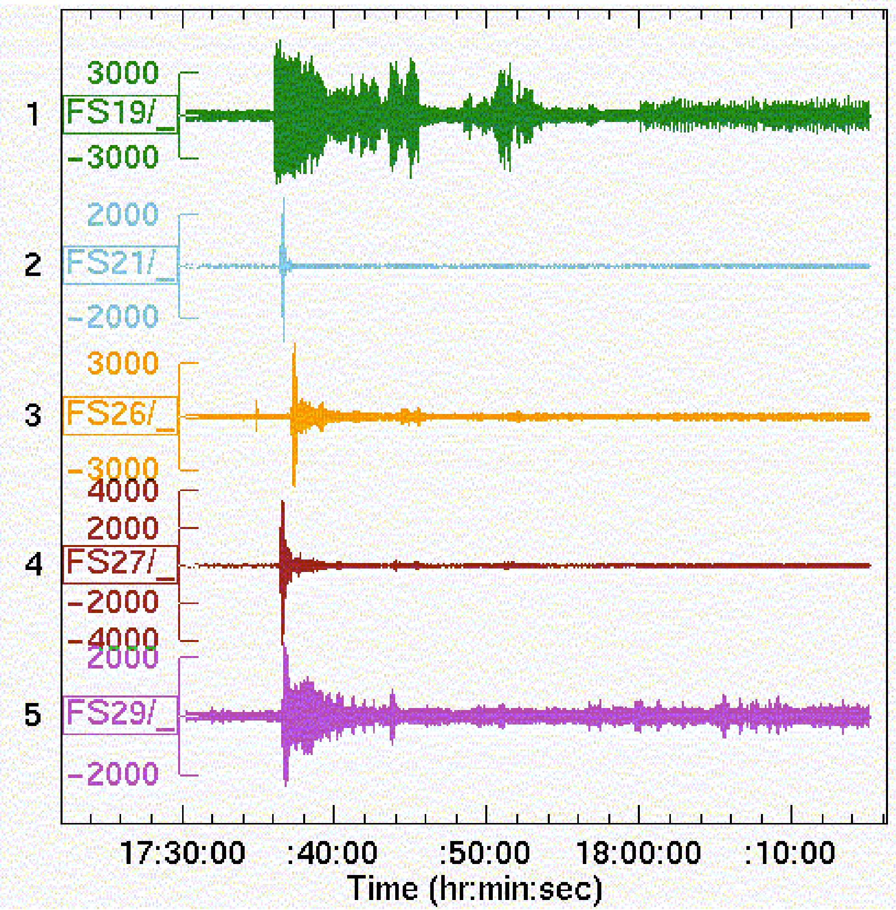

Chase 21 explosion: ASC spectra

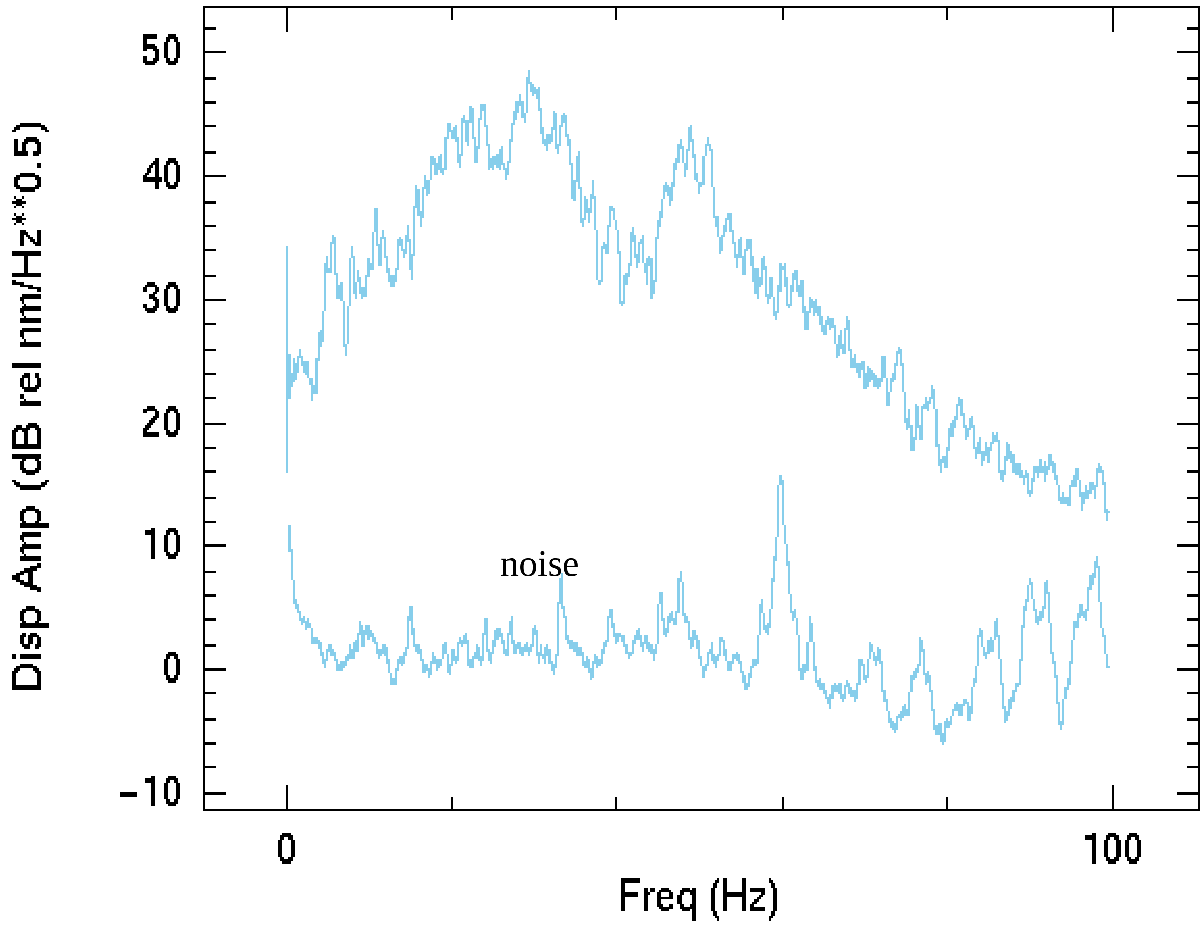

An analysis of second arrival would show that it has less high frequency energy and a longer duration. This is mainly due to the interaction with the continental slope.

Example of volcanic eruption and underwater explosion

Each trace shows energy above the indicated frequency.

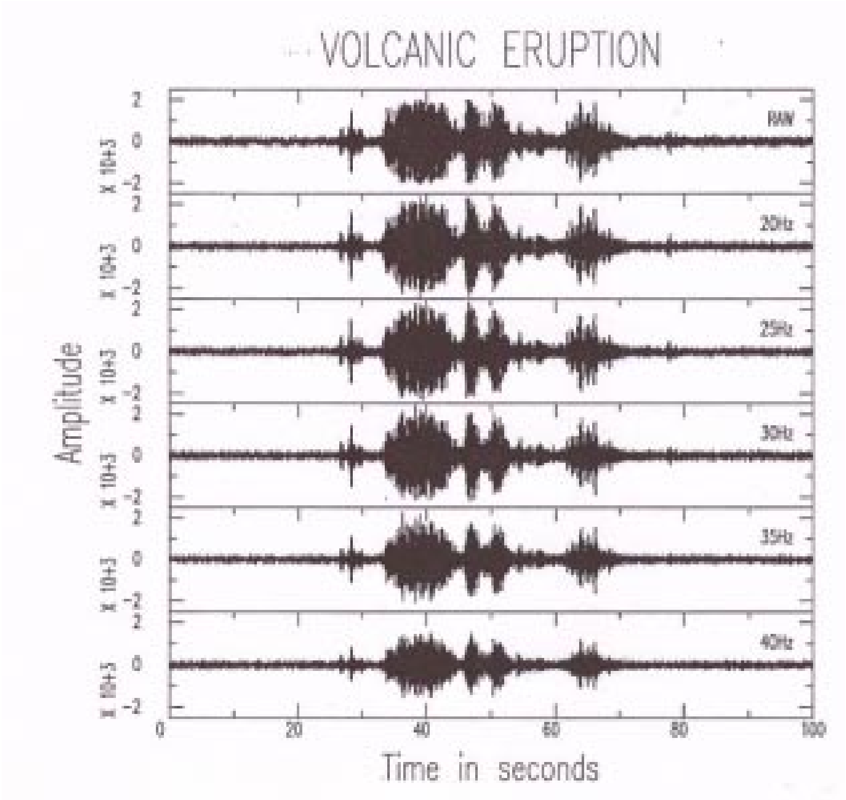

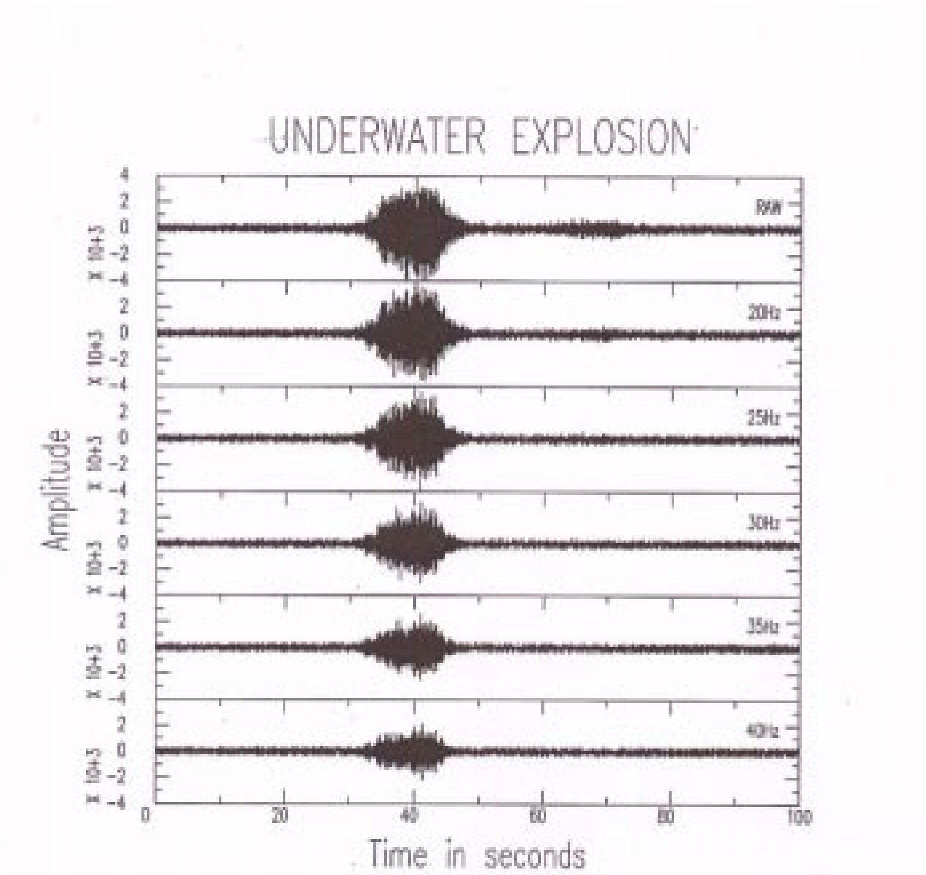

Volcanic eruption has explosive "behavior" and will likely be classified as an H-phase

Example of submarine earthquake and underground explosion

Each trace shows energy above the indicated frequency.

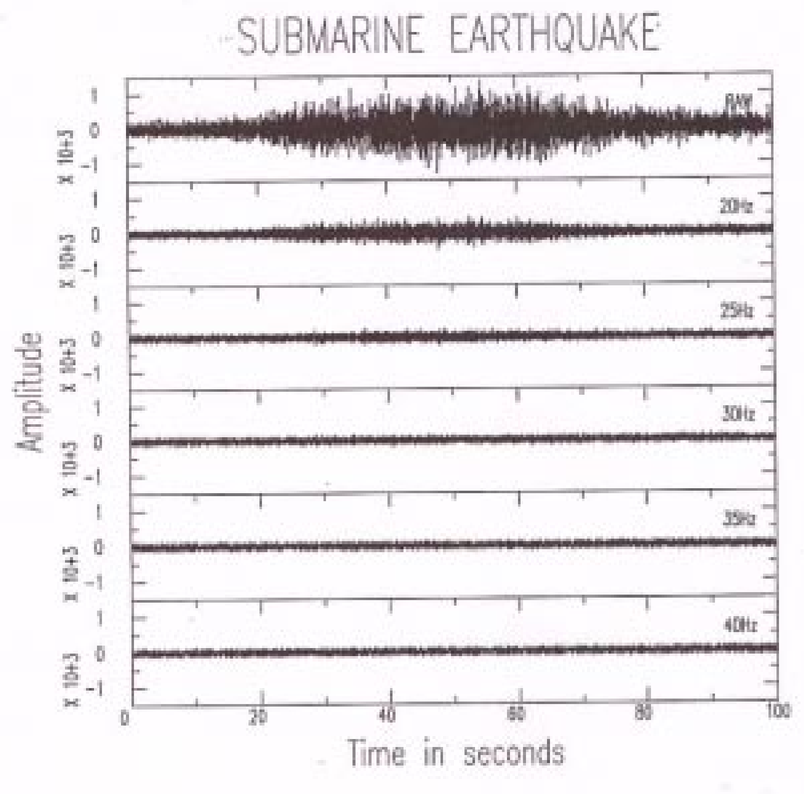

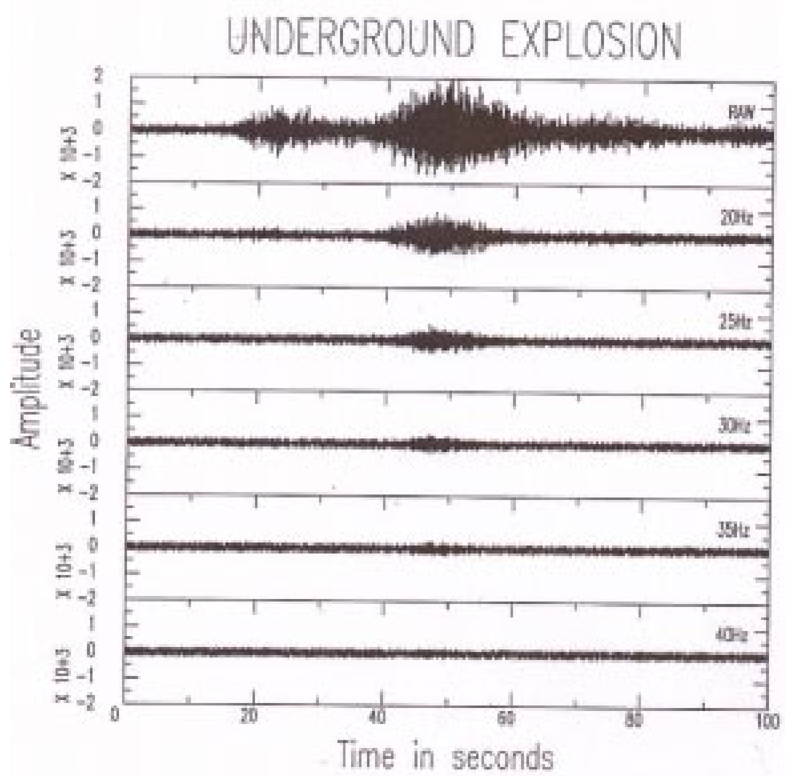

Submarine earthquake and underground explosion have long duration. The T-phase has a low frequency content.

Example of atmospheric explosion

Each trace shows energy above the indicated frequency.

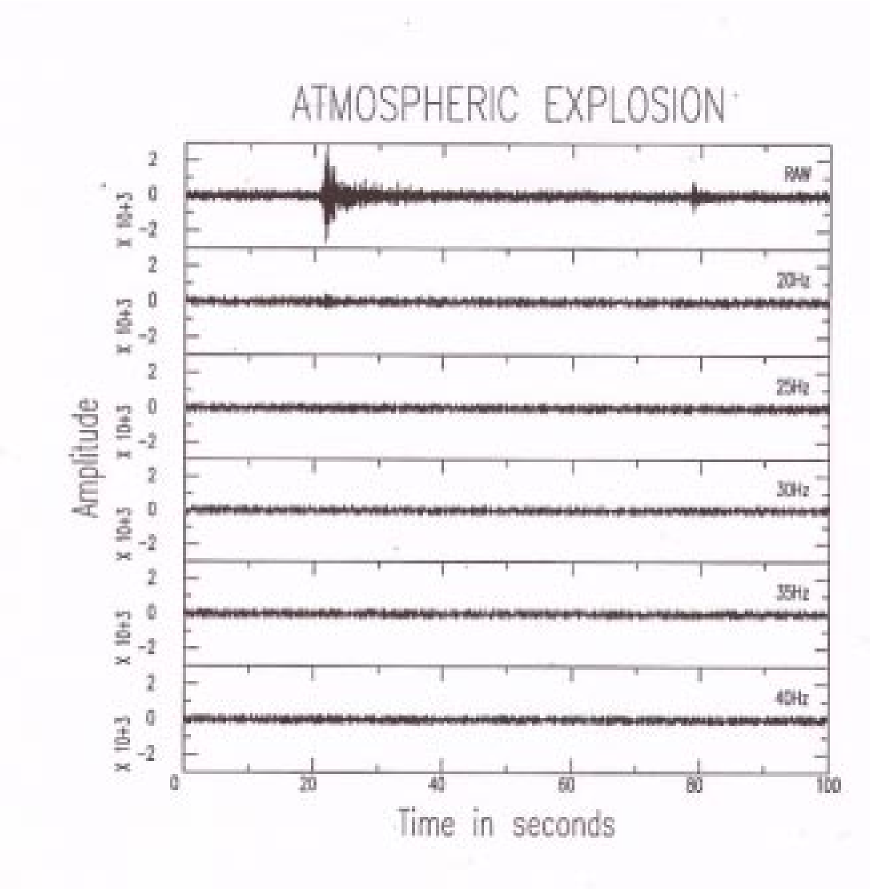

The atmospheric explosion has short duration and low frequency content. Currently it would probably be detected as noise.

Characteristic time series

The location of these events are unknown.

The underground explosion is likely an atoll-explosion. The second signal has travelled though the ocean (H-phase).
The origin of the first signal is not clear.

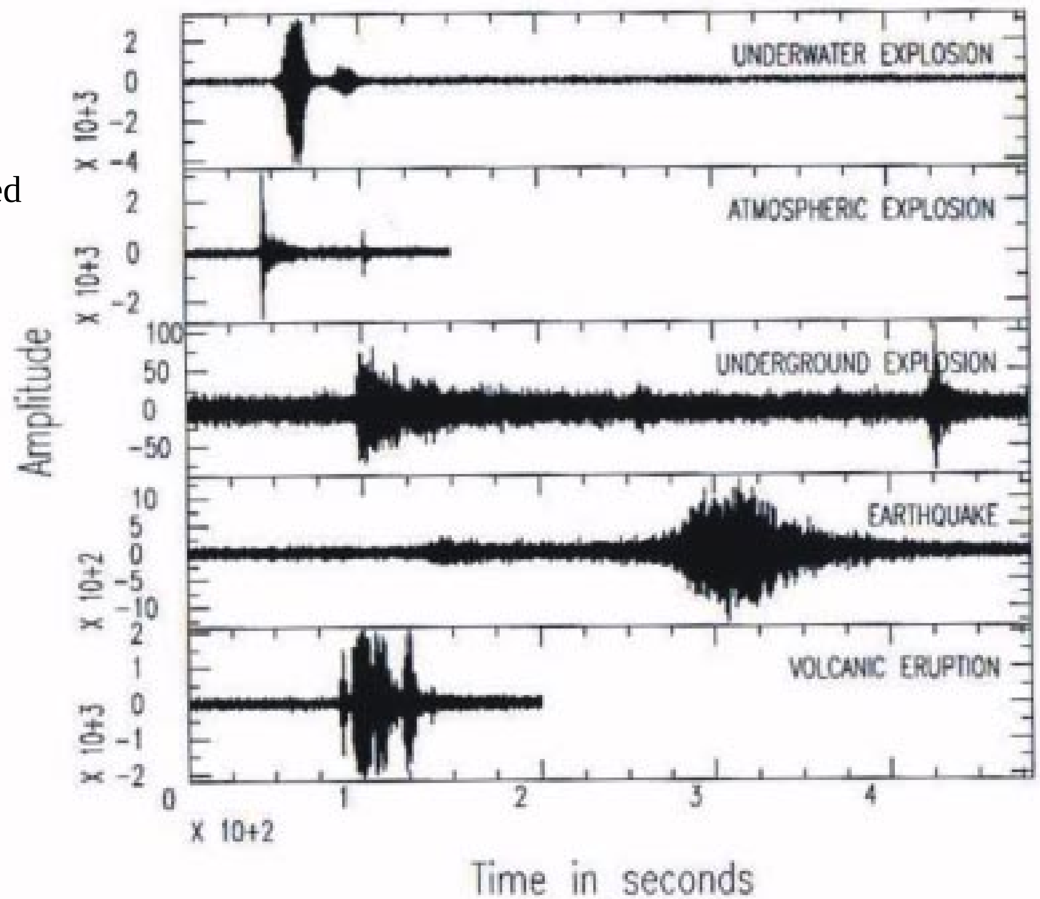

(figure provided by J. Schrodt, AFTAG)

T-phases

The coupling is not completely understood.

The coupling is most efficient when seamount sticks into the SOFAR waveguide. This can be away from the epicenter

Coupling via a flat seabottom is also possible, but the coupling is less efficient.

Hydrophone 1 will first see the arrival from D and then from B. Arrival B will have larger amplitude than D.
Hydrophone 2 will only see arrival A. Arrival C cannot propagate past the seamount due to modal cutoff.

Assuming the seamounts are separated by100 km and neglecting the vertical contribution to travel time, arrival D will arrive 100 km(1/1.482s/m-1/4s/m) =50 s before arrival B

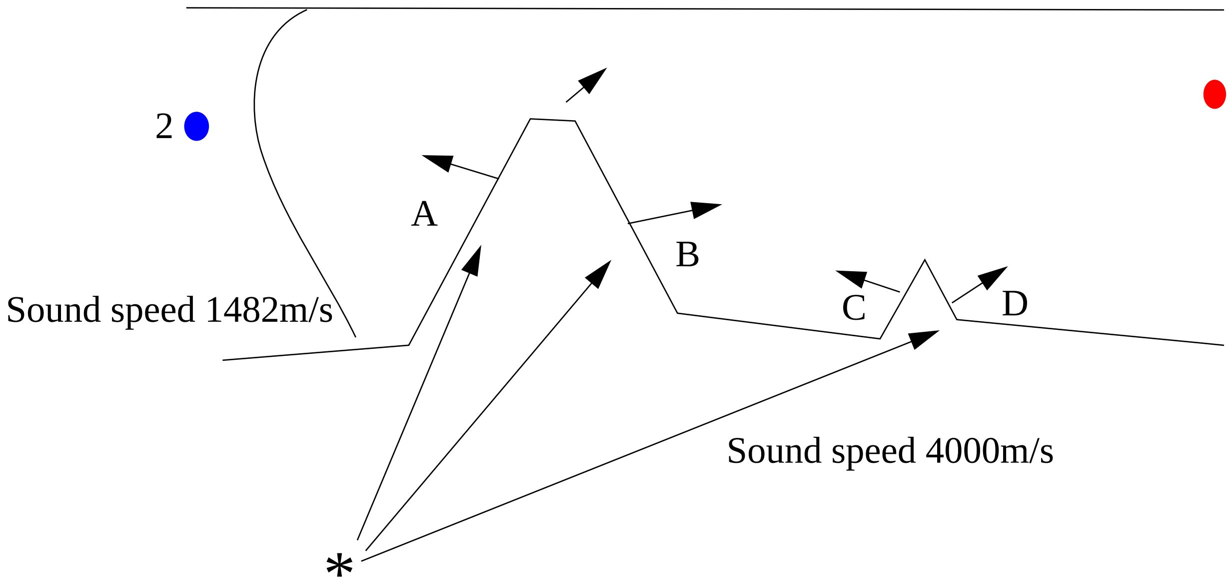

$$t = t_{earth} + t_{ocean} = \frac{r_{earth}}{4.} + \frac{r_{ocean}}{1.482}$$

T-phase variation with azimuth

T-phase coda from a variety of earthquakes at epicentral distances of 30-40 degrees from wake.
t=0 is relative to the epicenter using a reduction velocity of 1500m/s.

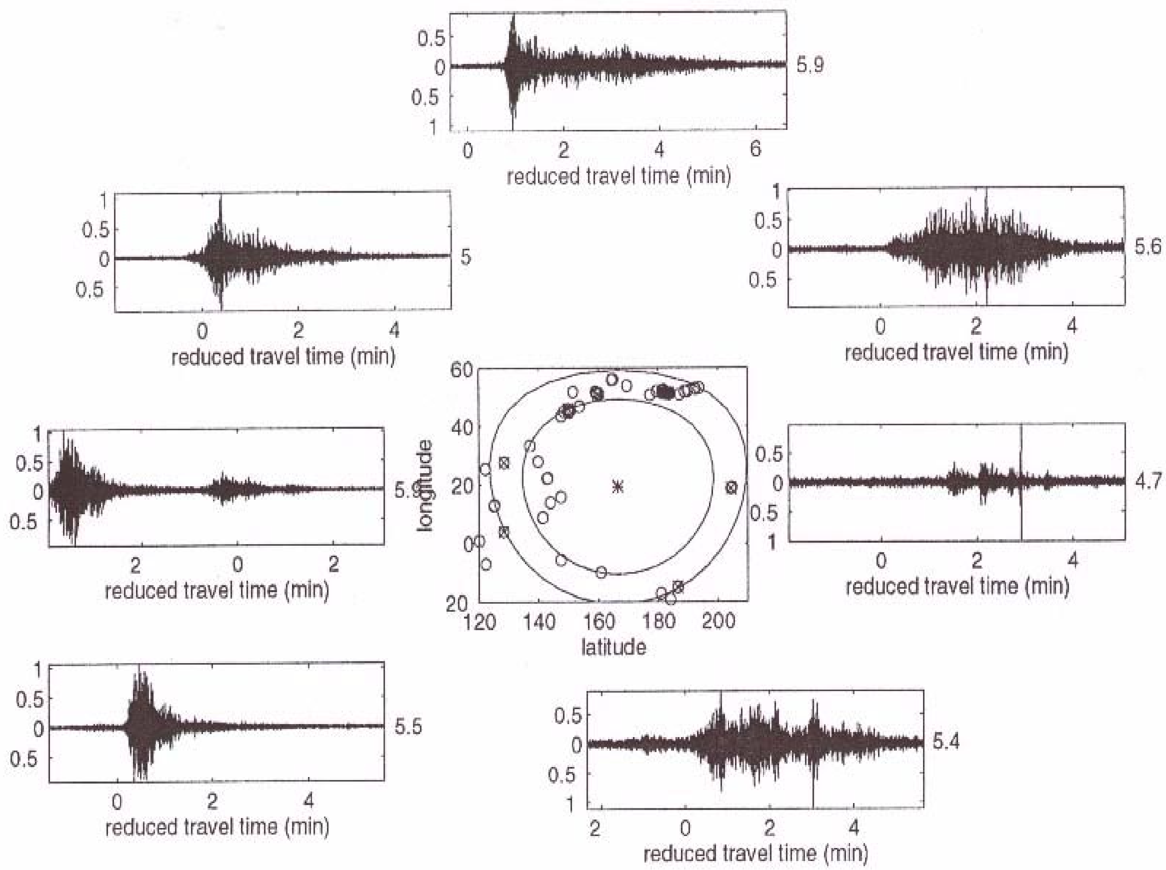

Bubble pulse (2)

Bubble pulse does not always appear. It does not appear for an explosive source too close to the surface or in the solid earth. It did not appear for the french atoll explosions and some of the C-4 (4 pound) explosions off California did neither show it.

The formula is empirically derived based on navy explosions.
The delay time between each pulse is given by

$$T_i = K_i w^{\frac{1}{3}} (z + 10.1)^{-\frac{5}{6}}$$

Where w is yield in kg
z is depth in meters
K_i is an empirical factor for the first 3 bubble pulses (2.11, 1.48, 1.20), as the bubble rises the time separation becomes less.

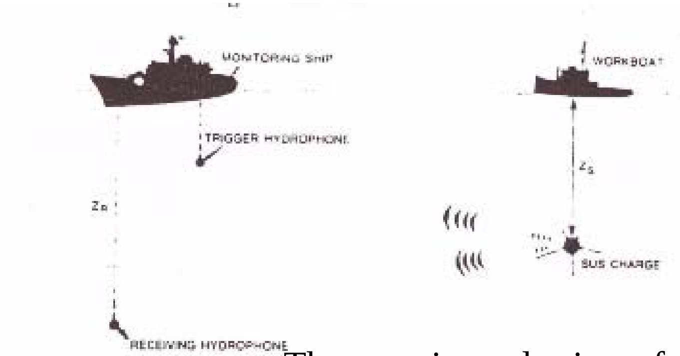

The negative pulse is surface reflection

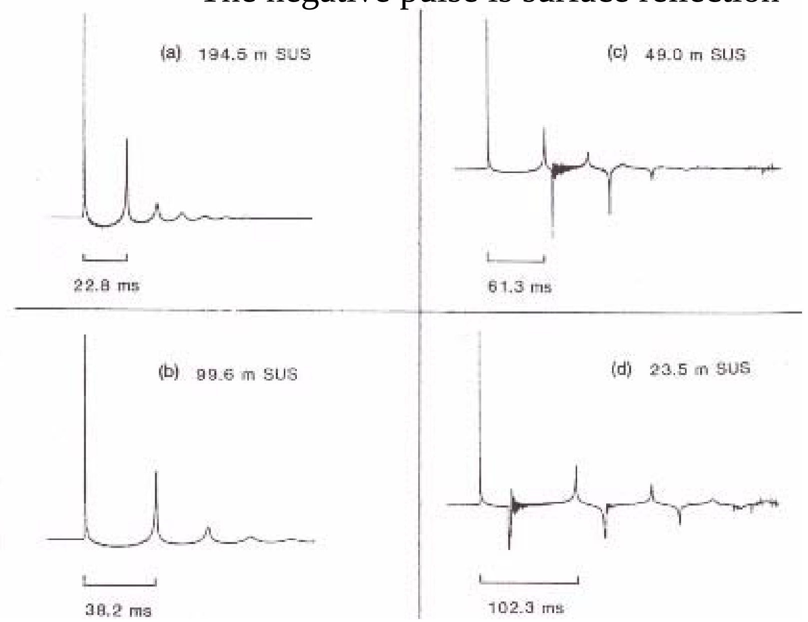

Currently source depth for hydroacoustic events is not determined.

Based on an estimated time delay the source-depth yield trade off can be determined.

The delay time will show up in the spectrum as scalloping with a period of 1/T1. This feature is best automatic detected in the cepspectrum.

Time series of explosions as a function of depth.

Explosions in a deep lake

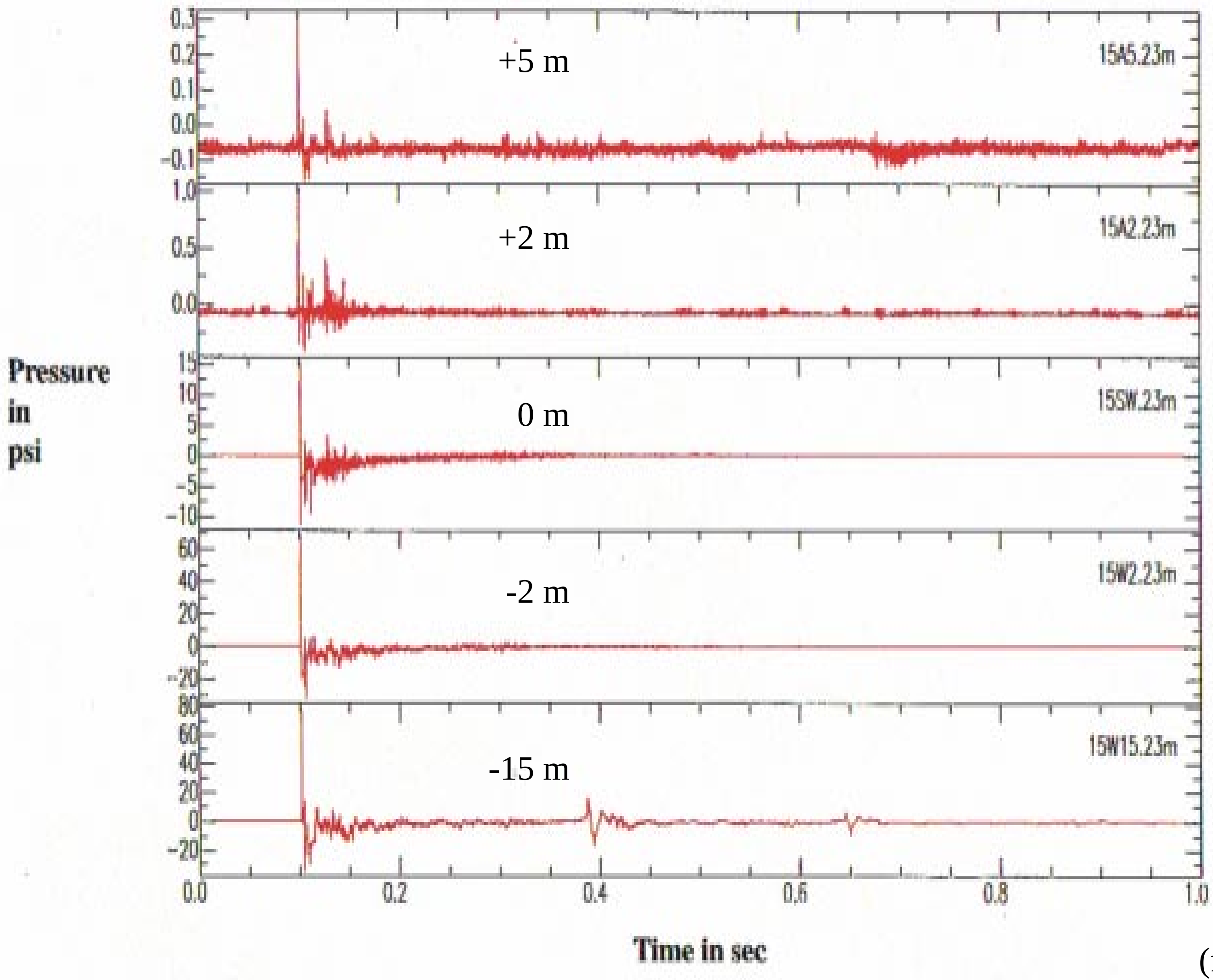

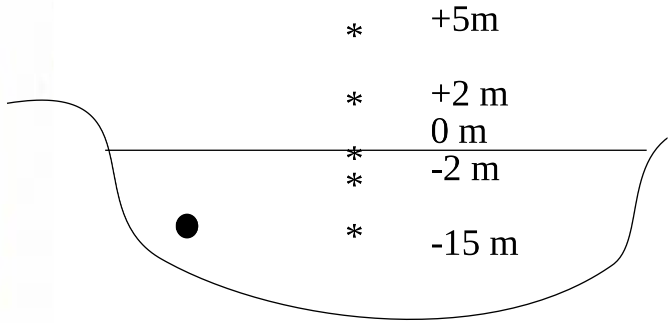

Bubble pulse period for 15 m source depth:

$$T_i = 2.11(15)^{\frac{1}{3}}(23 + 10.1)^{-\frac{5}{6}} = 0.28s$$

(figure provided by P. Harben, LLNL)

California explosions (C-4), 10 Nov. 1997 (1)

A series of Naval explosions was carried out off California (San Francisco). It was recorded at Wake, Psur and *partially* at VIB. Partially because, according to the analysts, I was difficult to find the phases at VIB. However 3 H-phases are needed in order to keep the arrivals in the REB-database. Further analysis makes this clear.

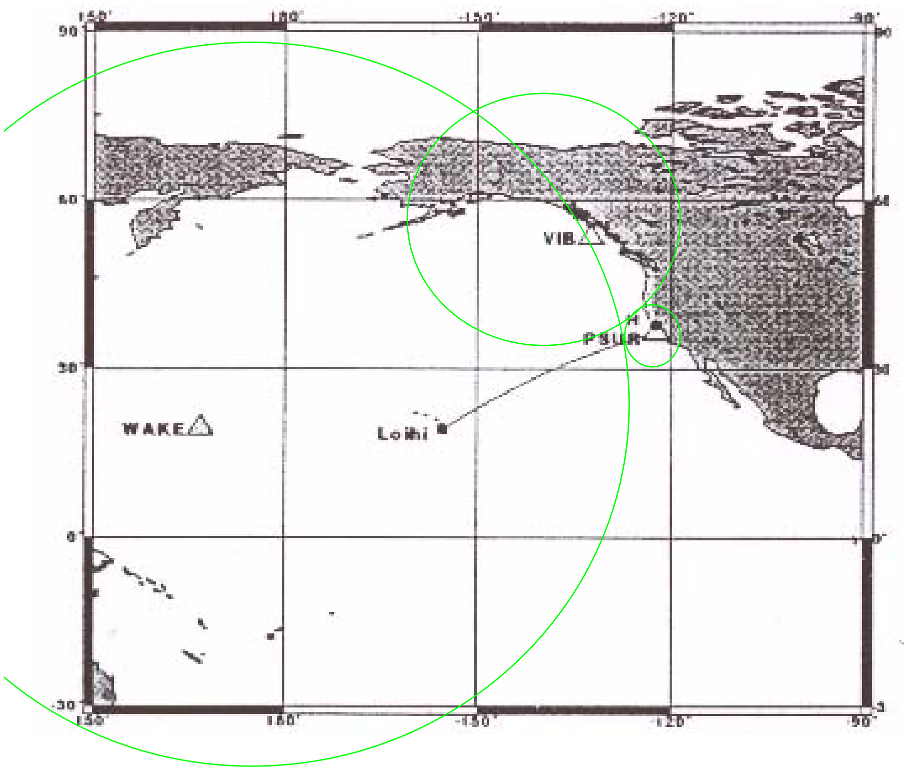

Curves of constant travel time

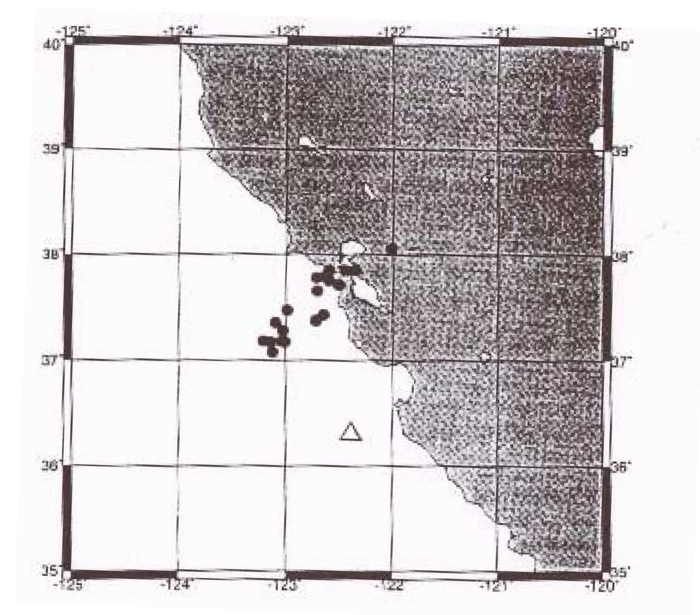

The location of the shots is unknown, but evidently some of the shots has been mis-located, as they are located on land. The location for H-phases is based entirely on traveltime. The variation of the location seems to be mostly in the radial direction of Wake, it could indicate that Wake has the main influence on the error in location.
However, as discussed later the arrivals picked at VIB is of question able quality. This makes location difficult.

California explosions (C-4), 10 Nov. 1997 (2)

The received signal at Point Sur.

Green line indicate arrival time.

Red is FFT length.

The source depths were unknown.

But using the bubble pulse formula,
The period is 0.38 s (0 m), 0.05 (100 m), 0.008s (1000 m). Thus repetitions are not related to the bubble pulse.
They could be related to out of plane scattering form nearby features.
But why should that be so regular.

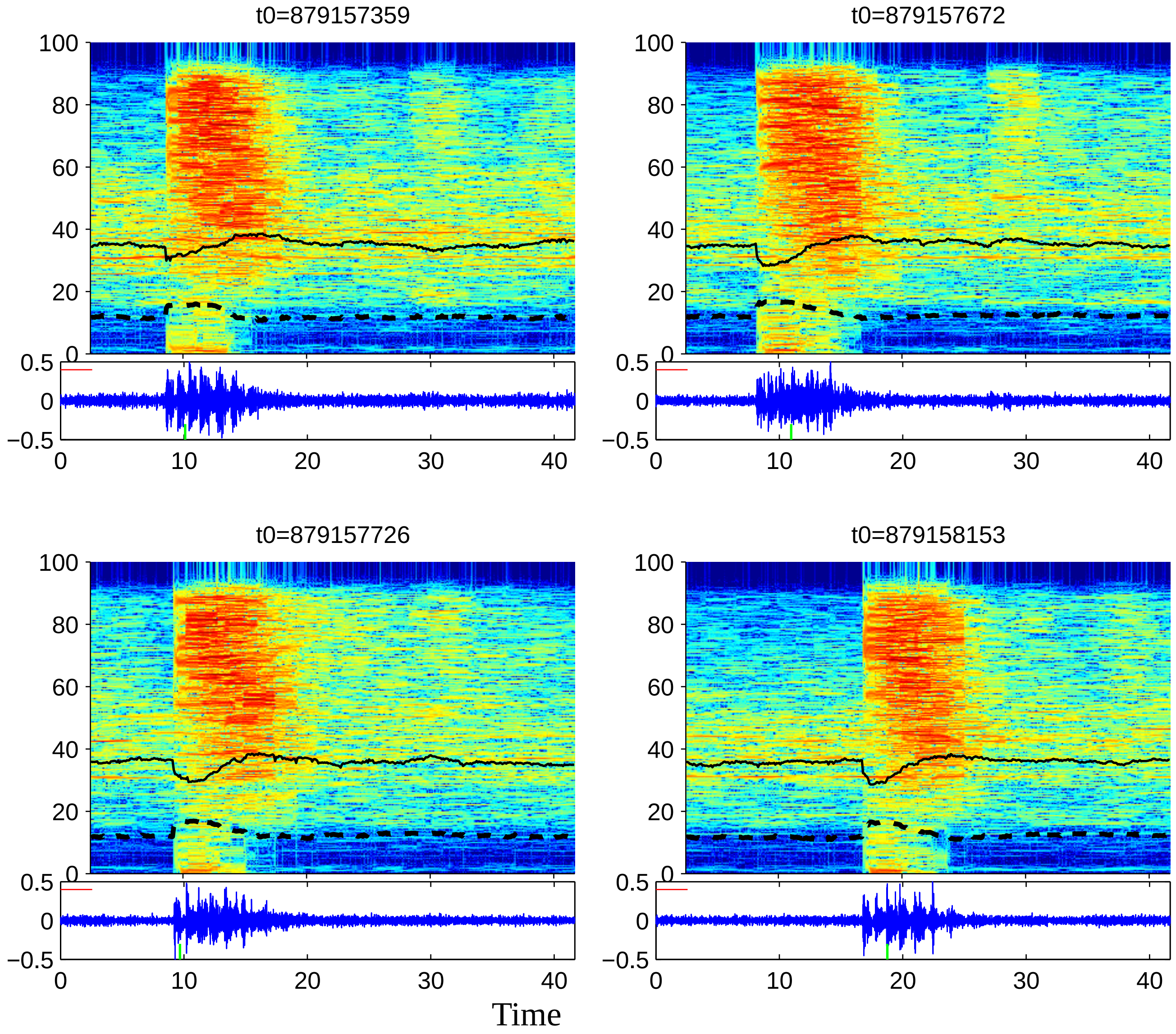

Notice the sharp onset.

The solid dark line is the mean frequency.
The pulse has first more energy at lower, frequencies followed by higher frequencies.

The source-receiver distance is only about 100 km, thus the arrival is not yet typical of a guided wave.

Multiples

A possible explanation of the ringing pattern could be multiples in the water column.
For an isovelocity wave guide this can be solved by the method of images.
Here it is assumed that the source is close to the surface

For the first three multiples we obtain:

$$R_1 = \sqrt{r^2 + ((D - z_s) + (D - z_r))^2}$$

$$R_2 = \sqrt{r^2 + ((D - z_s) + (D + z_r))^2}$$

$$R_3 = \sqrt{r^2 + ((D - z_s) + D + (D - z_r))^2}$$

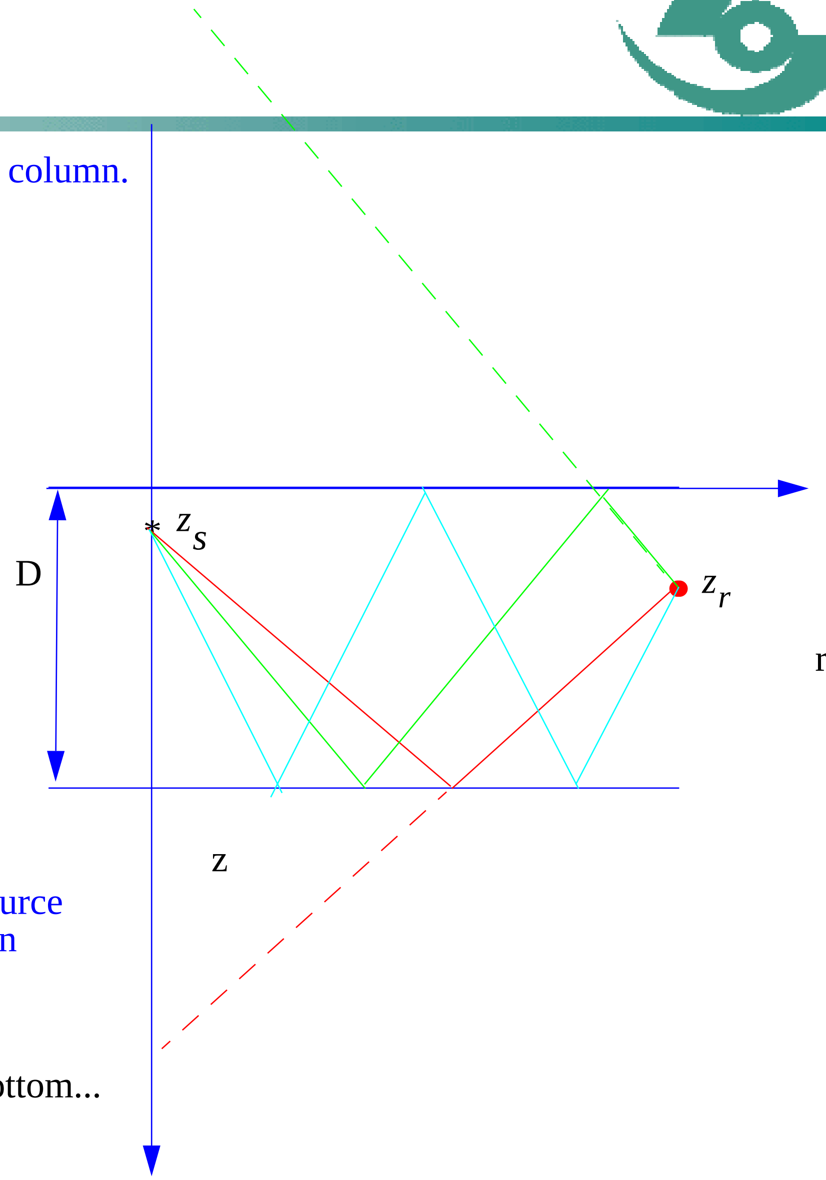

For this explanation to hold the shots must be located much closer to the source for a range of 10 km, receiver depth 1.3 km and ocean depth 2 km we obtain

$$R_1 = 10.3,\ R_2 = 10.5,\ R_3 = 12.2$$

Also this theory requires further examination, and inclusion of a sloping bottom...

California explosions (C-4), 10 Nov. 1997 (3)

The received signal at WK30.

Green line indicate arrival time.

Red is FFT length.

Notice the 60-Hz noise.

The appearance of the four wave forms are different. It could be due to different source depth.

For all signals a slow, 5-10 s build up is observed. This is typical for an ocean waveguide propagation.

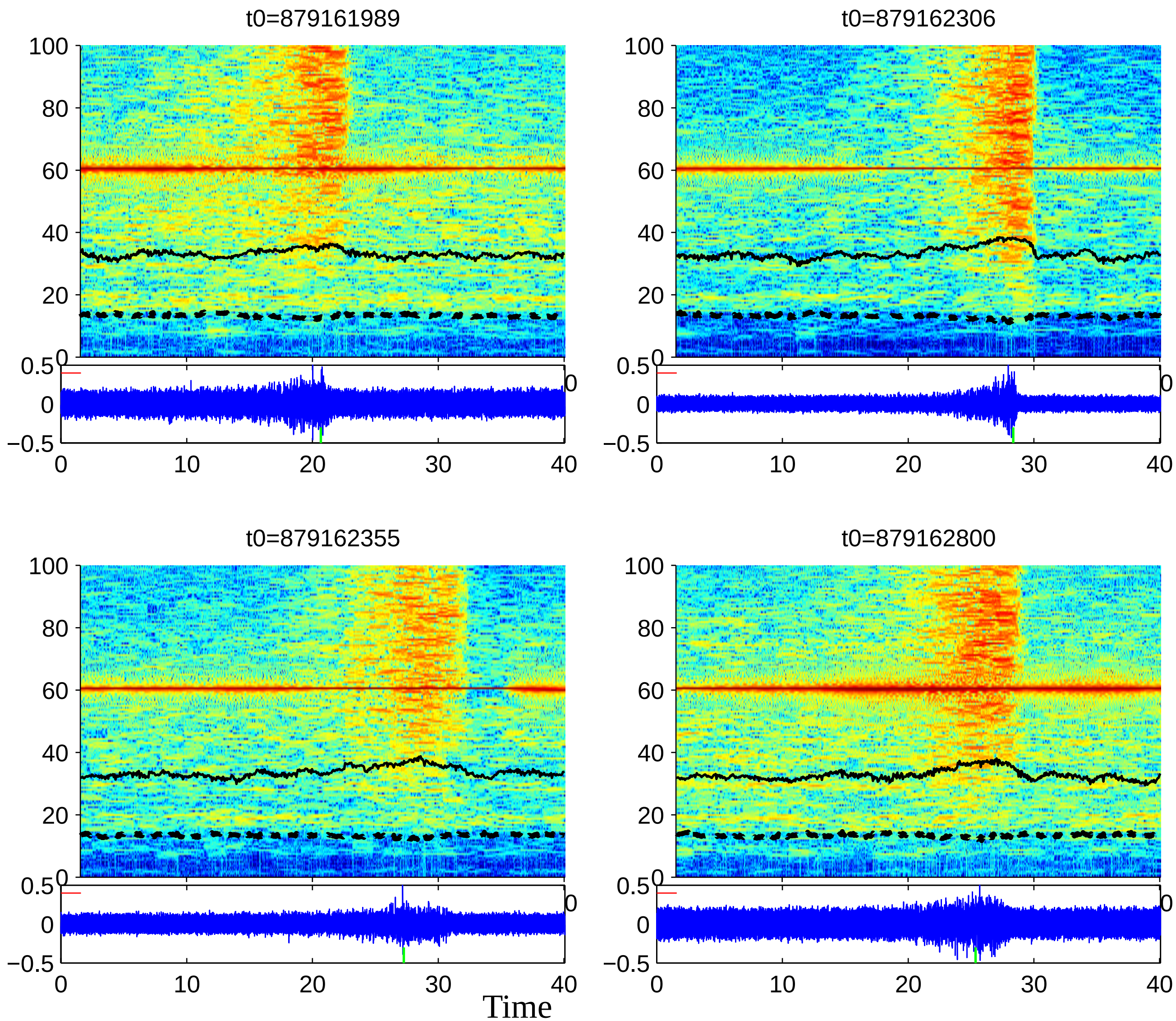

California explosions (C-4), 10 Nov. 1997 (4)

The received signal at VIB.

Green line indicate arrival time.

Red is FFT length.

Notice the 38-Hz generator noise.
It will be removed in a station upgrade.

VIB is the first T-phase station. The quality and use of T-phase stations is still a research area.

According to the analyst the arrivals picked at VIB is arbitrarily. The picks were necessary in order to maintain the arrivals in the database. (3 H-phases are needed to build an event)

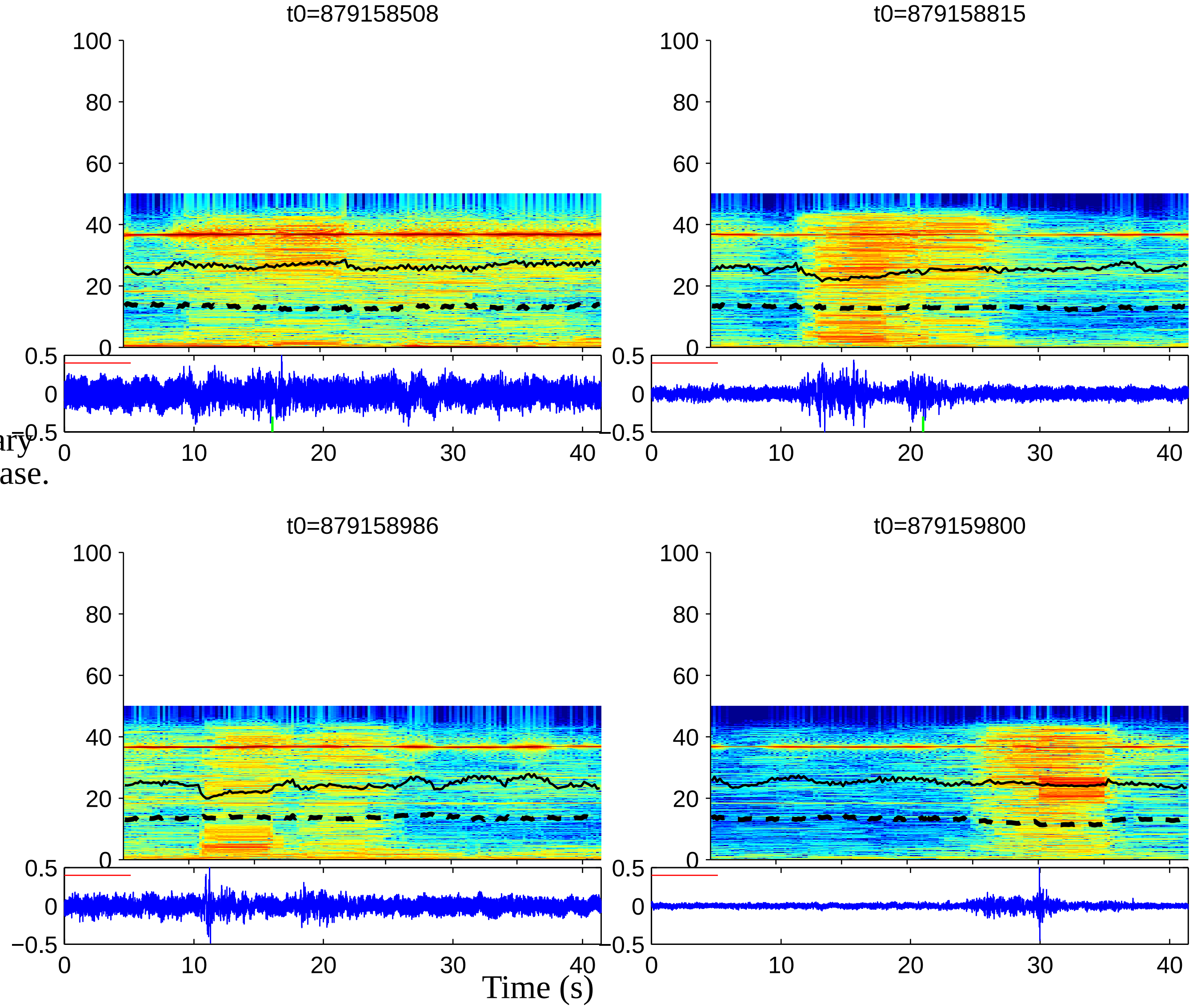

California explosions (C-4), 10 Nov. 1997 (5)

A problem is picking the arrival time. For hydroacoustics is done based on Probability Weighted Time (closely related to main peak). For Psur the arrival time is in the middle of the signal, while for Wake it is in the end of the signal. This is OK, as the travel time would be computed accordingly.

The traveltime picked at VIB is discussable.

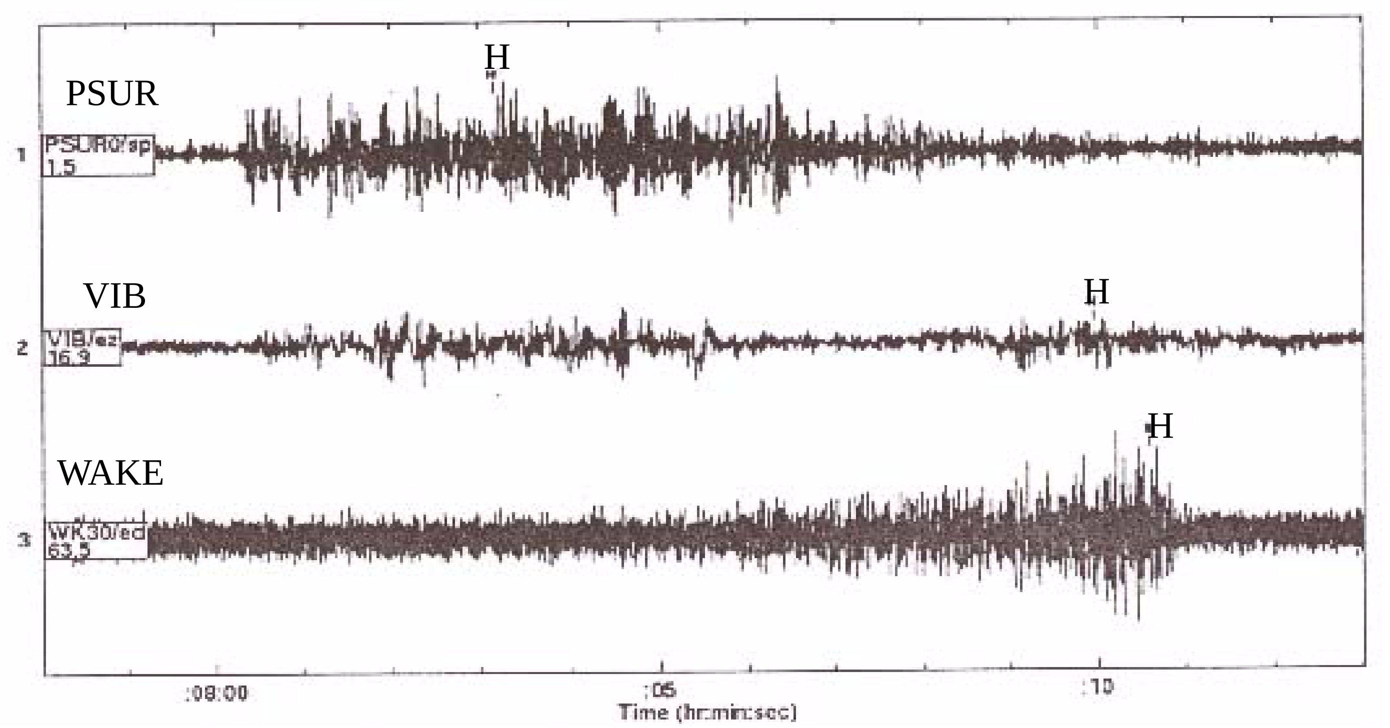

Hydroacoustic network

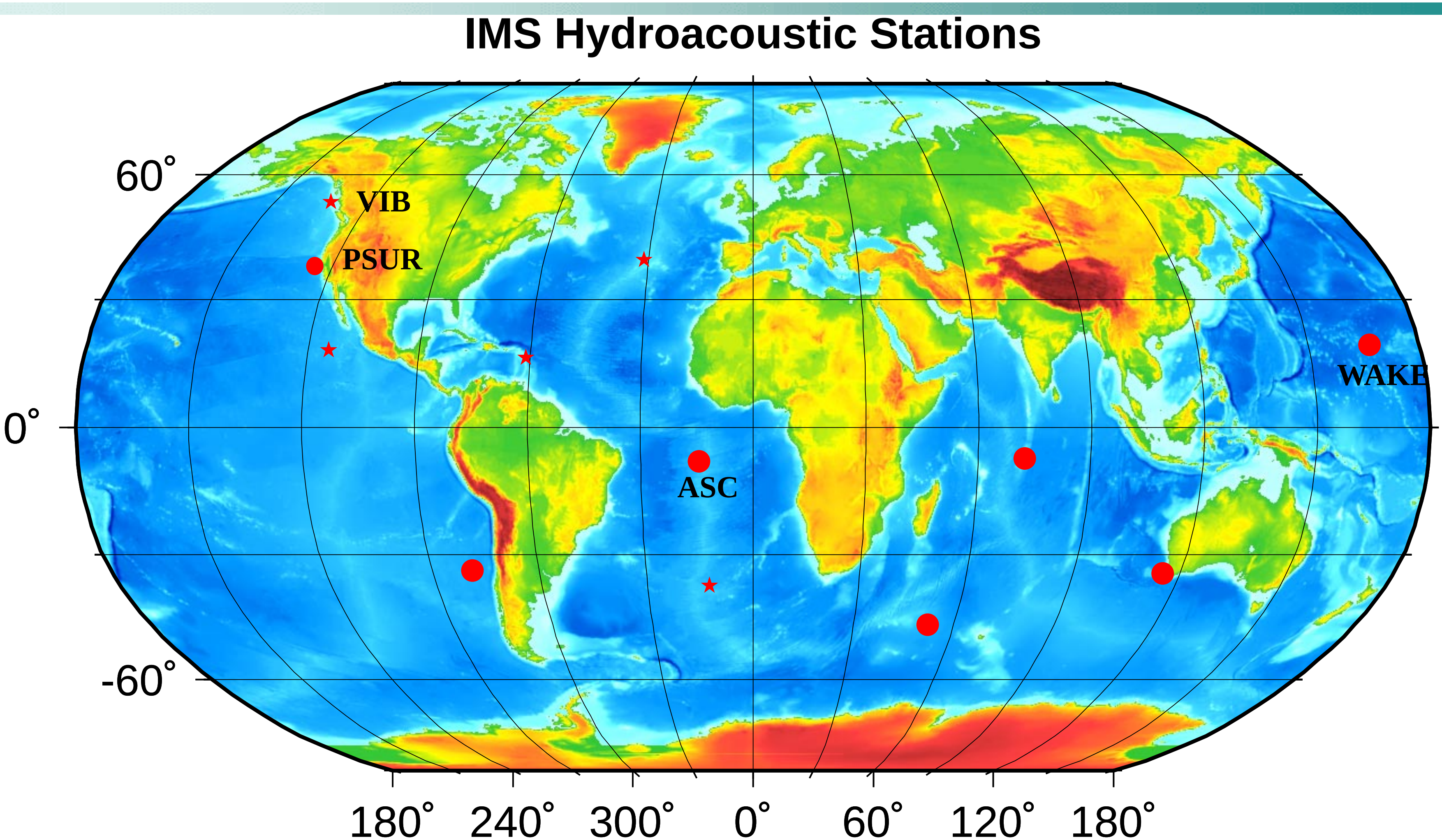

T-phase stations (5): star

Hydrophone stations (6): dots

(Point Sur: not in IMS, but to be received at IDC)

Hydroacoustic station configuration

Hydrophone station

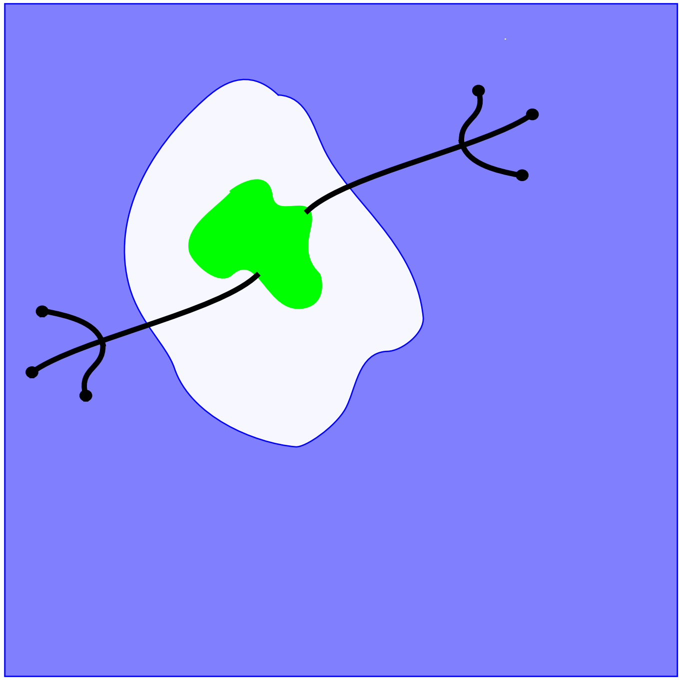

T-phase station

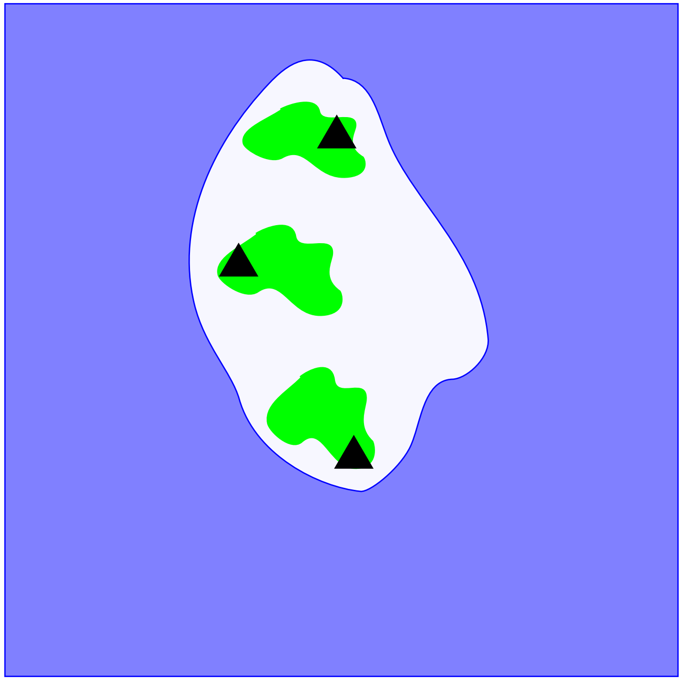

Up to 3 seismometers
Either vertical or 3 component seismometers
A factor 10 cheaper than Hydrophone stations
Quality of stations not known

The transmission loss from sofar channel to T-phase station is a factor 10-100.

Hydrophone station

A station will consist of two triplets of hydrophones

The hydrophones will be in the SOFAR channel, at a depth of 1 km , 10-100 km from the island.

The triplet hydrophones will be spaced 2 km apart.

The triplet will allow us to determine angle of arrival.

Point Sur has one hydrophone

Wake has two hydrophones

Ascension has five hydrophones

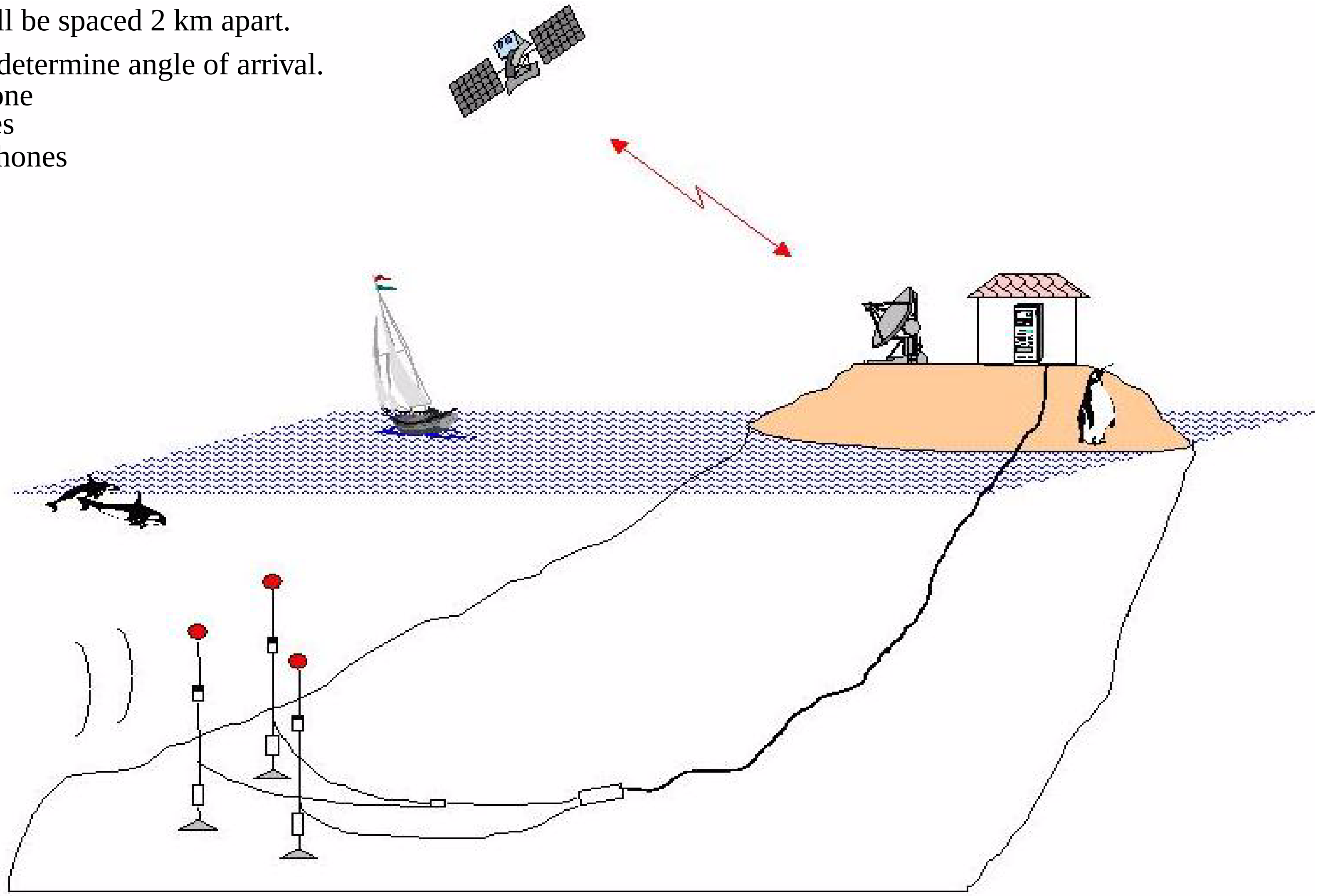

Hydroacoustic Processing

DFX Automatic Detection and feature eXtraction
StaPro Station Processing: Automatic phase identification
GA: Global Association: automatic event/ phase association

Interactive processing
ARS- Analyst Review Station, DFX recall processing

Automatic signal detection (DFX)

hydroacoustic signals picked with a STA/LTA detector (Shot Term Average/Long Term Average)

The running STA/LTA average is computed

Shot term window is 10 s (seismic is 1 s)

LTA is an exponential tapered window
Long term time constant is 150 s (seismic is 60 s)
[Often called long term window]
The window extends in principle to minus infinity.

9 band passed filters are used in detection
2-4, 3-6, 4-8, 6-12, 8-16, 12-24,
16-32, 32-64, 2-80Hz

When a detection is found in one band the
hydroacoustic processing starts!
(processing in all bands).

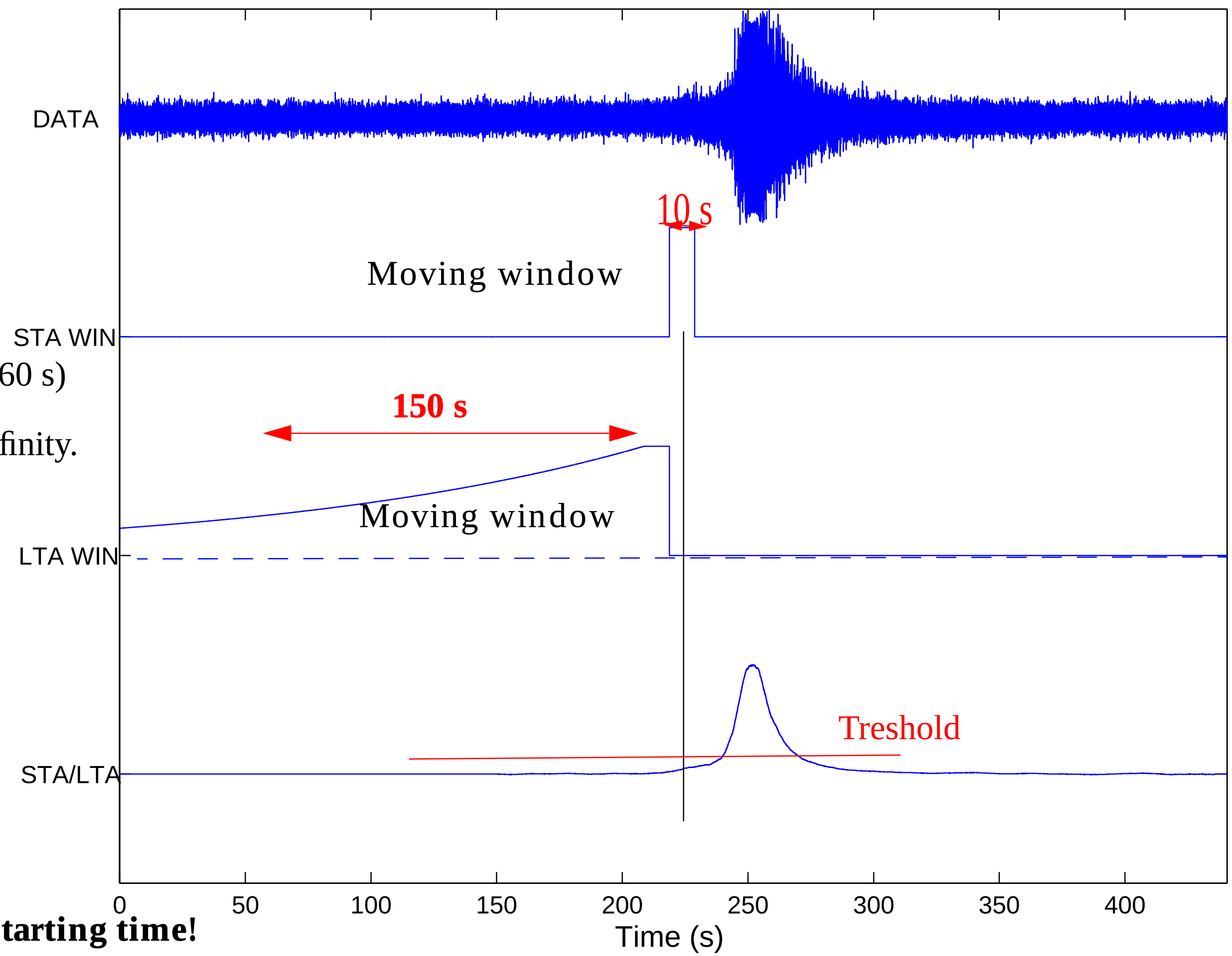

LTA depends on data before the 150 s.
Thus detections depend on processing starting time!

Detection on PSUR data, Fangataufa 1 OCT 1995 event

While both the STA and LTA is sensitive to the noise it is hardly seen in the STA/LTA ratio. The real arrival at 2700s is clearly detected.

STA window is 15 s

LTA time constant 150 s

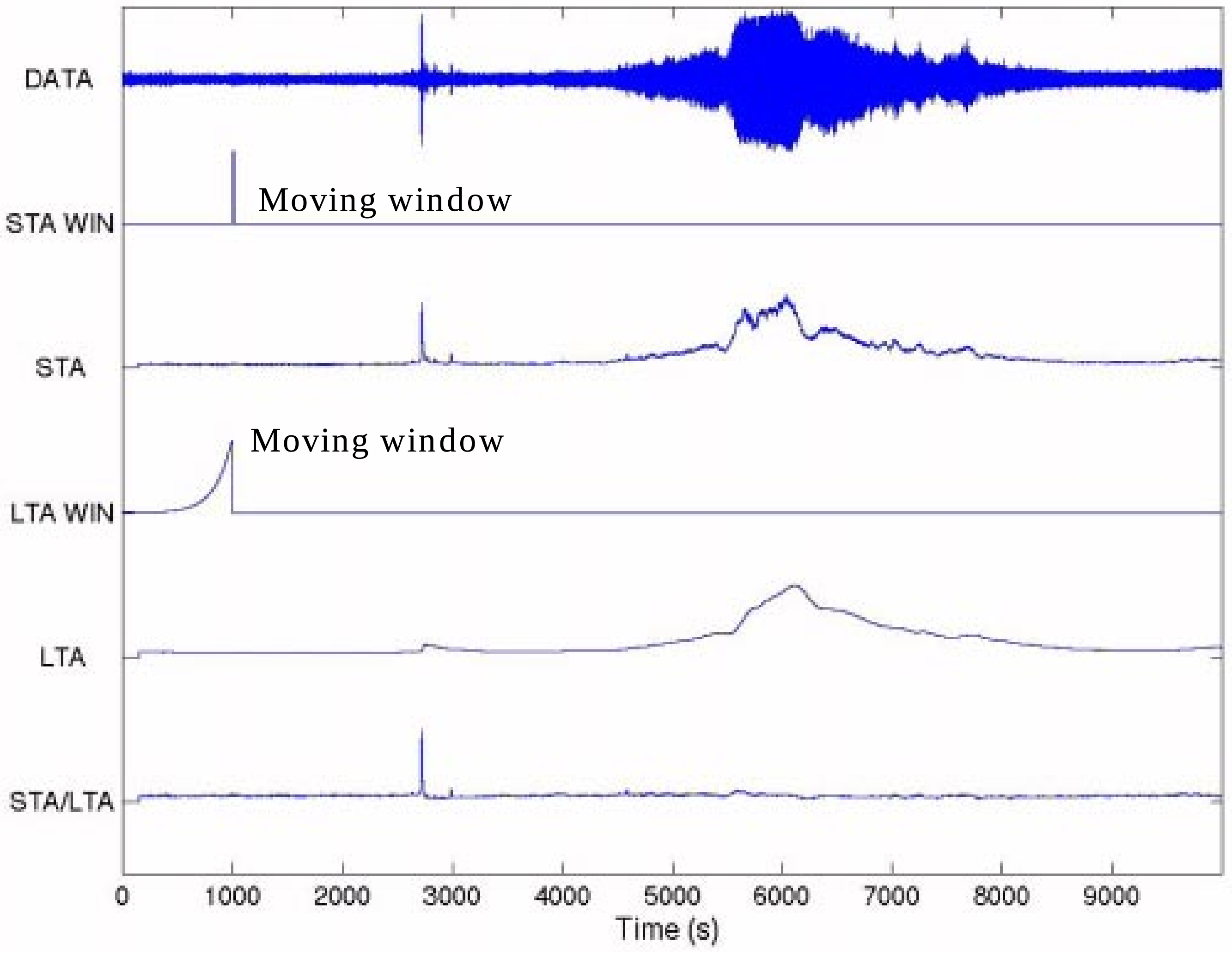

Hydroacoustic Feature Extraction (DFX)

Processing is done in multiple frequency bands:
2-4, 3-6, 4-8, 6-12, 8-16, 12-24,16-32, 32-64, 2-80Hz

The purpose of the feature extraction is to estimate relevant features that can first be used in identification of the arrival (program StaPro) and in the association and location (program GA). All relevant features are store in databases, that way the quality can easy be assessed.

Populates hydro_feature table:

primary keys: arid, low_cut and high_cut (i.e. band pass of filter)

Up to 9 entries per arrival (= number of band pass filters)
This table contains all the extracted features for each arrival.

Populates arrival table:

For the band with highest energy the arrival time, arrival time uncertainty and SNR is extracted from the hydro_features table

Onset and Termination time:

The onset and termination time is determined in each frequency band.
If a termination time cannot be determined then no features are measured in this band.

Onset is first found by the STA/LTA criterion.

Termination is when the signal falls below the termination treshold after the two criteria are meet:

- The minimum treshold must be reached.
- The termination most occur after the max SNR in the first 105 s

However, the signal length cannot exceed a max length

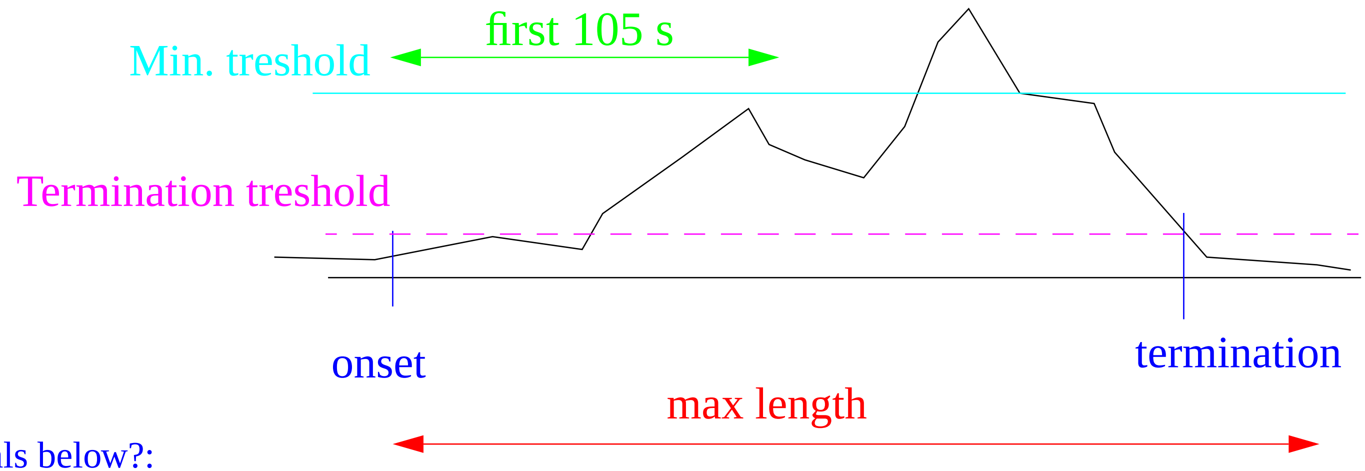

What is termination for the two arrivals below?:

Hydroacoustic arrival time is determined by Probability weighted time (PWT)

A well defined arrival time is difficult to measure for hydroacoustics. For example, onset time is difficult to specify due to the slow build-up of hydroacoustic arrivals, and the peak arrival can fluctuate due to noise.

Hydroacoustic arrival time is determined by Probability Weighted Time (PWT)

For low SNR the four peaks are as likely to be the main peak

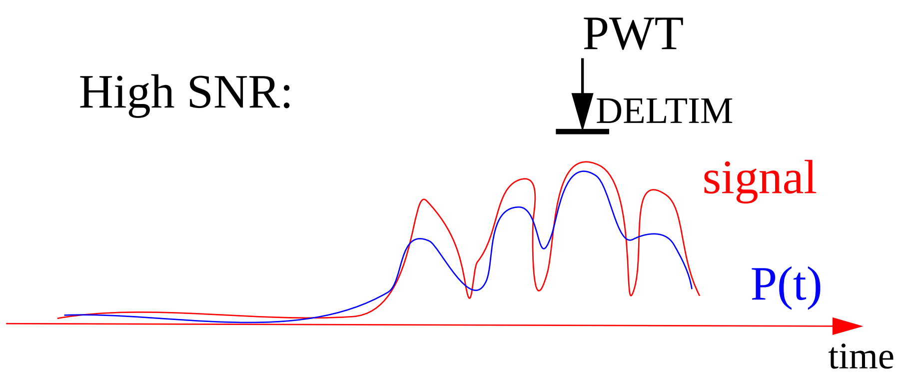

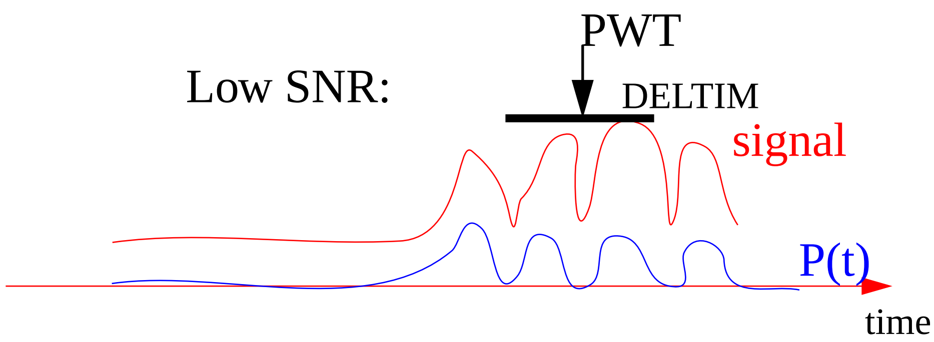

For each time sample i the pressure e_i is assumed $N(\mu_i, \sigma)$ distributed

Given an observed signal e_i we calculate the probability P(t) that observation e_i is the peak of the signal.

Arrival time = $E[P(e_i)]$

Arrival time error DELTIM = $\mathrm{std}[P(e_i)]$

Problems:

- A noise spike has DELTIM=0 (quality control could maybe detect this, but it is not so easy!)
- Sometimes a wrong peak is selected.

Elements in Hydro_features table (1)

1 Administrative

1. ARID: Arrival ID.
2. LDDATE: Load date.

2 Filter type

3. LOW_CUT: The low frequency cutoff value.
4. HIGH_CUT: The high frequency cutoff value.
5. FORD: Filter order.
6. FT: Filter type (usually a Butterworth).
7. FZP: Filter causality. Usually a zero-phase causal filter is used.

3 Pulse window

8. ONSET_TIME: Time, in epoch seconds, where the signal is estimated to begin. It is first based on a sliding average power window. This onset time is then refined using an Akaike Information Criterion (AIC) adjustment.
9. TERMINATION_TIME: Time, in epoch seconds, where the signal is estimated to end. It is also based on a sliding power window, however, with many refinements (Laney,1997a).

4 Energy and amplitude measures

10. PEAK_TIME: Identical to PROB_WEIGHT_TIME.
11. PEAK_LEVEL: The level in dB re μPa at the max peak.
12. TOTAL_ENERGY: Estimated total energy in dB re μPa between ONSET_TIME and TERMINATION_TIME. It is the sum squared of the trace corrected for the estimated noise and multiplied by the sampling rate.

Elements in Hydro_features table (2)

13. NUM_CROSS: Number of times the pressure squared exceeds the AVE_NOISE by a factor noise_onset. The noise_onset is defined in the hydro-rec.par file and is currently 1.2
14. AVE_NOISE: The average of the squared pressure in the noise segment (15 s long) it is expressed in dB re μPa. Computed before the ONSET_TIME.

5 Time measures

15. PROB_WEIGHT_TIME: The probability weighted time, based on (Guern, 1997)
16. SIGMA_TIME: The standard deviation for the PWT time, based on (Guern, 1997)
17. MEAN_ARRIVAL_TIME: mean arrival time of the estimated signal energy (first moment, in time).
18. TIME_SPREAD: The RMS time spread of the estimated signal energy (second moment, in time).
19. TOTAL_TIME: Total time, in seconds, where the signal exceeds the noise_onset threshold.
20. SKEWNESS: Skewness a of the estimated signal energy (third moment, in time).
21. KURTOSIS: Kurtosis of the estimated signal energy (fourth moment, in time).

6 Cepstrum analysis

22. CEP_VAR_SIGNAL: variance of the cepstrum.
23. CEP_DELAY_TIME_SIGNAL: Time in seconds to the largest value in the cepstrum
24. CEP_PEAK_STD_SIGNAL number of standard deviations from the mean to the largest amplitude.
25. CEP_VAR_TREND variance of the detrended cepstrum
26. CEP_DELAY_TIME_TREND: Time in seconds to the largest cepstrum value for the detrended spectrum
27. CEP_PEAK_STD_TREND number of standard deviations from the mean to the largest amplitude.

Signal Features:

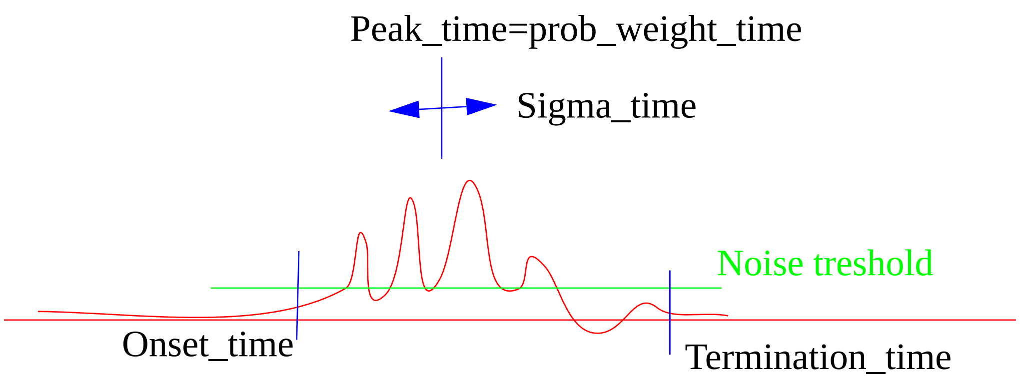

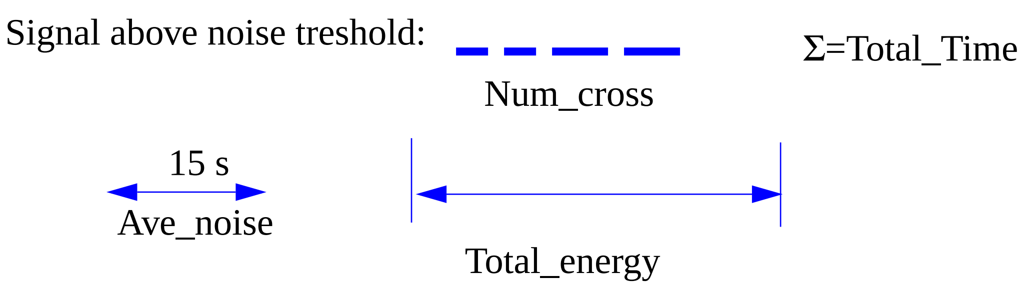

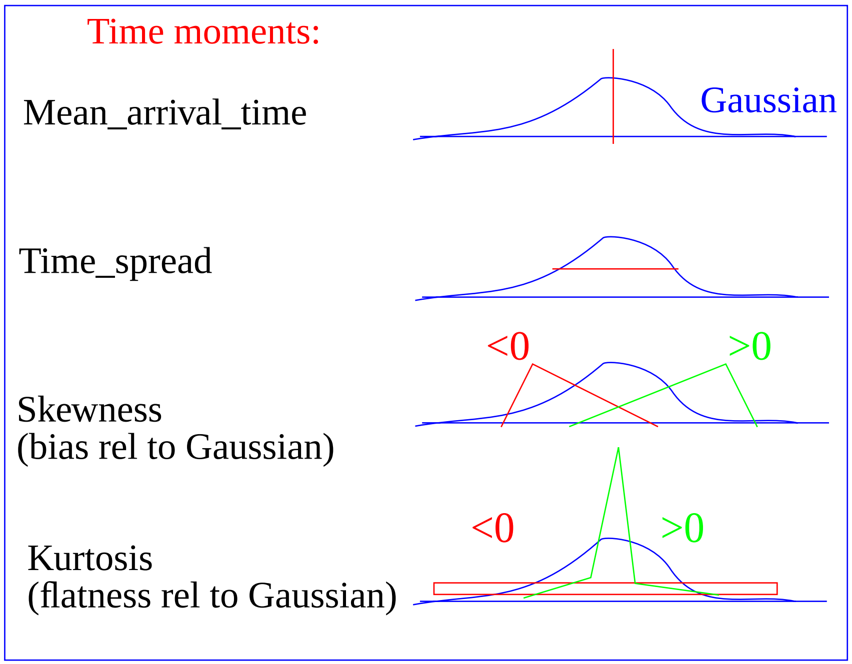

Identification based on automatic processing, wake 6 Dec. 1998 (1)

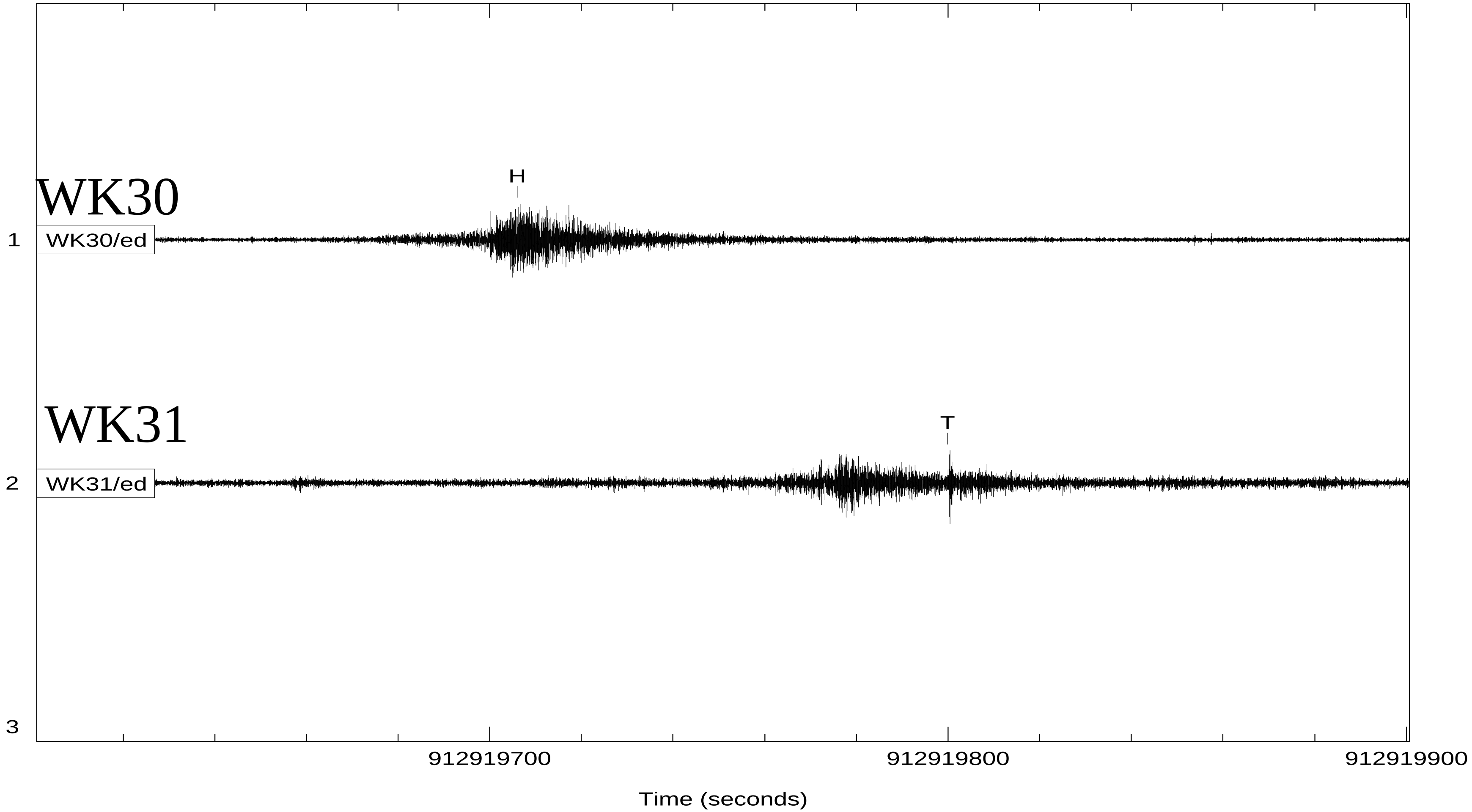

Why is one arrival classified as H and one as T?

Why is the timing so late on WK30?

Wake Island geometry

WK30 and WK31 are 238 km apart. The axis of the SOFAR channel is at about 1km depth, so there is no obvious local blockage [in practice arrivals from the North will be blocked on WK30]

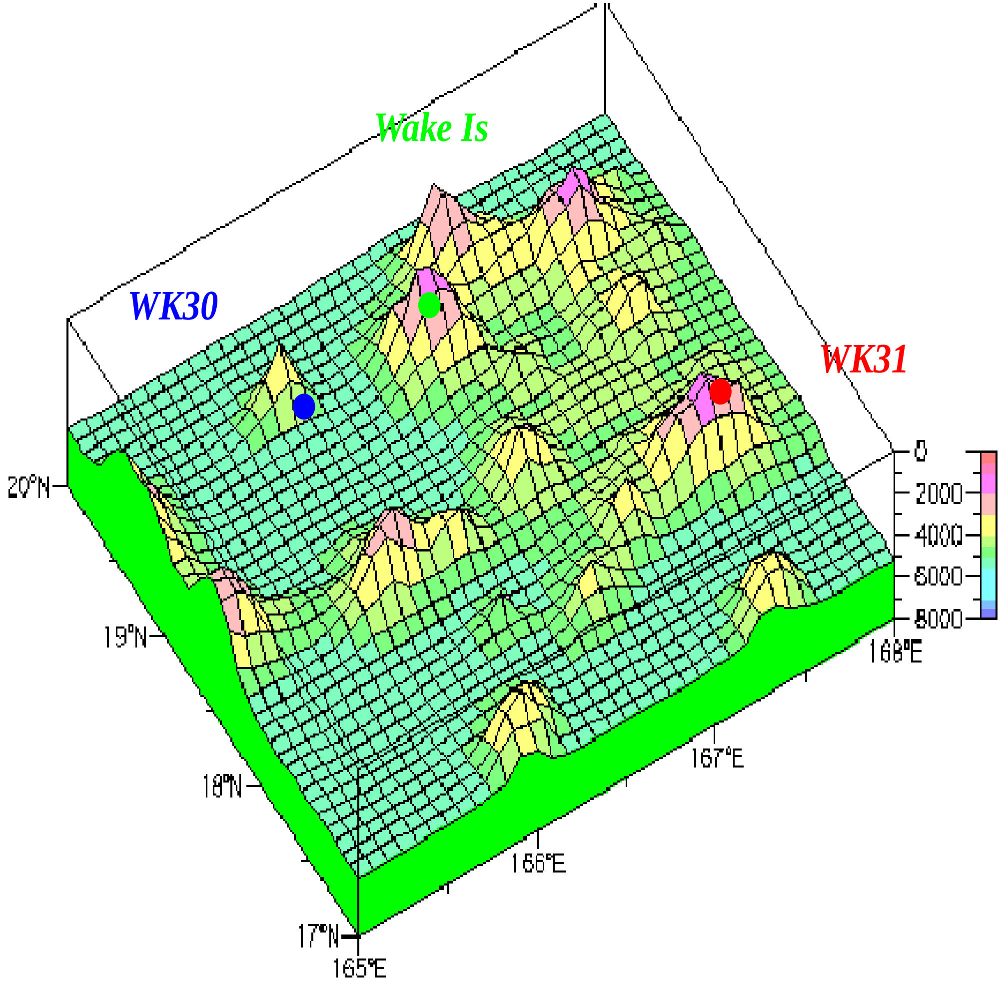

Spectrograms from one Dec. 6, 1998 event (2)

WK30: H-phase

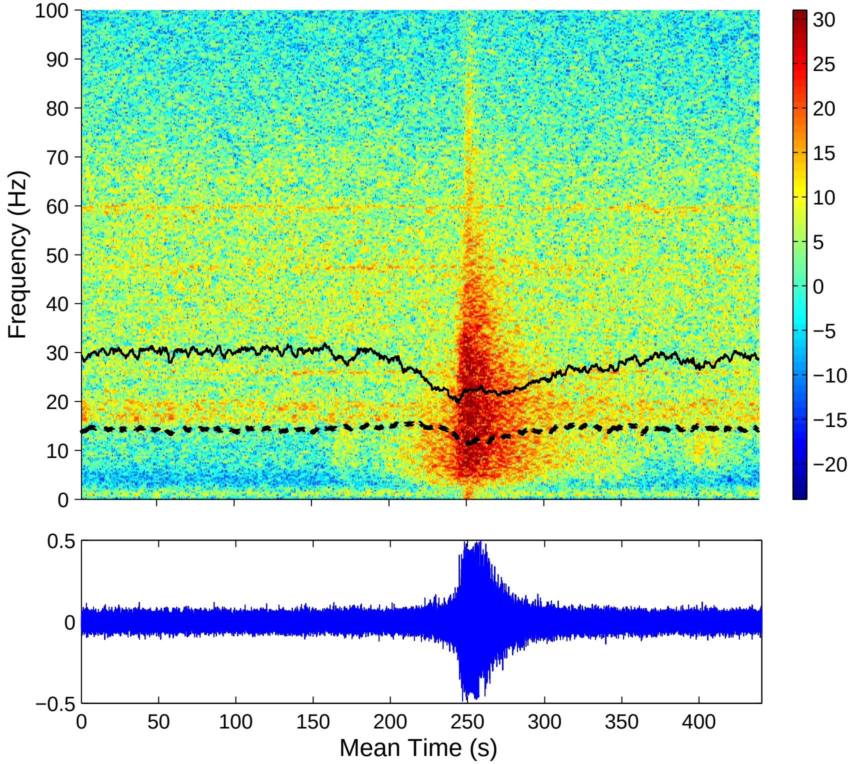

WK31: T-phase

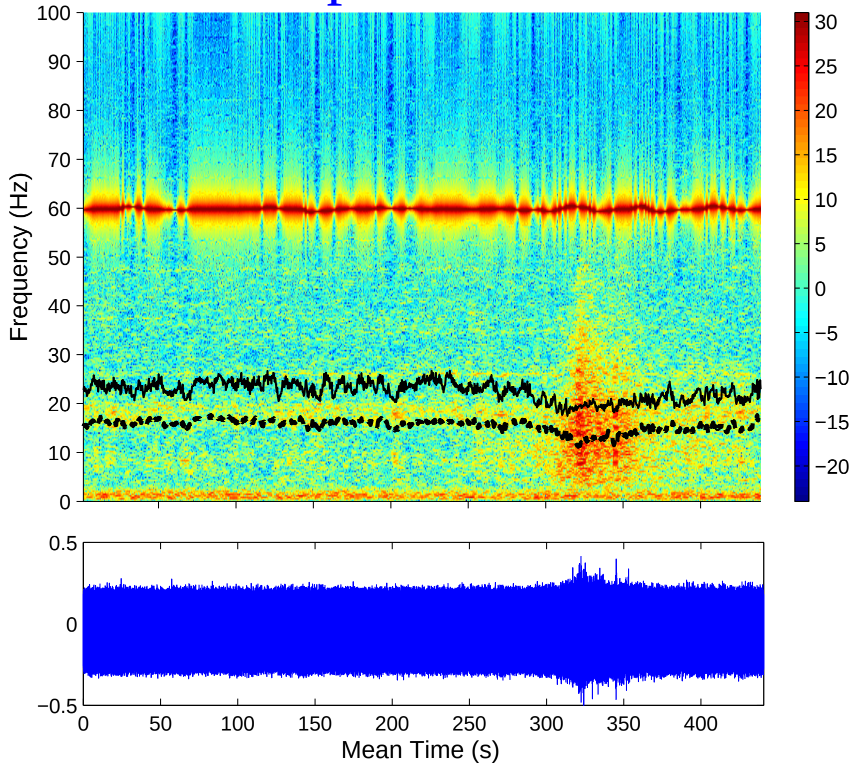

- High 60-Hz electrical noise on WK31
- Clipping of signal observed on WK30

It is expected that the clipping on WK30 caused the arrival to be classified as an H-phase.

Clipped signal on WK30, Dec. 6, 1998 event (3)

Zoom in on the WK30 signal does show clipping, this gives a broad spectrum in the spectrogram.

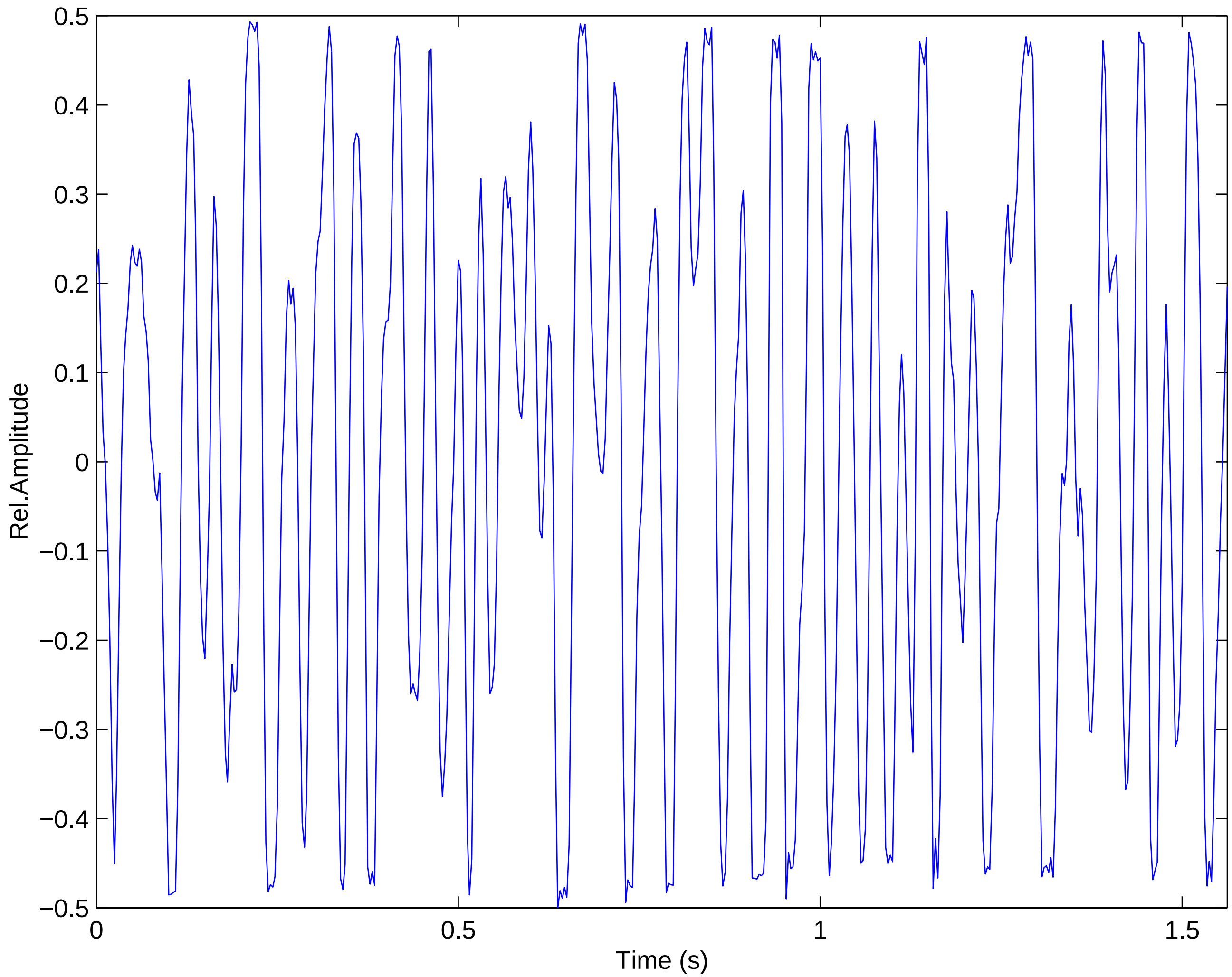

Filter analysis of WK31 arrival, 6 Dec. 1998. (4)

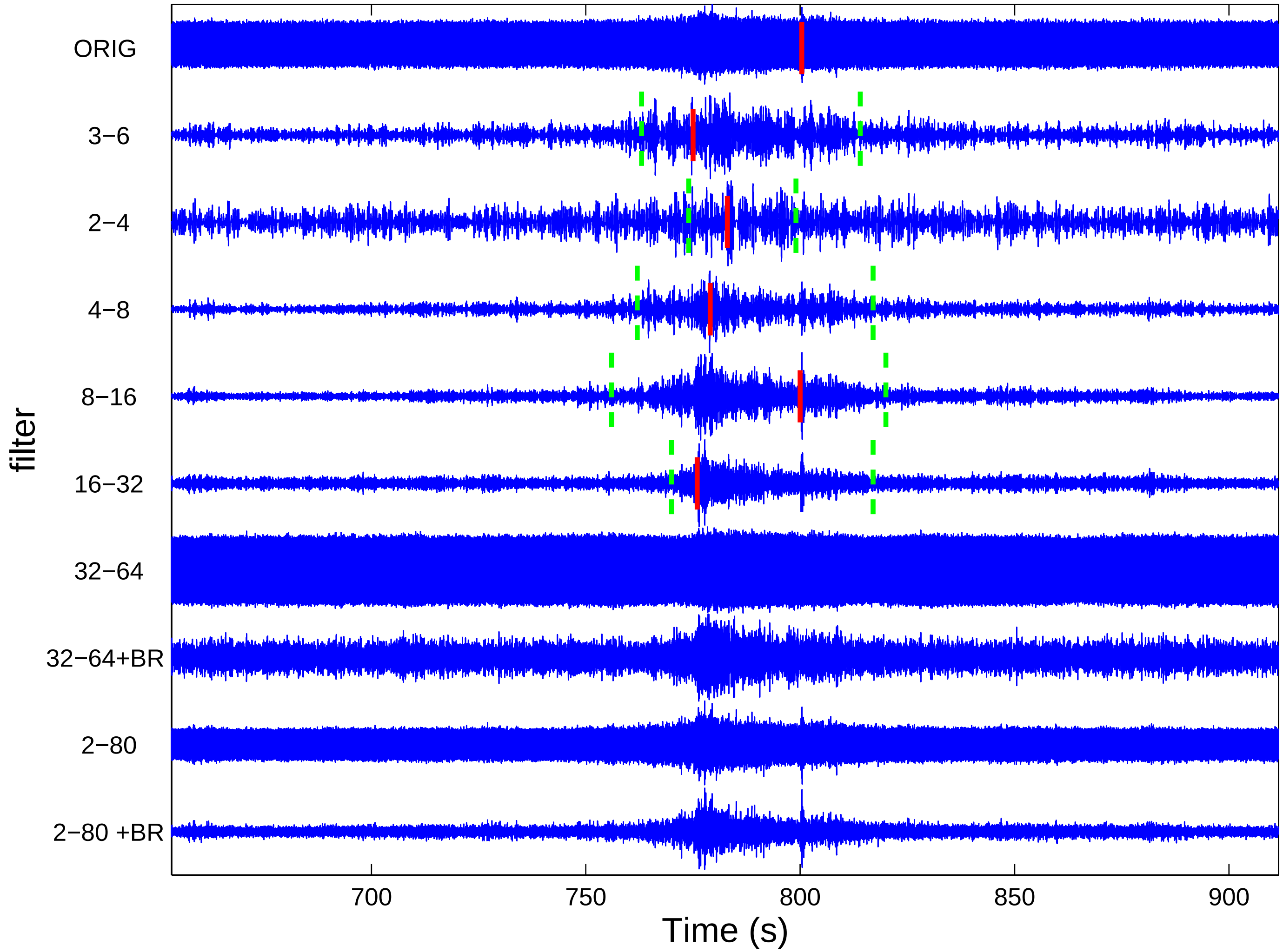

Onset and termination time

PWT

(the 60 Hz noise is dominating)

(but filtering repairs the problem)

The 8-16Hz band has most energy, arrival time (PWT) is from that band.
DELTIM=0.8 s (the measurement error). That seems too low.

Envelope filter analysis of WK31 arrival, 6 Dec. 1998. (5)

The envelope can be computed by rectifying the signal and then using a running avearging.
[But here it is based on the magnitude of the signal and it Hilbert transform]

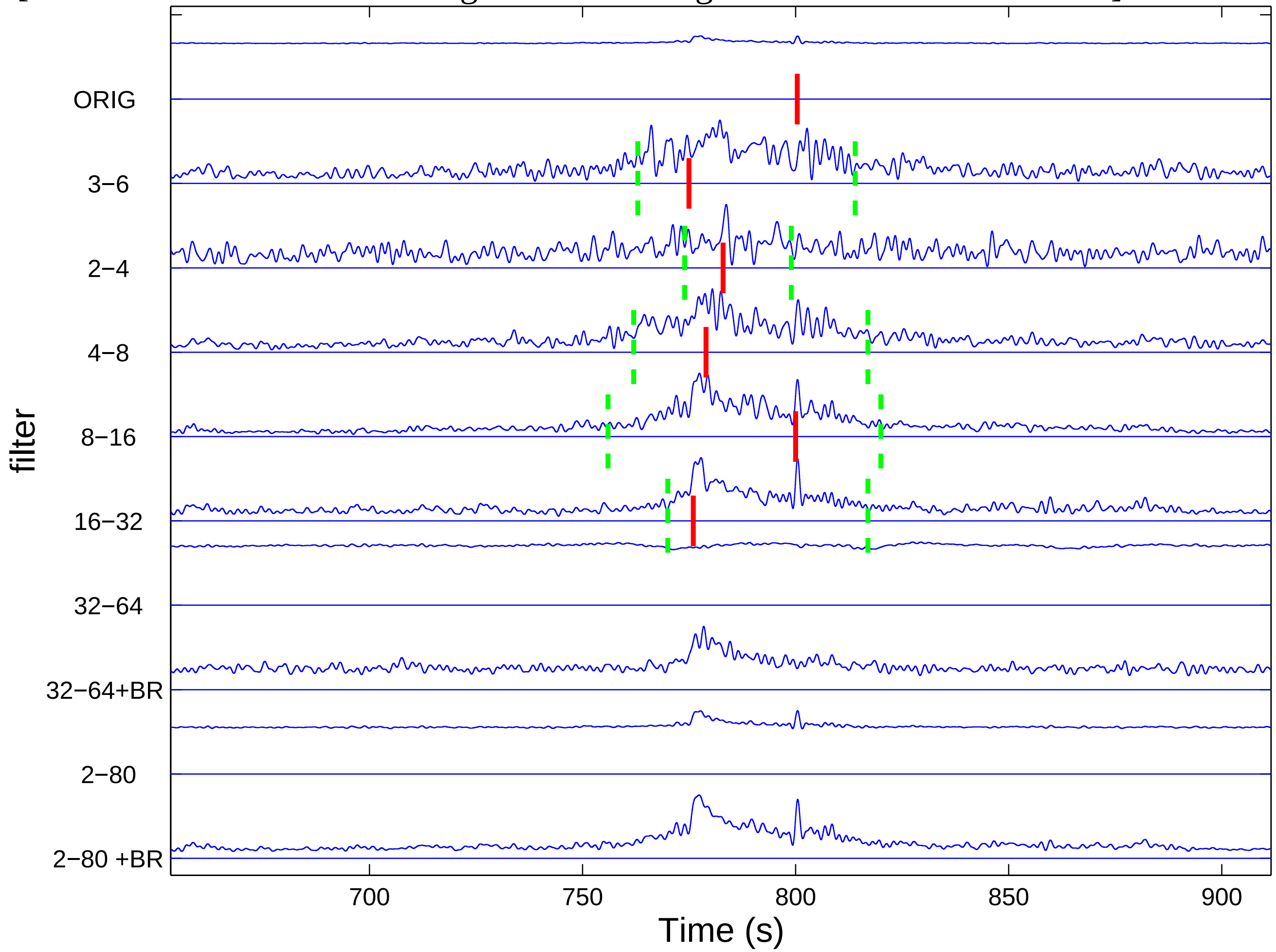

Onset and termination time

PWT

It looks peculiar as it is based on noise only

By comparison with previous slide the determination of the arrival seems now more stable.
The main arrival in the 8-16 Hz band is now in about 780 s, the highest peak is there. (No processing yet)

Determination of Angle of arrival, Dec. 6, 1998 arrival (6)

If the same phase type was detected on both station(WK30 and WK31) the angle of arrival could be determined.

From the measured time delay (here 75 s) the angle of arrival can be determined:

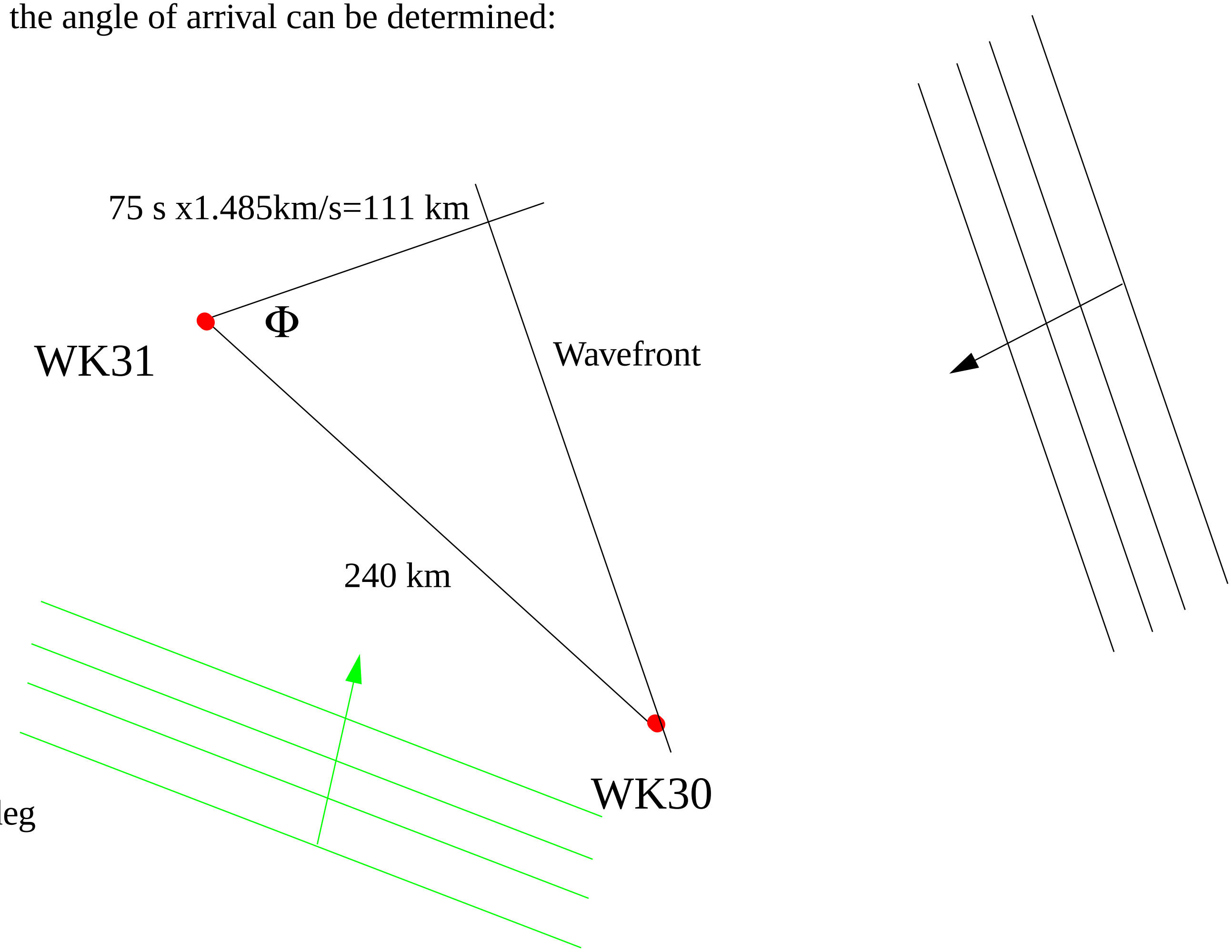

Where by Φ = acos(111/240)=62 deg.

The azimuth from WK31 to WK30 is 133 deg

The azimuth is 133+/- 62= 71 or 195 deg.

For two hydrophones there are two possible angles with three hydrophones a unique angle can be determined

Phase Identification is done by “Station Processing” (StaPro)

Phase identification (T, N or H) is done by StaPro

In Release two neural network weight implemented at
WK30, WK31, PSUR

Empirical Phase identification rules at
VIB, ASC23, ASC24, ASC26 + New stations

The neural network:

- Each hydrostation has its own neural network weights
- For each arrival a subset of the data from the hydro_features table is feed to the neural network and based on this the classification is done.
- The network must first be trained using real arrivals as well as synthetic arrivals.

Empirical Phase Identification rules (1)

1) For a given arrival the low frequency band (LFB) is the 3-6 Hz band and high frequency band (HFB) is 32-64 Hz band. The following parameters are then computed based on the `hydro_features` table (for definition of the variables from the `hydro_features` table see Appendix A):

- EnergyRatio: total_energy(HFB) -total_energy(LFB)
- Duration: termination_time(LFB)-onset_time(LFB)
- TimeSpread: total_spread(LFB)
- FractionalTime: total_time(LFB) / duration
- CrossingDensity: num_cross(LFB) / duration

2) If there are no HFB detections then the EnergyRatio is set to a small number, so that the signal will be identified as a T-phase or N-phase. If there is no LFB detection the signal cannot be a T-phase.

Empirical Phase Identification rules (2)

3) Based on these five measures the signal is declared a **T-Phase** if ALL the following rules are satisfied

- EnergyRatio < -15.5 dB
- TimeSpread>5 s
- CrossingDensity>12

4) If not a T-phase the signal is an **N-phase** if ANY of the following rules are satisfied

- EnergyRatio < -15.5 dB
- Duration<6 s
- TimeSpread>35s
- FractionalTime<0.4
- CrossingDensity>20
- Or features missing so that the 5 measures could not be computed.

5) The remaining unidentified phases are identified as **H-phases**.

Example: Identification of 6 Dec. event

What is this event identified as based on the empirical rules? (Sorry for format, but it is directly from the database)

select ARID, PEAK_TIME, PEAK_LEVEL, TOTAL_ENERGY, MEAN_ARRIVAL_TIME as mean_ar_tim, TIME_SPREAD, ONSET_TIME, TERMINATION_TIME as term_tim, TOTAL_TIME, NUM_CROSS, AVE_NOISE, LOW_CUT fmin, HIGH_CUT as fmax, PROB_WEIGHT_TIME as pwt, SIGMA_TIME as st from idcx.hydro_features where arid=23328270;

ARID	PEAK_TIME	PEAK_LEV	TOT_ENER	MEAN_AR_TIM	TIME_SPR	ONSET_TIME	TERM_TIM	TOT_TIME	NUM_CR	AVE_NOISE	FMIN	FMAX	PWT	ST
23328270	912919706	132.3	137.8	912919710	15.34	912919670	912919758	52.89	1087	106.56	2	4	912919706	.21
23328270	912919706	137.8	143.5	912919712	15.71	912919653	912919777	80.64	2098	106.58	3	6	912919706	.48
23328270	912919708	141.4	145.9	912919712	15.19	912919651	912919782	84.80	2814	107.97	4	8	912919708	.67
23328270	912919705	144.7	147.2	912919712	13.61	912919665	912919777	73.97	3402	109.90	6	12	912919705	.03
23328270	912919705	144.1	147.2	912919712	11.76	912919677	912919767	58.70	3524	111.15	8	16	912919708	3.86
23328270	912919707	144.1	146.3	912919712	8.71	912919695	912919755	37.83	3934	112.94	16	32	912919707	.69
23328270	912919705	137.9	138.1	912919710	5.35	912919700	912919726	13.18	2882	115.27	32	64	912919705	.70
23328270	912919706	149.3	151.5	912919711	10.91	912919677	912919755	45.77	4618	119.13	2	80	912919706	.32

Automatic Hydroacoustic phase association

Hydroacoustics arrivals are processed together with arrivals from the other waveform technologies.
Thereby arrivals are logically coupled together and only the seismic network is sufficiently developed to be independent.
However the networks have different detection capability and unrelated arrivals from different networks can be grouped together to build an event. This is also possible for one network, and there is no solution yet.

Exhaustive grid search is conducted to form events and associate arrivals for hydroacoustic arrivals.
Because they only use traveltime. This would not be necessary if arrival azimuth was determined.

Associations are based on time and phase type only.

Due to the uncertainty in the ocean coupling for T-phases they cannot participate in the location. They are only associated.

There H-phases can build an event alone.

With Release one this was possible with WK30, WK31 and NZ01 and NZ06 (none was generated).

With Release two this is possible with WK30, WK31 and PSUR.

In a future release groups belonging to the same station will be treated together (e.g. WK30 and WK31).
Thereby the two possible azimuth can be determined and not just arrival time.

In Release one 55 events were build by one seismic and two hydroacoustic H-phase arrivals. These are questionable!
Often small pacific events were detected in Norway and at Wake.

Automatic Hydroacoustic phase location

Location is to find the origin of an event.

T-phases are only associated.

The location is determined based on initial guess of the origin and refined using a Gauss-Newton iterative approach.

H-arrivals participate on an equal basis with seismic arrivals.

How much influence each arrival has on the location is determined by the a priori timing error for each arrival.

Since H-phases has lower a priori error than seismic phases they are more important in the localization of in-water events.

Blockage maps (1)

Blockage maps are used to eliminate unrealistic associations. They should not eliminate arrivals that could not be possible. Based on this it is reasonable not to block arrivals from north at WK30.

An arrival has to be in the non-blocked part for a station in order to be associated.

Determined from land masses.

Small islands has been removed from consideration.

Seamounts or shallow water passages can block the signal that has not been taken into account.

T-phases originates from the earth, and a 2-degree buffer is included to incorporate in-land events

Blockage map for Ascension:

Blockage maps (2)

Blockage map for WK30:

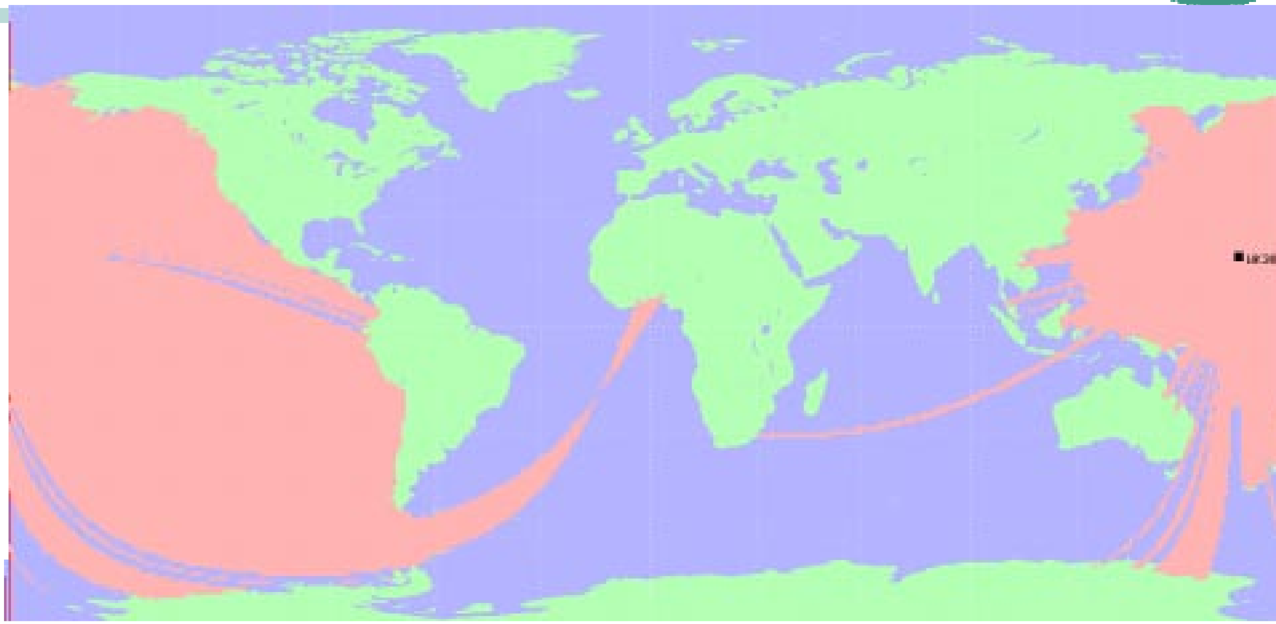

Blockage map for Point Sur:

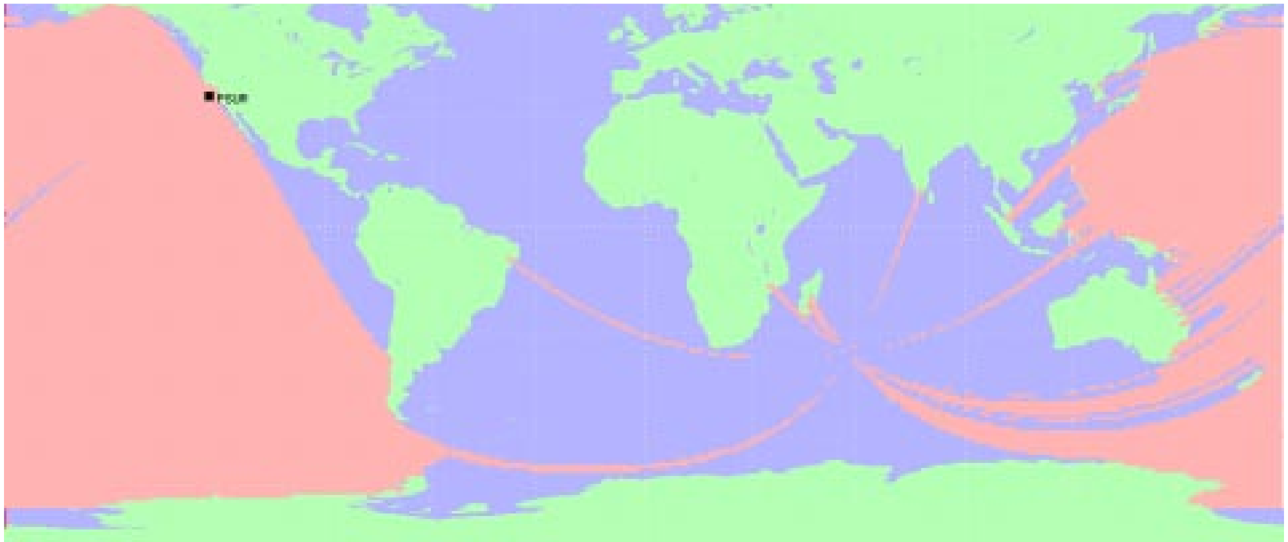

Blockage maps (3)

Combined Blockage map:

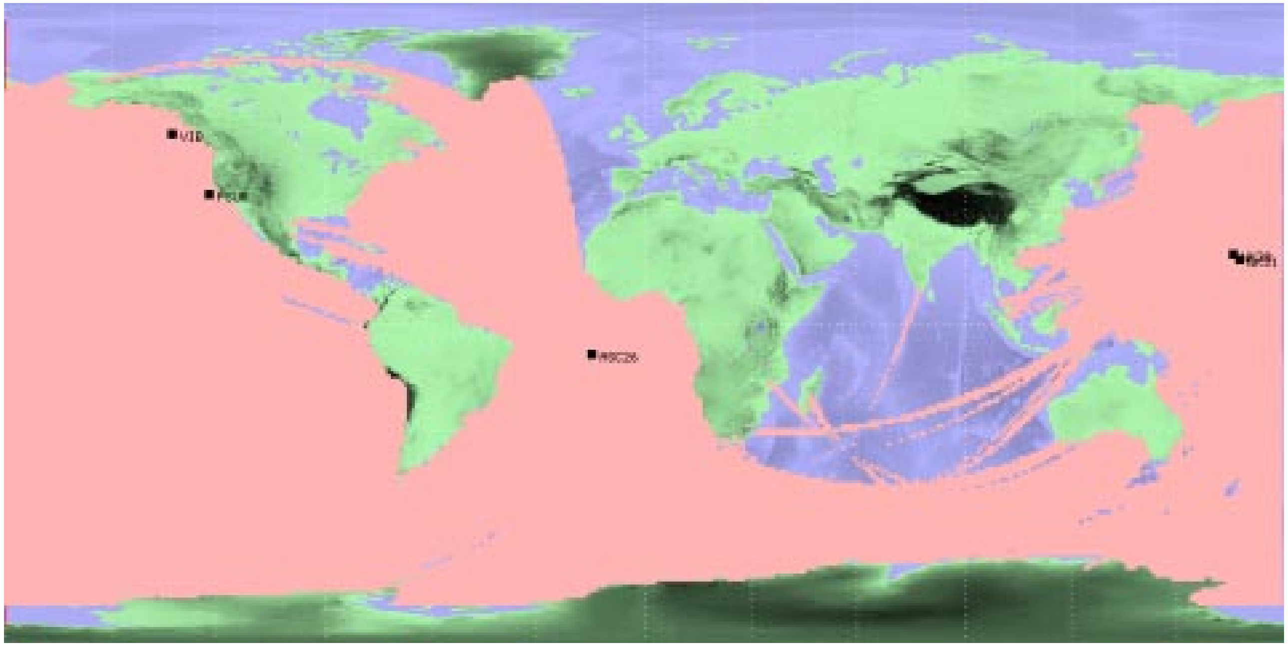

Blockage maps are very efficient in disassociate arrivals. The fine structure of the blockage maps are questionable.

For example the paths in the Indian ocean: some of the paths will be blocked due to shallow water,
if the SOFAR channel is blocked then energy will likely be scattered where the SOFAR channel is blocked.

while other path will be strongly horizontally refracted (how much is unknown).

A solution to this could be to eliminate all the “tricky” paths.

2-D seasonal travel time tables.

Travel times based on the probability weighted time using synthetic arrivals based on data bases of ocean sound speed and bathymetry.

The ocean sound speed is seasonally dependent, and therefore traveltimes has been computed for each of the four seasons (spring, summer, fall and winter).

Travel time reduced with 1482 m/s

The blockage map is indicated in the plots, as blockage is determined by land masses, they do not completely agree.

Due to colder (slower) water, the northern and southern paths has slower reduced travel time.

The difference in summer and winter traveltime is not obvious from these plots.

WK30 Summer:

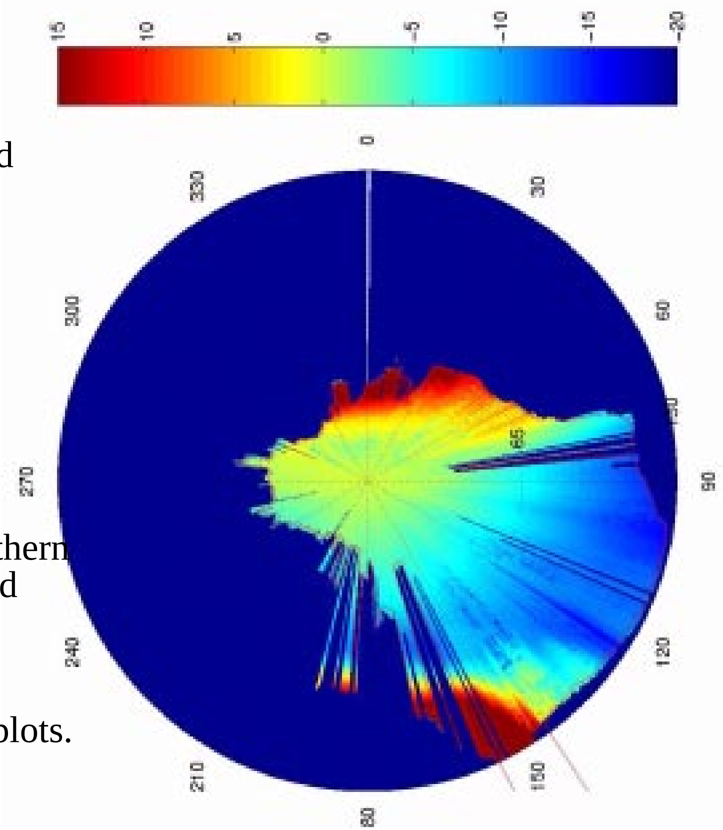

WK30 Winter:

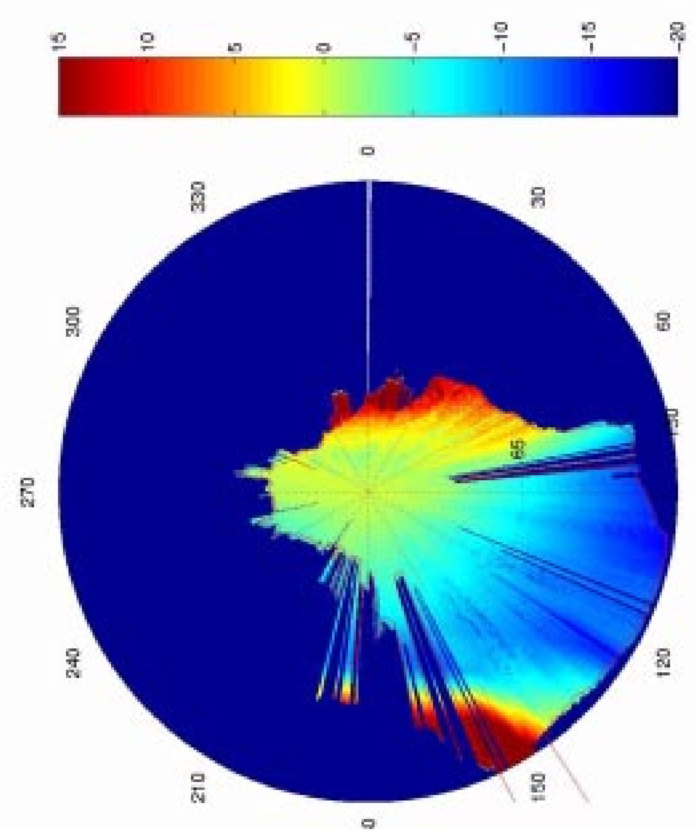

2-D seasonal travel time tables (2)

Difference in traveltime between summer and winter for wk30 (maximum difference in plot is 2 s)

The sound speed in the deep ocean is independent of the season.

The sound speed increases with temperature.

Only when the SOFAR channel is close to the surface will there be a large seasonal variation.

The depth and size of the termocline is also seasonally dependent.
Both warmer and stormier seasons tends to lower the termocline.
It can influence the travel time.

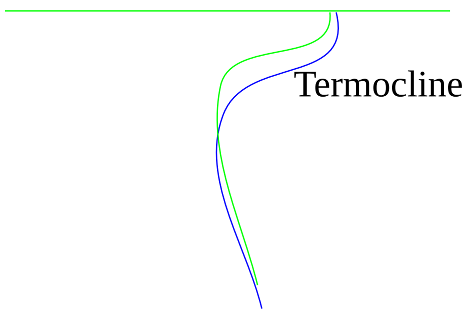

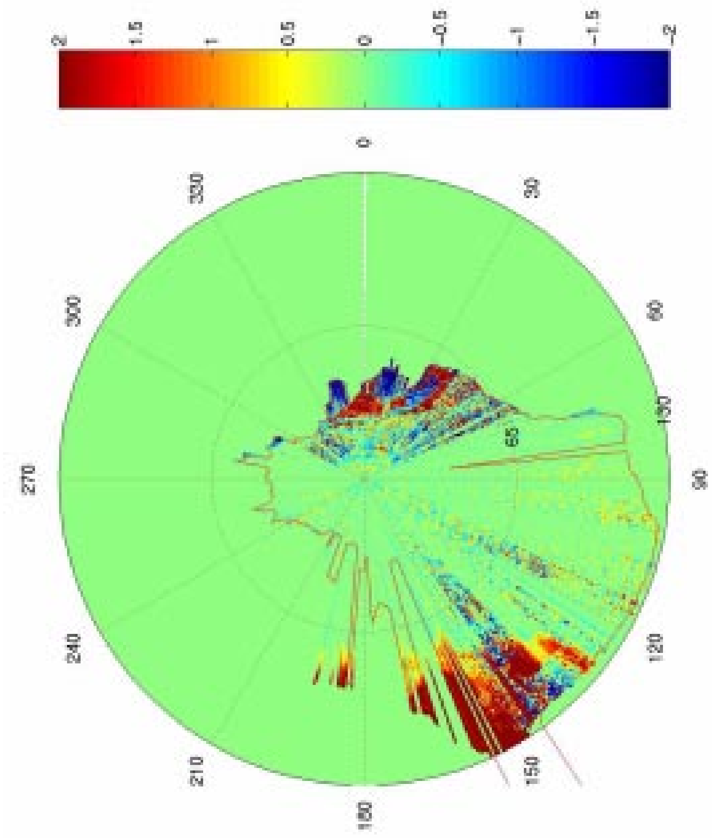

Automatic located events with phases associated at Wake Island

H-phases

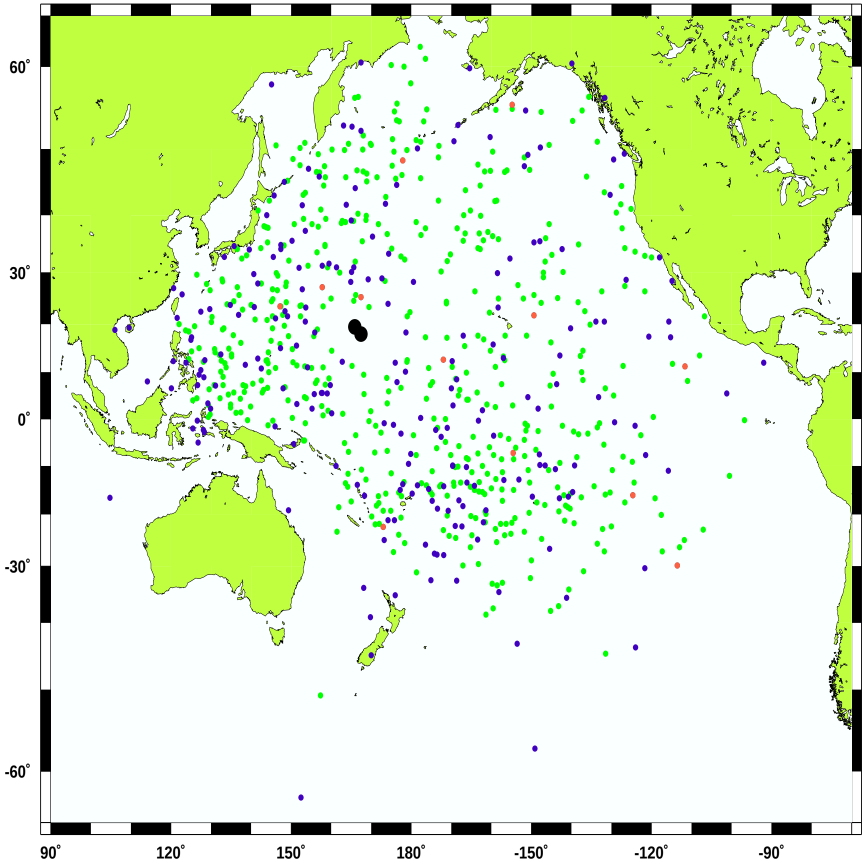

T-phases

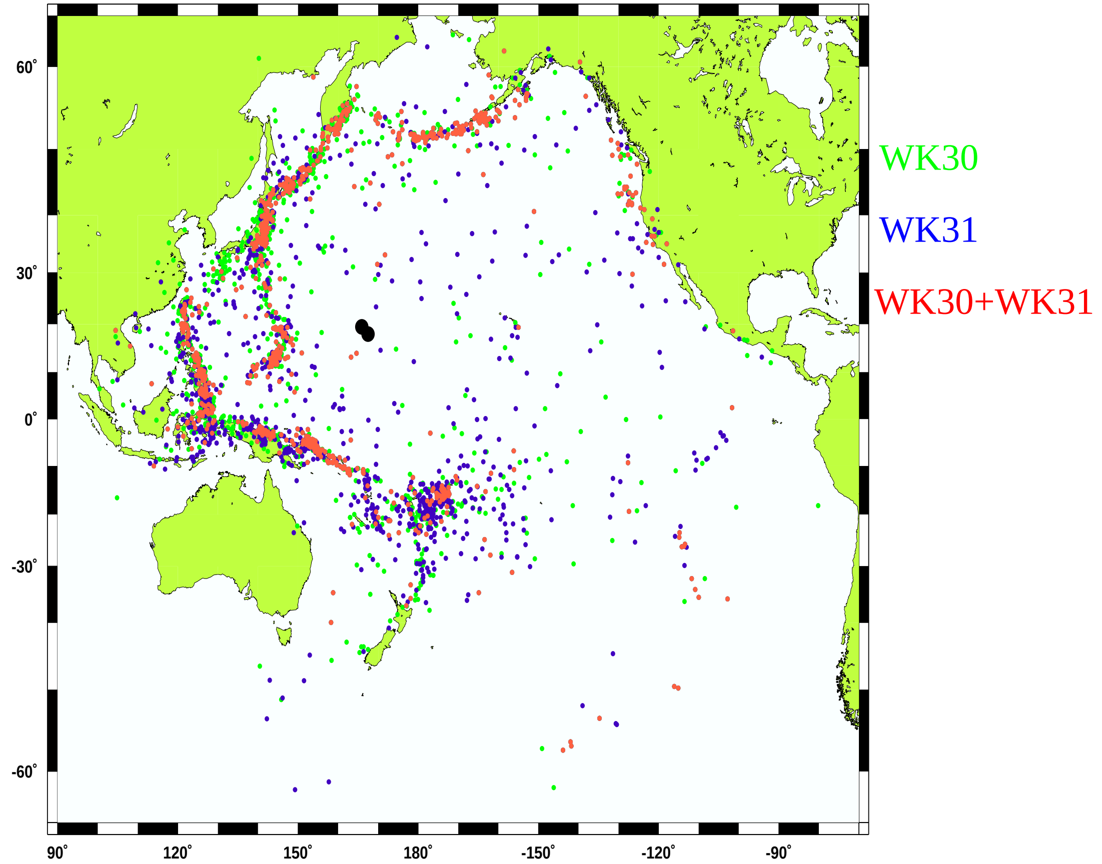

- Most T-phases in regions of high seismic activity
- Location of events with associated H-phases are questionable
- Only 12 “H-events” was detected on both WK30 and WK31. There was 3 times more H-phases detected on WK30 than WK31.

Error ellipse for events with H-phases associated at Wake Island

The exact location of an event cannot be found. The error ellipse indicates with 90% probability the location of an event.
Thus error ellipse is important in assessing the accuracy of a location.

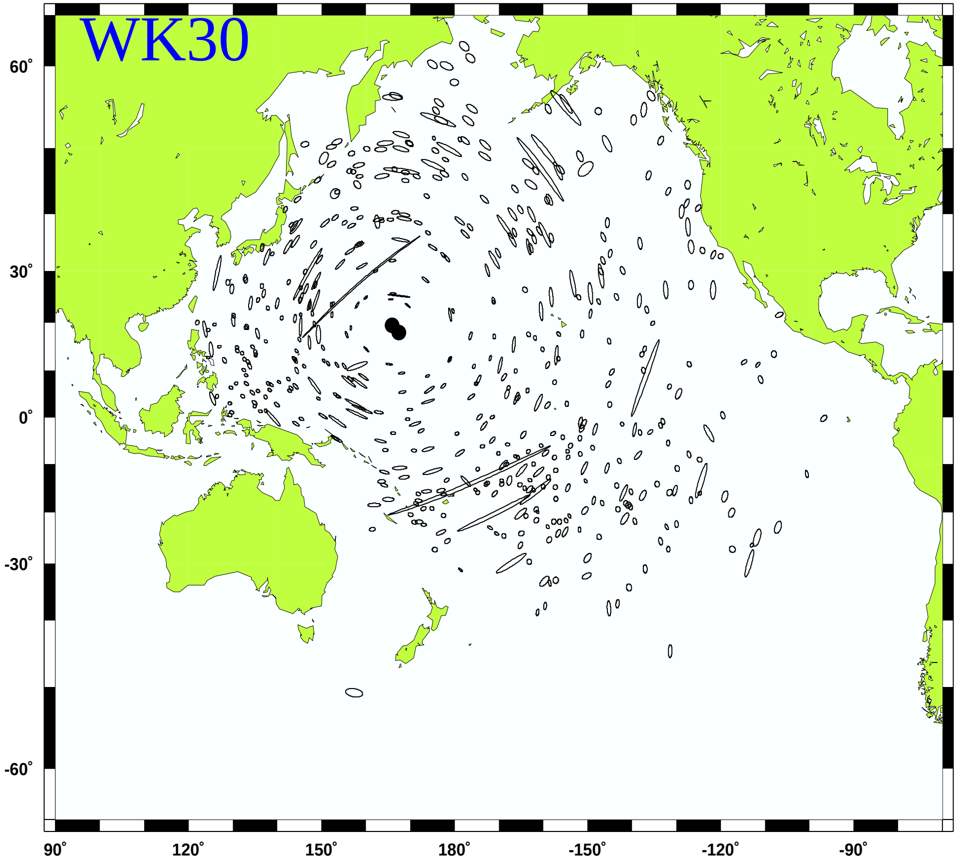

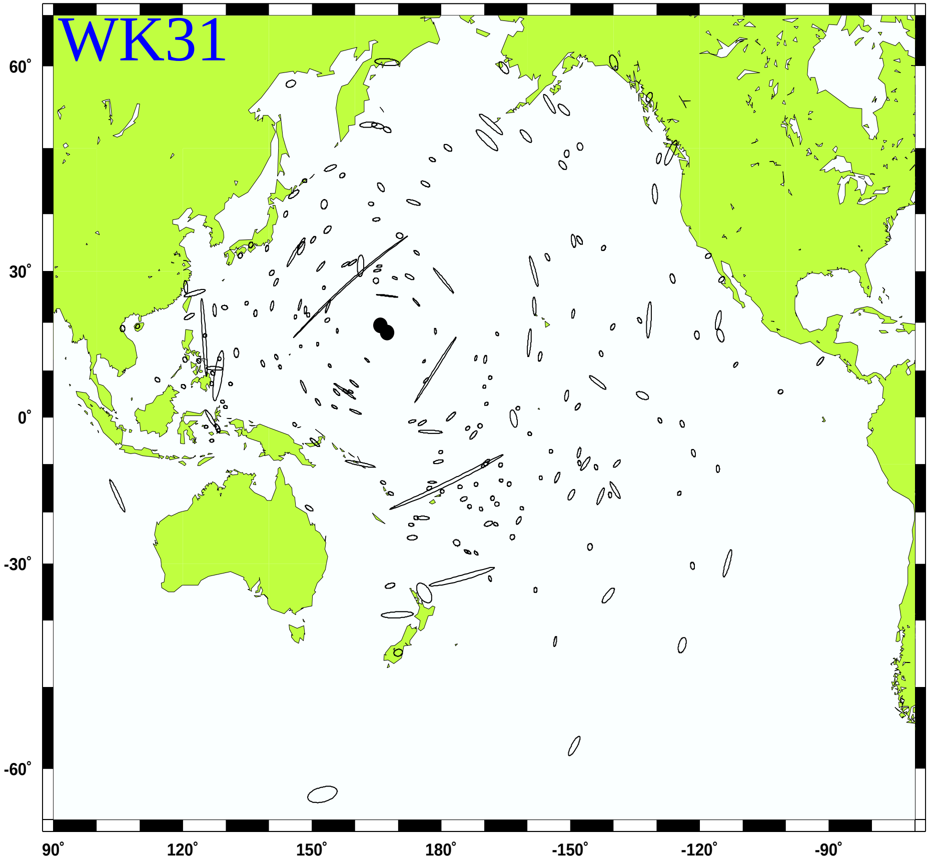

Most of these events has only one H-phase associated

The radial pattern indicates that the associated H-phases has low error contribution relative to the other associated phases

Definition of error ellipse

The error ellipse x_e is determined from the estimated location x based on the 90% fractile of the Chi-squared distribution with M degrees of freedom:

$$(\boldsymbol{x}-\boldsymbol{x}_e)^T \boldsymbol{V}_x^{-1}(\boldsymbol{x}-\boldsymbol{x}_e) = \chi_p^2(M)$$

This is the slowness in each direction

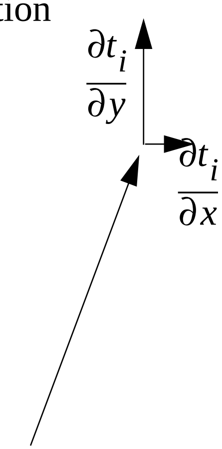

$\boldsymbol{V}_{\boldsymbol{x}}$ is the parameter correlation matrix.

$$\boldsymbol{V}_x^{-1} = A^T A = \sum_i^N a_i^T a_i \quad , \quad a_i^T = \sigma_i^{-1} \begin{bmatrix} \frac{dt_i}{dx} \\ \frac{dt_i}{dy} \\ \frac{dt_i}{dt} \end{bmatrix}$$

$\boldsymbol{V}_x^{-1}$ depends on local slowness for each arrival normalized with the *a priori* error σ_i for each contributing arrival *i*, *i=1,...,N*.

Ocean slowness 1/1480 s/m. Seismic slowness is 1/3000 -1/15000 s/m.
To have same weighting, hydroacoustic timing errors should be 2-10 larger than seismic

The timing errors σ_i are assumed uncorrelated [Full correlation may be more correct for Wake--but more complicated!]

$$\sigma_i^2 = \sigma_A^2 + \sigma_M^2$$

Measured (DELTIM) + Modelling error

Distribution of DELTIM for hydroacoustic arrivals

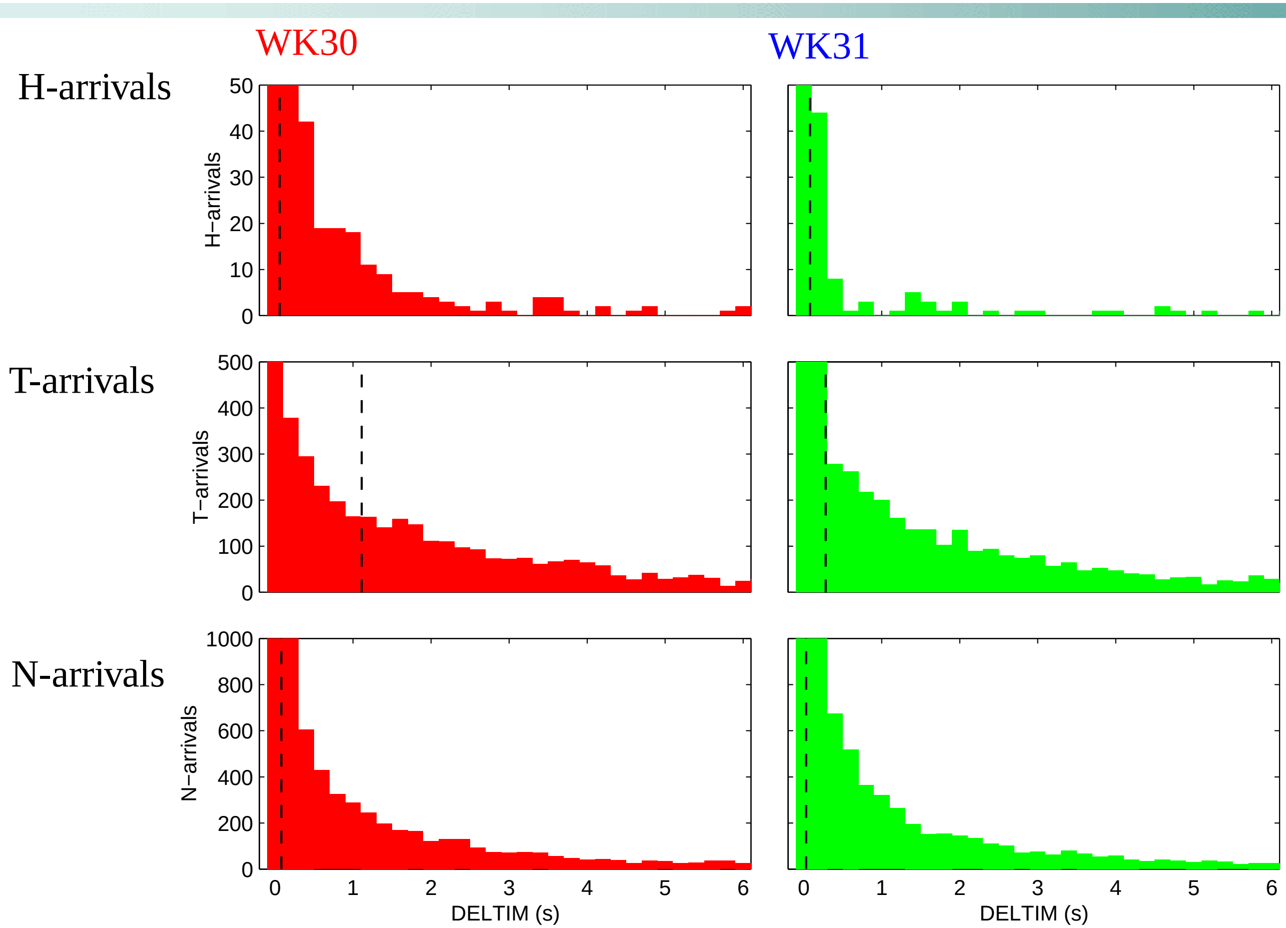

The figure shows the histogram of DELTIM
Based on all arrivals on Wake during R-1

Seismic network has DELTIM 0.7-1.7s
Physically: Hydroacoustic DELTIM should be larger

Modelling Errors

They have many causes:

-Too simple description of environment (10000km/1482m/s- 10000km/1481m/s=4.5 s)
-Seasonal variations. Up to about 20 s (range 50 deg) for northern paths, usually less than 1 s
-Fluctuations from database sound speed up to 2 s
-Partial blocking- Mode stripping.
-Internal waves: Important for energy distribution in the arrival phase.
-Daily fluctuations up to 0.07 s over 1000km
-Horizontal refraction +ellipsoidal correction caused Perth-Bermuda errors of 30 s rel to great circle path.
-Uncertainty in determining arrival time PWT 0.1 s

-T-phase coupling from source to ocean error about 60 s.
-T-phase station modelling error from ocean coupling to station 3 s

-Numerical errors 5 s

-Guess: In total H-phase errors about 2s+ 0.2Δ, where Δ is the distance in degrees

-For primary seismic phases in iasp91 modelling error 1-3.5 s.

To have same weighting in location, hydroacoustic timing errors should be 2-10 larger than seismic.
Based on the next figure (plus the DELTIM values) it can be concluded that hydroacoustic arrivals have more weighting in location.

The modelling error for H and T-phases

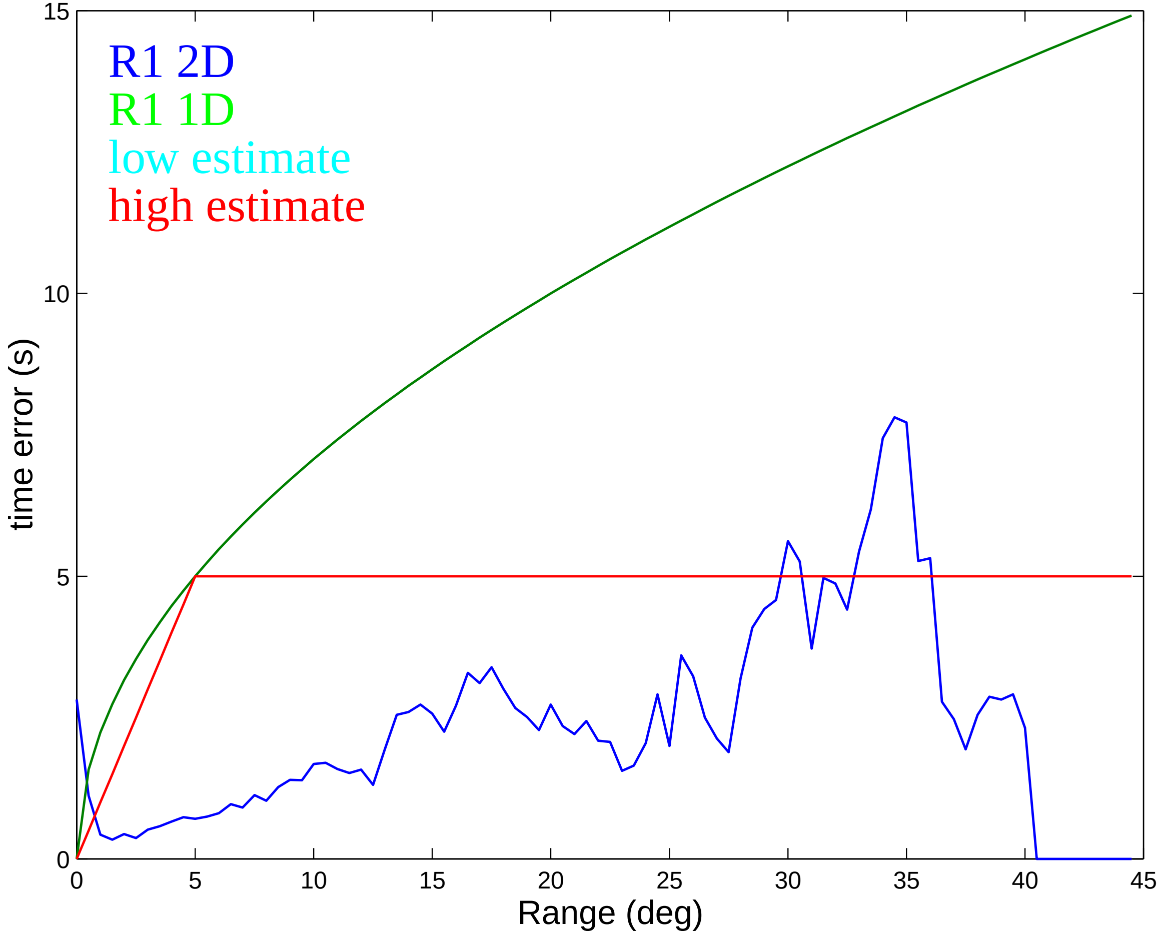

Event screening

After all automatic processing and analyst reviews, the detected events are screened in order to identify possible explosions. These are based on quite simple criteria (only outline is given):

1) All seismic events where minimal bathymetry is greater that 500 m for the entire error ellipse are screened out.
It is unlikely to have an explosion at greater depth.

2) For events without observed hydroacoustic signals on hydrophone stations: the event is screened out if the entire error ellipse has unblocked path to that station.
Hydroacoustic is so efficient that it will always detect a large explosion.

3) For all events with hydroacoustics signals: Apply event screening to all events that do not contain a bubble pulse:
Screen out events where the hydroacoustic signal has little energy in the 32-64 Hz band.